SCUOLA
NORMALE
SUPERIORE

The prodromal phase of Parkinson's disease:

a mouse model study focused on

alpha-synuclein pathology and dysfunction in the colon

PhD candidate: Lucia Rota

Supervisor: Emanuela Colla

Index of contents

Abstract

Parkinson's disease (PD) is the most common movement disorder and the second most common neurodegenerative disorder, with a prevalence of 1 to 2 individuals per 1000 at any age, increasing to 1% of the population above 60 years. The pathological hallmarks of PD are neuronal proteinaceous inclusions called Lewy bodies and neurites – rich in alpha-synuclein (αS) – and death of dopaminergic neurons in the pars compacta of the substantia nigra, which can only be detected in patients' brains *post mortem*. Diagnosis is mainly based on the observation of the typical motor symptoms (tremor, rigidity, bradykinesia) caused by these molecular alterations. Although PD is considered a movement disorder, patients also suffer from a variety of non motor alterations, some of which (e.g. constipation) can occur even decades before the onset of the motor ones. Moreover, Lewy pathology has been found in patients not only in the central (CNS), but also in the peripheral and enteric nervous systems (ENS), suggesting a correlation between αS inclusions in these sites and non motor symptoms, and a possible spreading of the pathology from the periphery to the brain. This study is focused on gastrointestinal (GI) dysfunctions and specifically constipation, for which the relationship with PD development is still poorly understood.

For this research we used a transgenic (Tg) mouse model over-expressing human A53T αS under the control of the murine PrP promoter (line G2-3), one of the first genetic model developed to study α-synucleinopathies (which include PD). These mice develop neurological abnormalities after 9 months of age that manifest with motor symptoms which become progressively more severe culminating into a fatal paralysis within 14-21 days. Diseased mice show an accumulation of intracellular, phosphorylated and ubiquitinated αS inclusions, neuroinflammation and neuronal degeneration in the CNS. For the purpose of this study, sick αS Tg mice at 12-14 months, presymptomatic mice at 1, 2, 3, 6, 9 and 12 (if still healthy) months, and age-matched nTg littermate controls were used. Presymptomatic αS Tg mice displayed a drastic delay in GI transit time of almost 2 hours from 3 months old that increased with age, reaching more than 3 hours delay at 6 months. Such delay was associated with abnormal formation of stools for αS Tgs, that resulted in less abundant but longer pellet excreted, although normal for dry and wet weight. After that we recorded the contractile activity from longitudinal and circular muscle preparations of colon and ileum, to verify the intestinal function. In line with our previous observations, electrically evoked contractions of the colon, but not of the ileum, showed a reduced response in both muscle layers in αS Tg mice already at 3 months of age, mainly due to an impaired cholinergic transmission of the ENS. Furthermore, molecular analyses were carried out to check on αS enteric distribution. Interestingly, insoluble and aggregated αS was found in enteric neurons in both myenteric and submucosal plexi only in the colon and not in the small intestine of 3

months old Tg mice, and exacerbated with age, mimicking the increase in transit delay and contraction deficits showed in behavioral and electrical recording experiments.

Following this GI characterization of PrP A53T αS Tg mice, we designed a disease modifying therapy to be carried out with an antisense oligonucleotide (ASO) against αS, in presymptomatic animals. After an *in vitro* evaluation, the selected ASO was administred to 10 weeks old Tg mice for 7 days, through osmotic pumps or rectal administration. Very surprisingly, Tg mice which received the ASO displayed a significant reduction in their GI transit time compared to the values before starting the treatment and to the PBS control group, for both administration routes. Together with the improvement in constipation, ASO treatment induced a reduction, although not significant, of the total level of αS in the distal colon for both delivery methods.

This research demonstrates for the first time that the PrP human A53T αS Tg mice line G2-3 is a unique model to investigate GI dysfunction in prodromal PD, thanks to the net spatio-temporal separation of αS-driven pathologies in the ENS and in the CNS. Moreover, the promising results obtained in this model by using an ASO peripherally support the correlation between GI behavior and αS levels and the hypothesis that lowering the total level of αS can be a successful disease modifying therapy against PD.

Abbreviations

Alpha-synuclein (αS)

Alpha-synuclein human gene (SNCA)

Antisense oligonucleotide (ASO)

Blood brain barrier (BBB)

Blood nerve barrier (BNB)

Central nervous system (CNS)

Distal colon (D)

Dopamine (DA)

Dorsal motor nucleus of the vagus nerve (dmX)

Electrical stimulus (ES)

Endoplasmic reticulum (ER)

Enteric nervous system (ENS)

Full length (FL)

Gastrointestinal (GI)

High molecular weight (HMW)

Lewy bodies (LBs)

Lewy neurites (LNs)

Non transgenic (nTg)

Non amyloid β-component (NAC)

Over night (o/n)

Parkinson's disease (PD)

Proximal colon (P)

Peripheral nervous system (PNS)

Paraformaldehyde (PFA)

Phosphate-buffered saline (PBS)

Prion protein (PrP)

Room temperature (RT)

Standard error mean (SEM)

Substantia nigra (SN)

Substantia nigra pars compacta (SNpc)

Substantia nigra pars reticulata (SNpr)

Small ubiquitin-related modifier (SUMO)

Tris-buffered saline (TBS)

Transgenic (Tg)

Whole gut transit time (WGTT)

Introduction

Parkinson's disease

Parkinson's disease (PD) is the most common movement disorder and the second most common neurodegenerative disorder, after Alzheimer's disease. The prevalence of PD increases with aging: it counts 1 to 2 affected individuals per 1000 at any age (Von Campenhausen et al., 2005), 1% of the population above 60 years (de Lau and Breteler, 2006) and 4% above 85 years (de Rijk et al., 1995). The age of onset is usually between 65 to 70 years, and only for a rare recessive form it occurs before the age of 40, in less than 5% of the cases (Tysnes and Storstein, 2017). PD is an irreversible and slowly progressive neurodegenerative movement disorder that impairs movement control. Together with multiple system atrophy, dementia with Lewy bodies (Peelaerts et al., 2018) and pure autonomic failure (Kaufmann et al., 2017), PD belongs to a group of diseases named α-synucleinopathies, because of the abnormal accumulation of intracellular proteinaceous inclusions mostly made of aggregated alpha-synuclein (αS). Specifically, the pathological hallmarks of PD are the loss of dopaminergic neurons in the substantia nigra pars compacta (SNpc) and the presence of αS positive intraneuronal inclusions called Lewy bodies (LBs) or Lewy neurites (LNs), depending on whether they are located in the soma or in the neurites, respectively (Goedert et al., 2013). LBs and LNs were discovered by Freiderich Lewy in 1912, but only after almost a century it has been described that they are mainly composed by fibrillar aggregates of post-translationally modified αS and ubiquitin (Spillantini et al., 1997), together with a large number of other constituents, such as tau, parkin and neurofilaments (Arima, 1999; Schlossmacher et al., 2002; Shults, 2006).

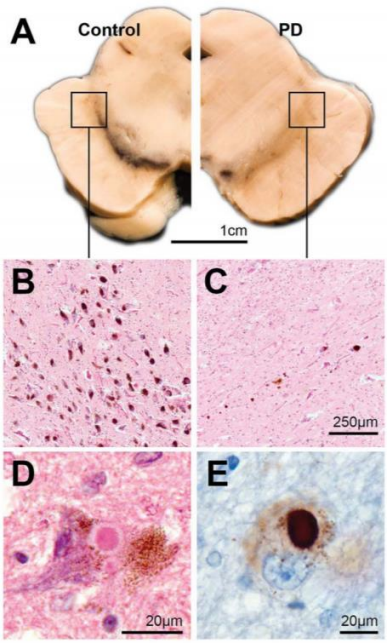

Fig.1.1 The pathological hallmarks of clinical PD. A) Transverse hemisection of the midbrain of a control and a patient with clinical PD, showing the marked reduction in the black pigment within the substantia nigra region. B, C) Haematoxylin and eosin stained sections showing at higher magnification the pigmented neurons of the substantia nigra in a control (B) and a PD patient (C). D, E) Intracytoplasmic LBs in remaining pigmented neuron of the substantia nigra of a subject with clinical PD, showing the eosinophilic core and paler halo in haematoxylin and eosin staining (D) and the dark aggregation of αS using immunoperoxidase with cresyl violet counterstaining (E) (Obeso et al., 2017).

Etiology of PD

As for many neurodegenerative diseases, the etiology of PD is still unknown for most identified cases. PD is a multifactorial disorder, for which several factors (genetics, aging, environment) are thought to play a role in causing the pathology. Concerning the environmental aspect, it has been shown that exposure to certain pesticides (e.g. rotenone, paraquat, maneb), heavy metals (e.g. Fe, Mn, Cu), toxins such as 1-methyl-4-phenyl-1,2,3,6 tetrahydropyridine (MPTP) can lead to PD (Polito et al., 2016). Tobacco, alcohol and coffee consumption are examples of environmental factors negatively correlated with the risk of developing PD (Kalia and Lang, 2015).

As for the genetics, two main forms of PD can be distinguished, the hereditary or familial form, which accounts for about 5-10% of total cases, and the idiopathic or sporadic form for all the others (Lill, 2016). Several gene loci have been linked to the familial form of PD, and first degree family members of affected patients have a 2- to 3-fold increased risk to develop the disease compared to control subjects in the general population (Sveinbjornsdottir et al., 2000; Savica et al., 2016). To date, the mutations present in the αS gene (SNCA) and the LRRK2 gene account for the majority of genetic PD pedigree identified and are responsible for the autosomal-dominant transmission of the disease. In most of these cases, the symptomatology and pathogenesis do not differ from the sporadic form of PD. Autosomal-recessive forms of PD have also been described. The most frequent is associated with mutations in the Parkin gene. The transmission of this form is more rare and differs from the other cases (both genetic or sporadic), including an early onset (before 30-40 years of age). It is interesting to notice that, even in cases of sporadic PD, several PARK-designated polymorphisms (SNCA, UCHL1, LRRK2, PARK 16, GAK) and a few others (MAPT, GBA, NAT2, INOS2A, GAK, HLA-DRA, APOE) have been linked to a higher risk of developing the disease, because of a genetic predisposition. Specifically, the polymorphic length and single-nucleotide polymorphism (SNP) variations in the SNCA gene are known to be the most significant risk factors, followed by the occurrence of the G2385R and R1628P missense SNPs in the LRRK2 gene. In addition to SNCA and LRRK2, which can be both associated to the monogenic disease and a major risk factor, heterozygous β-glucocerebrosidase mutations and tau variants are examples of PD-associated risk factor (Klein and and Westernberger, 2012; Rana et al., 2013; Kalia and Lang, 2015).

PARK locus	Gene	State	Inheritance	Function
PARK1/4	**SNCA**	Confirmed	AD	Protein aggregation; prion-like transmission; synaptic function
PARK2	**PARKIN**	Confirmed	AR	Mitochondrial maintenance; mitophagy; ubiquitin-proteasome
PARK3	Unknown	Putative	AD	Unknown
PARK5	UCH-L1	Putative	AD	Ubiquitin hydrolase
PARK6	**PINK1**	Confirmed	AR	Mitochondrial function; mitophagy
PARK7	**DJ-1**	Confirmed	AR	Mitochondrial function; cell stress response
PARK8	**LRRK2**	Confirmed	AD	Protein and membrane trafficking; neurite structure; lysosomal autophagy; synaptic function
PARK9	**ATP13A2**	Confirmed	AR	Lysosomal autophagy; mitochondrial function
PARK10	Unknown	Confirmed	Risk factor	Unknown
PARK11	GIGYF2	Putative	AD	Tyrosine kinase receptor signalling; insulin-like growth factor pathway
PARK12	Unknown	Confirmed	Risk factor	Unknown
PARK13	HTRA2	Putative	AD	Mitochondrial function
PARK14	PLA2G6	Confirmed	AR	Mitochondrial function
PARK15	FBX07	Confirmed	AR	Mitochondrial maintenance; mitophagy; ubiquitin-proteasome
PARK16	RAB7L1	Confirmed	Risk factor	Protein and membrane trafficking; lysosomal autophagy
PARK17	VPS35	Confirmed	AD	Lysosomal autophagy; endocytosis
PARK18	EIF4G1	Putative	AD	Protein translation
PARK19	DNAJC6	Confirmed	AR	Synaptic function; endocytosis
PARK20	SYNJ1	Confirmed	AR	Synaptic function; endocytosis

Tab.1.2 PARK loci and identified genes linked to familial PD. The five genes underlined in bold account for the monogenic form of the disease. The most characterized point mutations in the SNCA gene are A53T, A30P and E46K. Heterozygous mutations in the LRRK2 gene are responsible for autosomal-dominant PD (Zimprich et al., 2004). Heterozygous loss-of-function mutations in the PARK2 gene are responsible for the autosomal-recessive form, also referred to as juvenile PD because of its early onset (Valente et al., 2004).

Motor circuits in PD

The loss of SNpc neurons in PD patients gradually leads to a severe striatal dopamine (DA) deficiency, which is responsible for the major motor symptoms. For this reason, the main treatment still in use is L-DOPA, a DA precursor which replaces the striatal DA and thus improves motor dysfunction. In healthy subjects, motor cortical areas are involved in the planning and execution of movements. In order to perform smooth and fine motor tasks, motor cortical areas have to communicate with deep brain circuits, among which a pivotal role is played by a group of nuclei called basal ganglia (Mink, 1996). The basal ganglia count several interconnected subcortical nuclei: the striatum (caudate and putamen), the globus pallidus externus, the globus pallidus internus, the substantia nigra (SN), and the subthalamic nucleus. This network differentially connects with motor cortical areas (Obeso et al., 2000). In particular, there are two loops, the direct and indirect pathways, which originate from two different populations of striatal projecting neurons and project to different nuclei. These pathways have opposite effects on movement, meaning that the direct pathway promotes it, whilst the indirect one inhibits it (Kravitz et al., 2013). The crucial role of the nigrostriatal circuit is to exert the dual effect of exciting the direct pathway and inhibiting the indirect one. The SN is made of two distinct structures, the SNpc and the SN pars reticulata (SNpr). The neurons of the SNpc contain neuromelanin and use DA as neurotransmitter. The main recipients of nigral projections are the striatum, the subthalamic nucleus and the globus pallidus. In PD patients, the loss of DA neurons in the SNpc affects only the nigrostriatal circuit and leads to a severe DA denervation of the striatum (Blandini et al., 2000). The loss of nigrostriatal DA neurons leads to bradykinesia or akinesia in PD patiens, since the indirect pathway inhibition of motor cortex overtakes the direct pathway excitation of motor cortex, finally causing a general inhibition of motor cortical regions.

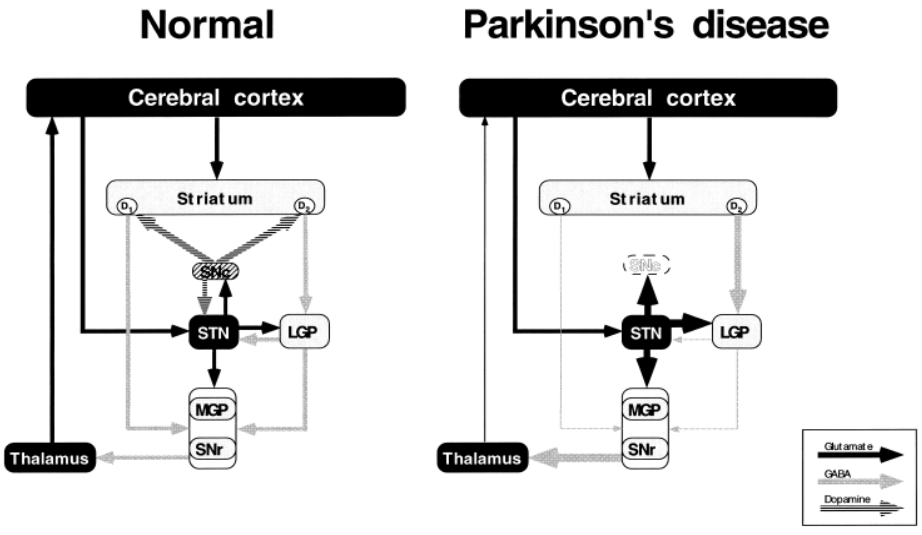

Fig.1.3 Schematic diagram illustrating the changes occurring in the basal ganglia functional organization in PD, compared to normal condition. Relative thickness of arrows indicate the degrees of activation of the transmitter pathways. Medial globus pallidus, MGP; lateral globus pallidus, LGP; substantia nigra pars compacta, SNc; substantia pars reticulate, SNr; subthalamic nucleus, STN (Blandini et al., 2000).

Besides voluntary movements, DA can control higher brain functions such as motivated behaviors and emotional states. While changes in these latter circuits could partially explain certain non motor symptoms in PD, it has been shown recently how neuronal loss is not limited to DA neurons in the SNpc, but it also affects other neuronal populations such as serotoninergic neurons in the raphe and cholinergic neurons in the basal forebrain (Braak et al., 2003a; Bohnen and Albin, 2011). In fact, loss of cholinergic neurons in specific areas has been related to non motor symptoms such as memory loss and cognitive dysfunction, serotoninergic to depression and mood disturbances, and adrenergic to attention dysfunction (Pillon et al., 1989).

Motor and non motor symptoms

PD diagnosis is currently made upon the presence of typical motor symptoms (bradykinesia, rigidity and tremor) caused by death of DA neurons in SNpc. Bradykinesia is the slowness of initiation of voluntary movements with a progressive reduction of speed and amplitude, rigidity is defined as stiffness and increased tone of muscles, and PD tremor is specifically a 4- to 6-Hz rest tremor. All these features usually manifest unilaterally or at least asymmetrically. Recently, postural instability has been removed from initial diagnostic criteria, since it usually appears in patients during the late phases of the disease (Berardelli et al., 2013). As previously mentioned, the symptomatic therapy used for PD patients to date (L-DOPA) focuses on DA replacement strategies. Unfortunately, the progression of the disease and increased doses of L-DOPA lead to the appereance of motor complications, characterized by fluctuations between “on” and “off” periods (respectively presence and absence of motor symptoms control effect) and dyskinesias, defined as involuntary choreiform or dystonic movements. These complications are often worse for patients compared to the original symptoms, and can be accompanied by non motor complications such as psychosis. It is important to underline that already from the first observations by James Parkinson (1755 –1824) more than two centuries ago and by Jean-Martin Charcot (1825-1893) right after him, clinical features of PD patients have always revealed a very complex setting, with a plethora of non motor symptoms which unfortunately did not get the deserving attention in the following decades.

Fig.1.4 Drawing by Jean-Martin Charcot (1887) depicting the typical flexion posture of a PD patient. The French neurologist gave a great contribution to the clinical studies on PD, expanding and refining the early descriptions made by James Parkinson, about half a century before. (Goldman and Goetz, 2007).

The first contemporary account on non motor symptoms occured in fact after the introduction of L-DOPA in the 1960s, when clinicians and scientists started to report that the drug could improve several non motor dysfunctions such as sialorrhea, mood disturbances, constipation and dysuria (Barbeau, 1969; Yahr et al., 1969). Non motor symptoms were finally taken into account, but it took till the 21st century to really appreciate and measure their impact on PD (Martinez-Martin et al., 2011; Erro et al., 2013; Špica et al., 2013; Kalia and Lang, 2015). Overall, the variety of symptoms experienced by PD patients which affects both the central nervous system (CNS) and the peripheral nervous system (PNS) has obviously a deep impact on their quality of life, but probably the most important aspect of non motor dysfunctions is that not only they occur across all motor stages of PD, but some of them are present very early during its prodromal phase. In particular, GI and olfactory dysfunctions (partial or total loss of smell, named hyposmia or anosmia respectively) can arise even decades before the onset of motor abnormalities (Fasano et al., 2015; Schapira et al., 2017), and this is why their analysis can be potentially useful for early diagnosis and therapeutic intervention.

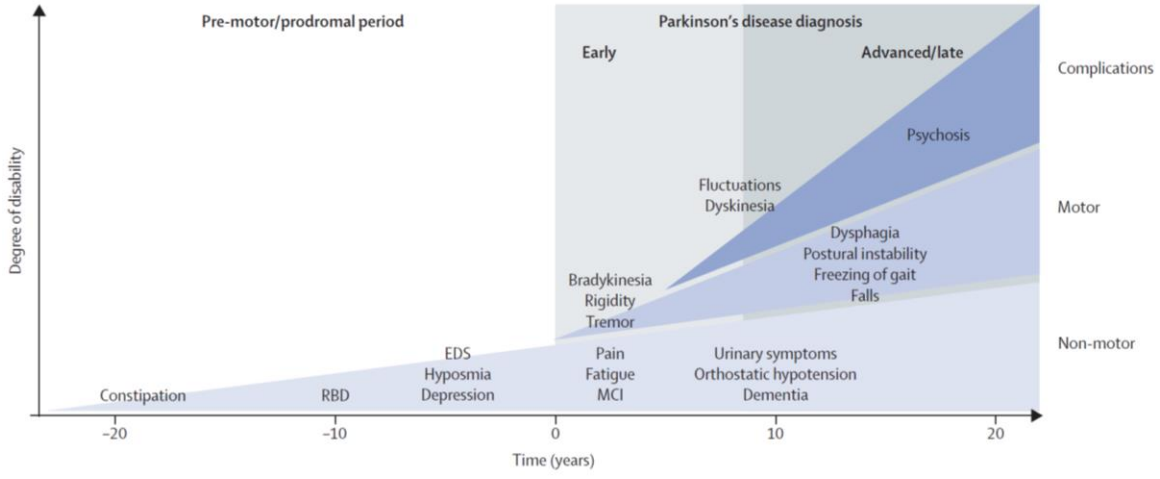

Fig.1.5 Time course progression of PD and related symptoms. Diagnosis of PD (at time 0) is made upon the onset of motor symptoms (tremor, rigidity, bradykinesia), preceded by a prodromal phase of 20 years or

more, characterised by specific non motor dysfunctions. Additional non motor features arise after diagnosis during the progression of the pathology, with a strong impact on the quality of life of patients. Axial motor symptoms, such as postural instability with frequent falls and freezing of gait, are no longer considered for diagnosis, since they tend to appear during the advanced stages. Long-term complications of L-DOPA therapy (fluctuations, dyskinesia, psychosis) contribute to disability of patients. EDS, excessive daytime sleepiness; MCI, mild cognitive impairment; RBD, REM sleep behaviour disorder (Kalia and Lang, 2015).

By affecting up to 80% of PD patients, constipation represents the most frequent GI dysfunction in PD (Cersosimo et al., 2013) and even Parkinson in his famous essay says "the bowels, which had been all along torpid, now in most cases, demand stimulating medicines of very considerable power" referring to constipation in patients suffering of the "shaking palsy". We now know that patients with a previous diagnosis of constipation have an increased risk of developing PD (Stirpe et al., 2016), e.g. less than one bowel movement per day is linked to a 2.7-fold increase in risk (Abbott et al., 2001). A more accurate definition of constipation reports infrequent bowel movements, impairment of propulsive colonic motility, prolonged colonic transit time, reduced rectal contractions and abnormalities in motor activity of the anal sphincter of the patients (Andrews and Storr, 2011). However, to date we still know very little about the relationship between bowel dysfunctions and development of PD, mostly because there is a lack of animal models able to recapitulate such symptoms in a manner translatable to human cases (see hereinafter).

Alpha-synuclein

αS, β-synuclein and γ-synuclein are the three proteins which compose the family of synucleins, discovered by Maroteaux in 1988 (Maroteaux et al., 1988). At first, αS was found to be present in the nucleus (the name etymologically means "with the nucleus") and in the presynaptic terminals of neurons. In 1997, this protein was linked to the autosomal-dominant form of PD, after the missense mutation A53T (a threonine substitution to an alanine at position 53) in the SNCA gene was found in a family pedigree with early onset PD (Polymeropoulos, 1997). Remarkably, the very same year another study showed that αS is the major constituent of LBs and LNs (Spillantini et al., 1997). These two independent findings gave for the first time a strong proof that the SNCA gene, both with mutated and wild-type isoforms, is associated to genetic and sporadic PD and other α-synucleinopathies.

The gene encoding for human αS contains 10 exons and is located in the long arm of chromosome 4 at position 22.1. Besides the A53T mutation, which to date is the most recurrent and better

characterized (Polymeropoulos, 1997), several other missense mutations in the SNCA gene, associated with familial PD and dementia with LBs, have been mapped in the following years, e.g. A30P (Krüger et al., 1998), E46K (Zarranz et al., 2004), H50Q (Appel-Cresswell et al., 2013; Proukakis et al., 2013), G51D (Lesage et al., 2013a) and A53E (Pasanen et al., 2014). In addition, duplication or triplication of the SNCA gene have been related to genetic PD, proving that the pathology can also be caused by only increasing the amount of the wild-type protein (Singleton et al., 2003; Ibáñez et al., 2004). All missense mutations and amplifications of the SNCA gene were associated with a dominant inheritance and an early onset of the disease compared to the sporadic forms. Due to the fact that overexpressing wild-type or mutated αS leads to neurodegeneration in various animal models (Feany and Bender, 2000; Masliah, 2000; Lakso et al., 2003), whereas ablating αS has little or no effect in mice (Abeliovich et al., 2000), αS toxicity has been linked to a gain-of-function mechanism, in which an altered version of the protein ultimately causes neuronal damage.

Physiology of αS

αS is an acidic protein made of 140 amino acids, with a molecular weight of about 14 kDa, mainly expressed in neurons and possibly oligodendrocytes (in very low amount and still under debate) of the CNS (Asi et al., 2014), but also in the PNS, in circulating blood cells and in hematopoietic cells of the bone marrow, under physiological conditions (Nakai et al., 2007; Gardai et al., 2013).

The structure of the protein can be divided in three regions:

1. the N-terminal domain (residues 1-60) is amphipathic and interacts with phospholipids present in membranes and micelles, it also contains the sites for missense point mutations responsible for monogenic familial PD;
2. the non amyloid β-component (NAC) (residues 61-95) is hydrophobic and plays an important role in self-aggregation (El-Agnaf et al., 1998); the name derives from the fact that this fragment of the protein was identified in senile plaques of AD patients although not as abuntant as the Aβ peptide;
3. the C-terminal domain (96-140) is acidic because of a higher proportion of charged residues and represents the main site of post-translational modifications, truncation (Li et al., 2005) and interaction with modulators of the aggregation e.g. metal cations (Binolfi et al., 2006).

The whole protein accounts seven imperfect 11-residues repeats with a conserved hexameric sequence (KTKEGV) predicted to form an amphipathic α-helix: four in the N-terminal region and three in the NAC region (George et al., 1995). This domain seems to serve also as a hidden mitochondrial targeting sequence, potentially linking αS to mitochondrial dysfunctions (Devi et al., 2008).

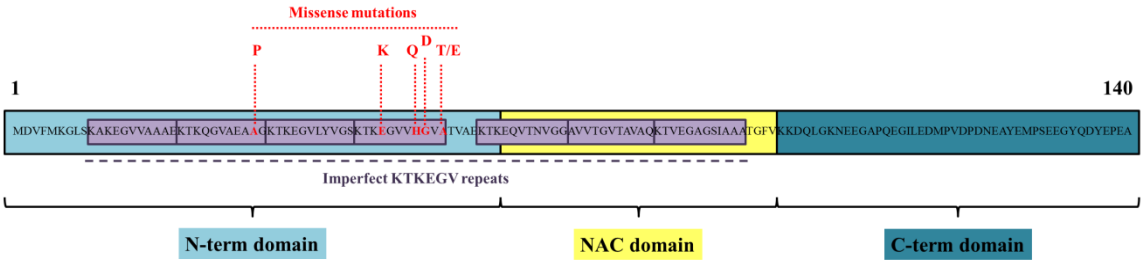

Fig.1.6 αS protein in humans. αS protein is made of 140 amino acids, in which several point mutations (highlighted in red) have been associated with genetic forms of PD (Polymeropoulos et al., 1997; Krüger et al., 1998; Lesage et al., 2013b; Appel-Cresswell et al., 2013; Zarranz et al., 2004). The protein can be divided into three regions: a N-terminal domain (light blue), deputed to membrane binding; the NAC domain (yellow), responsible for fibril formation (El-Agnaf et al., 1998) and a C-terminal domain (blue) relevant for the interaction with other proteins. There are seven imperfect repeats made of 11 residues each (depicted in purple), a highly conserved motif predicted to form an α-helix structure (George et al., 1995), which is located between the N-terminal region and the NAC core. It is interesting to notice that the missense point mutations discovered up to date are all located within the N-terminal region, suggesting that membrane binding may play an important role in the process of αS aggregation (Miraglia et al., 2018).

αS is intrinsically disordered, with an unfolded native conformation, soluble in the cytosol under physiological conditions (Weinreb et al., 1996). In fact, whilst αS from mouse brain purified by gel-filtration elutes as a single peak with a 63 kDa molecular mass, which means close to a folded tetramer, mass spectrometry and circular dichroism analysis detect a monomeric conformation of 17 kDa (slightly larger than expected, probably because of an *in vivo* N-terminal acetylation) (Burré et al., 2013). In line with these recent data, NMR studies show that acetylated αS, which is the main form in physiological conditions, is in fact a disordered monomer that adopts a more compact conformation in solution which prevents further interactions of the NAC domain within the cytosol (Theillet et al., 2016). The unfolded and disordered monomeric conformation of αS was confirmed in rat and human brain and erythrocytes isolated under denaturing and non denaturing conditions, and in bacteria expressing αS, whilst no oligomer species were present (Fauvet et al., 2012) in physiological conditions. On the opposite, another study has shown that αS extracted in non denaturating conditions and upon cross-linking in living cells (e.g. human erythrocytes, cell lines and brain tissue), is mainly a metastable homo-tetramer with a molecular

weight of 58 kDa. The tetramer is in a dynamic equilibrium with the unfolded monomer, which is more prone to aggregation (Bartels et al., 2011). Another independent study suggested a homo-tetramer structure for αS under physiological conditions (Wang et al., 2011) and demonstrated that its subunits are held together by hydrophobic interactions. Following these results, it was suggested that αS tetramer and monomer co-exist in physiological conditions and any perturbation of this state due to higher levels of the monomer is linked to αS aggregation and pathology. Consistently with this view, some missense mutations were shown to reduce the tetramer : monomer ratio and to trigger neurotoxicity (Dettmer et al., 2015a, 2015b). Recently, αS was found to bind synaptic vesicles *in vivo* not as a monomer but in a folded α-helical multimer conformation, larger than an octamer (Burré et al., 2014). This structure has a specific orientation which only happens when the vesicles are docked at the cell membrane.

αS is expressed by several neuronal populations within CNS and PNS, accounting for as much as 1% of total proteins in soluble cytosolic brain fractions, and it has been often shown that it plays a role in general neuronal function. Nevertheless, its precise function still remains elusive, just like for many of the misfolded proteins found in other neurodegenerative diseases. Although αS does not possess a transmembrane domain or a lipid anchor, it interacts stably with synthetic phospholipidic vesicles containing negatively charged head groups, various phospholipid membranes, fatty acids, micelles and with biological membranes (Fortin, 2004). Interestingly, monomeric αS bound to membranes can efficiently prevent lipid oxidation, suggesting another physiological role of the protein (Zhu et al., 2006). Fractionation of healthy brain extracts revealed a portion of αS in association with synaptic vesicles, explained by its preference for membrane with high curvature (Jensen et al., 2011), although as previously said the vast majority of αS behaves as soluble protein (Fortin, 2004). αS is one of the last proteins to localize at presynaptic terminals during development since it is not essential for their formation (Withers et al., 1997). The protein is able to bind membrane vesicles on the cytosolic side but also to reside in the vesicle lumen and be secreted through exocytosis (Lee, 2005). This close association with vesicular structures has led to the hypothesis that αS may regulate vesicular release and/or turnover and other synaptic functions in the CNS. In line with this view, a research group proved that αS knock-out mice exhibit exaggerated levels of DA release following stimulation, suggesting a modulatory role for DA neurotransmission (Abeliovich et al., 2000). Another study showed that αS regulates catecholamines release from the synaptic vesicles and its over-expression inhibits a vesicle priming step that occurs after secretory vesicle trafficking to docking sites but before calcium-dependent vesicle membrane fusion (Larsen et al., 2006). More recently, several studies clarified that αS is a chaperone of the SNARE complex (Burré et al., 2010; Nemani et al., 2010; Diao et al., 2013; Wang et al., 2014). This complex is made of vesicular SNARE proteins (v-SNARE) and target membrane SNARE proteins (t-SNARE), which allow

vesicular fusion to cell membrane after assembly. The assembly process is potentiated by αS through lipid and SNARE interactions.

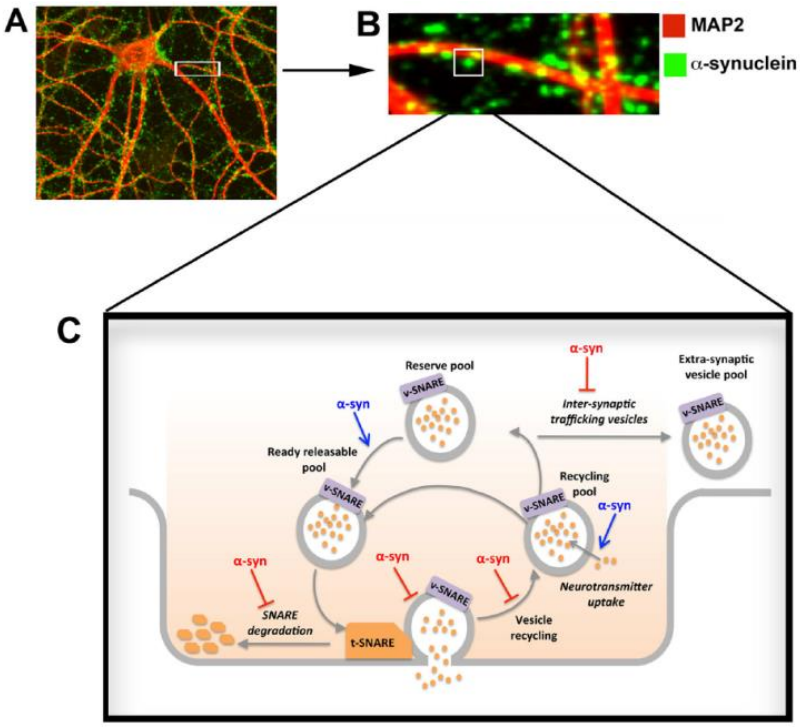

Fig.1.7 Functional properties of αS. A, B) Wide field and magnification of cultured cortical murine neurons, showing dendrites (MAP2 staining in red) and αS-positive presynaptic densities (green), indicating that αS is located in the presynaptic terminals. C) Scheming of αS roles at the presynaptic terminal in the regulation of vesicle trafficking and vesicle refilling (blue), and its interaction with t-SNARE or v-SNARE proteins and neurotransmitter release. αS accumulation induces an impairment of neurotransmitter release, vesicle recycling and trafficking between synaptic buttons and influence t-SNARE complex assembly stability (red), whilst its depletion induces an impairment of vesicle trafficking between the reserve pool and the ready releasable pool and a deficiency in vesicle refilling and neurotransmitter uptake (Lashuel et al., 2013).

Furthermore, αS has been associated to intracellular protein trafficking e.g. vesicle transport from the endoplasmic reticulum (ER) to Golgi (Cooper et al., 2006; Gitler et al., 2008; Thayanidhi et al., 2010; Oaks et al., 2013) and from Golgi to endosomes/lysosomes (Chung et al., 2013; Volpicelli-Daley et al., 2014; Breda et al., 2015; Mazzulli et al., 2016). In line with this, αS was also identified as an inhibitor of phospholipase D2, an enzyme implicated in membrane trafficking and specifically exocytosis (Bendor et al., 2014). Finally, it has been recently reported that αS acts as a molecular dynamase and directly binds to microtubules, thus promoting their assembly and stability, which makes it an active player also for axonal transport (Cartelli et al., 2016).

Pathology of αS

Apart from the debate on αS physiological state, the necessary step for the formation of LBs and LNs or in general insoluble αS inclusions is the transition of the protein to an aggregated β-sheet conformation. In their amyloid state, αS monomers form an antiparallel in-register β-sandwich fold, which in turn stacks into a parallel arrangement forming the so called protofilaments (Vilar et al., 2008; Tuttle et al., 2016). Protofilaments further assemble into mature fibrils. The process of aggregation is nucleation-dependent and occurs in a sequential series of steps, inside of which detours can still happen. Based on *in vitro* experiments we are now able to define a precise time course for this fibrillation process: at first there is a lag phase, in which the monomers convert into an oligomer-type of conformation (nucleation), then there is a growth phase and finally a steady state which terminates with the accumulation of β-sheet amyloid fibrils (Cremades et al., 2012). Oligomers are low molecular weight aggregates, which can be soluble or insoluble, and do not have a fibrillary organization. After the formation of the seeds, αS fibrils grow by the addition of monomers more likely than oligomers (Buell et al., 2014). To date, two different aggregate polymorphs, called fibrils and ribbons, have been described *in vitro* after using different aggregation protocols. Fibrils and ribbons differ biochemically and for seeding properties, and there may be more of these polymorphs still to discover (Bousset et al., 2013; Guo et al., 2013).
The role of αS oligomers and aggregates in PD has been largely studied and is still under debate. The fact that fibrillar αS is found in LBs strongly suggests an involvement of the aggregation process in the pathogenesis of α-synucleinopathies, nevertheless it has also been suggested that αS aggregation might merely represent a by-product of metabolism or even act as a neuroprotective player. In support of this hypothesis is the observation that LBs formation does not always correlate with neurological symptoms (Braak et al., 2003a), or that in some forms of genetic PD αS aggregation is not present (Schneider and Alcalay, 2017). On the other hand, a recent study demonstrated that all the αS types of aggregates (fibrils and ribbons) generated *in vitro* are potentially toxic and can trigger different histopathological phenotypes, supporting the concept of heterogeneity among α-synucleinopathies (Peelaerts et al., 2015). For what concerns αS oligomers, several forms have been described *in vitro*, with different sizes and morphologies, including spherical, annular and tubular structures (Lashuel et al., 2002). Another difference is that some are amorphous and non fibrillar assemblies, while others are described as on-fibrillization pathway. The aggregation process can be affected by many factors, e.g. protein concentration, specific physico-chemical conditions, the presence of certain ligands (including DA) and cross-linking (Buell et al., 2014). Therefore it is still unclear whether the heterogeneity among oligomers has a real physiological relevance or it is due to the protocol used for aggregation and working conditions. Recent studies helped unravel some of these issues, by directly following the oligomerization reaction using single molecule fluorescence techniques.

What they independently demonstrated is that the oligomers pool mainly consists of two different species, type A and type B, which assemble in the early stages of aggregation (Chen et al., 2015; Cremades et al., 2012). These two types of oligomers showed different chemical, structural and toxic properties. Type B oligomers are more resistant to protease K digestion than type A and need a longer lag time for formation, arising the hypothesis that they could derive from the conversion and rearrangement of type A oligomers. Moreover, type B oligomers present a higher amount of β-sheets that are instead negligible in type A (Fusco et al., 2017). *In vivo* experiments showed that type A oligomers could enter the cell and trigger aggregation in it, indirectly causing cell death type, whereas type B oligomers induced death of neuronal cells through the disruption of cellular ion homeostasis and production of reactive oxygen species, which separately caused mitochondrial dysfunction (Danzer et al., 2007; Fusco et al., 2017). Interestingly, Fusco and colleagues explained that both A and B oligomers can bind to biological membranes, but only B oligomers with their rigid β-sheet core are able to get through the lipid bilayer and therefore to directly disrupt the membrane (Fusco et al., 2017). According to this model, type A oligomers convert into more compact protofibrils and fibrils, thus being responsible for seeding formation of new aggregates and αS pathology propagation; type B oligomers are strongly detrimental for directly disrupting biological membranes but are off the pathway of self-propagation. In line with this view, our research group recently demonstrated that αS species associated to microsomes (a membrane fraction including ER, Golgi and synaptic vesicles) had different effects, in terms of seeding properties on intracellular aggregates, when they were isolated from sick αS transgenic mice with respect to adult but presymptomatic littermates, suggesting the presence of at least two different types of αS high molecular weight (HMW) species *in vivo*, corresponding to different stages of αS pathology (Colla et al., 2018). For instance, αS toxic species isolated from diseased mice (likely together with αS aggregates) were able to seed for intracellular inclusions and induce cell death of primary neurons, whilst αS toxic species isolated from presymptomatic mice caused cell death without stimulating endogenous aggregation.

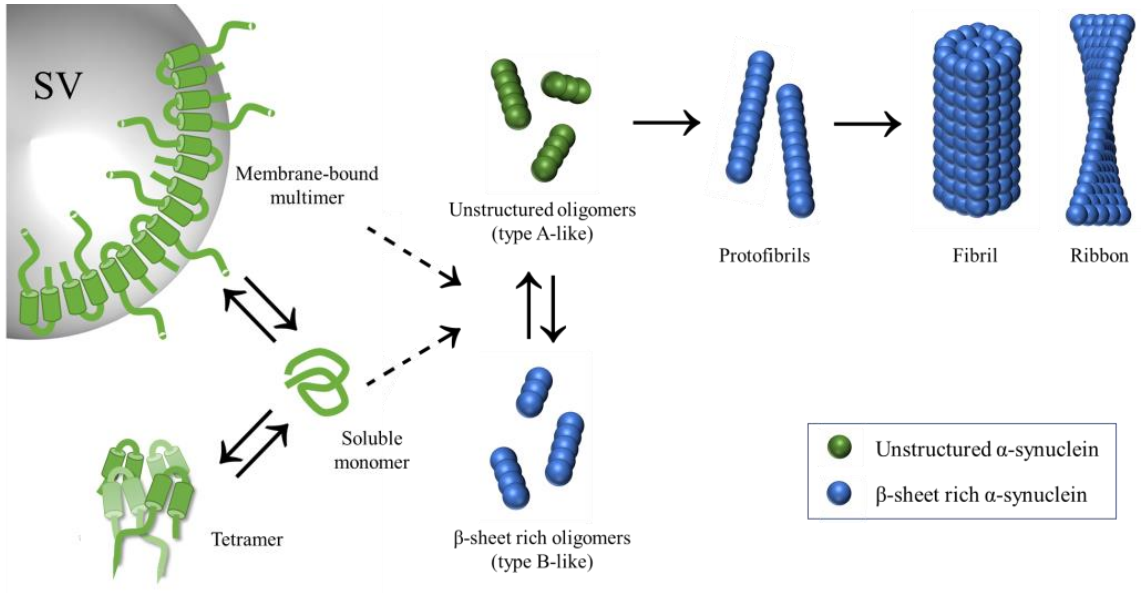

Fig.1.8 αS aggregation process. (Miraglia et al., 2018) In physiological conditions, αS is found as a highly disordered monomeric protein in a dynamic equilibrium with a multimeric conformation when bound to synaptic vesicles, SV (Weinreb et al., 1996; Fauvet et al., 2012; Burré et al., 2010; Burré et al., 2014; Theillet et al., 2016). Other studies proposed that αS in native state is a homo-tetramer and the disruption of this conformation causes the increase of the monomeric form (Bartels et al., 2011; Wang et al., 2011; Dettmer et al., 2015a, 2015b). αS aggregation is a nucleation process in which soluble monomeric αS is converted into insoluble β-sheet rich structures, tightly stacked in a parallel configuration (Lashuel et al., 2002; Vilar et al., 2008; Tuttle et al., 2016). Based on *in vitro* studies, we know that these structures account a heterogeneous pool of intermediate states named oligomers (Cremades et al., 2012; Chen et al., 2015), which generate protofibrils and ultimately aggregates, with a ribbon or a fibril conformation (Bousset et al., 2013; Guo et al., 2013). Both oligomers and aggregates have been described to be toxic, through different mechanisms (Danzer et al., 2007; Peelaerts et al., 2015; Fusco et al., 2017).

Post-translational modifications

αS has been shown to undergo a variety of post-translational modifications, which affect its conversion into oligomers and aggregates in different ways.

- Phosphorylation

Phosphorylation is the most frequent post-translational modification occurring in proteins at serine (S) or tyrosine (Y) residues, in both cases at the level of the hydroxyl group. For what concerns αS S129 is the major phosphorylation site, while three others were identified in the last years at S87, Y125, Y133 and Y136 (Fujiwara et al., 2002; Anderson et al., 2006; Chen et al., 2009; Paleologou et al., 2010). Immunohistochemical and biochemical studies have reported that ~90% of αS found in LBs and LNs is phosphorylated at S129 and the amount of phosphorylated

αS in healthy brains is only 4% of total αS, suggesting that the accumulation of pS129-αS is involved in the formation of LBs and LNs and the neurodegeneration occurring in PD patients (Fujiwara et al., 2002; Zhou et al., 2011). Several kinases were identified for αS. Casein kinases (CK1, CK2), G protein-coupled receptor kinases (GRK1, GRK2, GRK5 and GRK6), calmodulin-dependent kinase (CDK2) and polo-like kinases (PLK2, PLK3) are all possible candidates for phosphorylation at S129. The effects of this specific modification on αS propensity to aggregate are controversial depending on the specific kinase used for the study. E.g. the phosphorylation at S129 by CK2 and GRK6 causes increased oligomerization, fibrillation and neurodegeneration (Fujiwara et al., 2002; Sato et al., 2011), whilst phosphorylation at S129 by CK1 inhibits αS fibrillation (Paleologou et al., 2008). Specifically, S129 undergoes phosphorylation by CK1 in the fibrillary state, which means that this modification occurs after αS fibrillation and/or during the development and maturation of LBs and LNs (Paleologou et al., 2008).

- Ubiquitination

Ubiquitination is a fundamental biochemical process which regulates a variety of aspects for protein function, e.g. degradation, protein-protein interaction and subcellular localization. αS contains 15 lysine (K) residues and 9 of them were shown to undergo ubiquitination: K6, K10, K12, K21, K23, K32, K34, K45 and K96 (Sampathu et al., 2003; Tofaris et al., 2003; Nonaka et al., 2005; Rott et al., 2014). Ubiquitination of αS leads to changes in its activity, affecting its localization and degradation processes. Ubiquitination of aggregated or filamentous proteins has been implicated in the pathogenesis of many neurodegenerative disorders. Specifically, ubiquitin-positivity was shown for nuclear inclusion bodies made of expanded polyglutamine repeats in many polyglutamine diseases, for neurofibrillary tangles composed of hyperphosphorylated tau in Alzheimer's disease, for LBs and LNs containing hyperphosphorylated αS in α-synucleinopathies (Nonaka et al., 2005). Moreover, genetic studies have proved that dysfunctional proteins belonging to the ubiquitin-proteasome pathway are responsible for neurodegeneration. The ubiquitination modulated by SIAH-2, an E3 ubiquitin-ligase which mono and di-ubiquitinate αS *in vivo*, is similar to the endogenous ubiquitination pattern observed in biochemically purified LBs and involves K12, K21 and K23 residues. Under conditions of proteasomal impairment, SIAH-1, another E3 ubiquitin-ligase, promotes αS aggregation and apoptotic cell death (Rott et al., 2008; Beyer and Ariza, 2013).

- Nitration and oxidation

Cellular oxidative damage occurs when the production of reactive oxygen species overcomes the compensatory antioxidant capacity of the cell itself. A common consequence of increased oxidative stress is the nitration of tyrosine residues caused by peroxynitrite, a reaction product generated after combining oxygen and nitric oxide. αS contains four tyrosines (Y39, Y125, Y133

and Y136) which can all undergo nitration (Duda et al., 2000; Giasson et al., 2000; Burai et al., 2015) and four methionines (M1, M5, M116 and M127) which can all be subjected to oxidation under conditions of oxidative stress (Beyer and Ariza, 2013; Barrett and Timothy Greenamyre, 2015). It has been claimed that the abnormal levels of oxidative stress occurring in DA neurons are a major cause for PD progression. LBs are found enriched of nitrated αS and when this is administrated to the SNpc of rats, it leads to a strong reduction in DA neurons number (Yu et al., 2010). It has been suggested that the susceptibility of this neuronal type to αS pathology may be due to the fact that αS oxidation causes the accumulation of DA-αS toxic adducts. Furthemore, when nitrated αS is administred to cultured cells, it causes apoptosis in a dose-dependent manner through the formation of nitrated αS oligomers (Liu et al., 2011).

- Truncation

Different studies have reported a variety of specific sites for αS truncation (E110, D115, D119, P120, E130, Y133 and D135), all of which are found in the C-terminal region of the protein (Li et al., 2005; Liu et al., 2005; Lewis et al., 2010), although N-terminal truncation can also happen. The three main truncated fragments identified *in vivo* are referred to as Syn12, Syn10, Syn8. Syn12 and 10 are generated after truncation at P120 and E110 residues respectively, whilst Syn8 is the result of a double truncation at N- and C-terminal and is a fragment of about 80 aminoacids. Syn12 and 10 are present in both detergent soluble and insoluble fractions from mouse and human brains, whereas Syn8 is only present in the insoluble fraction and is specific for diseased brains. Furthermore, it has been shown that the accumulation of Syn12 and 10 occurs independently from of αS aggregation, while Syn8 needs the aggregation of αS in order to accumulate. αS truncation can be mediated by more than one proteolytic system, including 20S proteasome, Calpain I, Cathepsin D, Neurosin and Matrix Metalloprotease 3 (Li et al., 2005; Beyer and Ariza, 2013). The truncated forms Syn12 and 10 are known to be generated also under physiological conditions, nevertheless the amount of truncated αS strongly increases in case of genetic PD. Moreover, these truncated species preferentially accumulate in αS aggregates, especially the ones not associated with membranes (Colla et al., 2018), and have the ability to enhance fibril formation from full length αS (Li et al., 2005).

- Other modifications

Other post-translational modifications have been negatively correlated to αS pathology, meaning that they inhibit its propensity to aggregate. For this reason, studying these modifications can be useful for finding protective pathways for α-synucleinopathies and also for better understanding the modulators of αS physiological role. Lysine acetylation is a post-translational modification involved in several physiological functions. For what concerns αS, four residues have been shown to undergo acetylation (K6, K34, K45 and K97) (Lundby et al., 2012). N-terminal acetylation is a

very common modification of mammalian αS which stabilizes its native structure, thus inhibiting aggregation (Bartels et al., 2014).

Another modification which has been associated to PD and affects αS conformation is the transglutaminase-induced cross-linking. Transglutaminases are enzymes which catalyze the formation of an isodipeptide by linking one glutamine to one lysine. When these residues are on the same protein, like for αS, the effect is an intramolecular cross-linking, which leads to the formation of a more compact monomer. The consequence of this compact conformation is the inhibition of oligomerization, fibrillization and membrane binding of αS *in vitro*. Specifically, Schmid and colleagues have shown that the major transglutaminases substrates in αS sequence are the glutamine residues Q79 and Q109 which can cross-link to various lysine residues in the N-terminal region, and up to three intramolecular cross-links can occur on a single monomer (Schmid et al., 2009).

Sumoylation is a post-translational modification which consists in the attachment of small ubiquitin-related modifier (SUMO) and can affect a variety of cellular mechanisms. Sumoylation was recently suggested to be a solubility promoter of aggregation-prone proteins. αS has been reported to be sumoylated at two sites (K96 and K102) upon overexpression and whilst unmodified αS can form fibrils, sumoylated αS remains soluble. Moreover, the presence of as little as 10% sumoylated protein was shown to be enough to delay the aggregation process *in vitro* (Krumova et al., 2011). Another study demonstrated that SUMO binding regulates sorting of proteins (including αS) in extracellular vesicles, revealing another putative function of sumoylation as a ubiquitin-independent sorting signal (Kunadt et al., 2015).

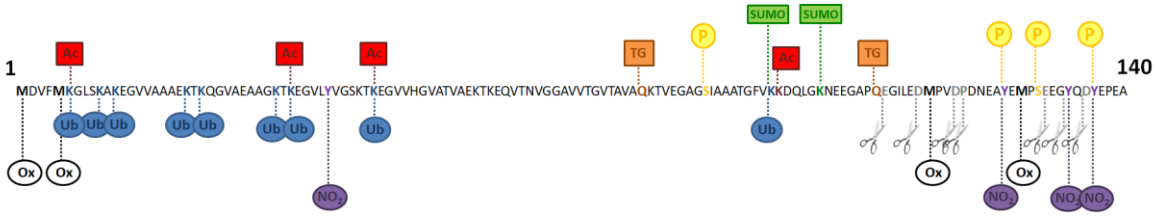

Fig.1.9 Post-translational modifications of αS. The complete 140 aminoacids sequence of αS is depicted and the sites where the modifications occur are highlighted. P in yellow for phosphorylation, Ub in blue for ubiquitination, NO_2 in purple for nitration, Ox in white for oxidation, the scissors in grey for truncation, Ac in red for acetylation, TG in orange for transglutaminase cross-linking, SUMO in green for sumoylation. Specifically, the group of post-translational modifications represented in circles are known to promote αS aggregation, whilst the ones in rectangles have been described to inhibit αS aggregation.

αS mechanisms of toxicity

As mentioned before, ubiquitination is a modification involved in many regulatory functions fundamental for cellular survival, among which protein degradation. Specifically, protein degradation mechanisms within the cell mainly consists in the ubiquitin-proteasome system and the autophagic-lysosomal pathway. For what concerns αS, the former is responsible for the degradation of oligomers, the latter for the degradation of aggregates (Tetzlaff et al., 2008). When the aggregation process driven by αS overexpression occurs, both systems can become dysfunctional. In fact, different *in vitro* studies showed the inhibition of proteasomal function (Petrucelli et al., 2002), impairment of chaperone-mediated autophagy (Yang et al., 2009; Song et al., 2014) and macroautophagy (Winslow et al., 2010) caused by αS overexpression.

As previously explained, αS binds to lipid membranes in both physiological and pathological conditions. While cytosolic and membrane bound states are both physiologically relevant, it is unclear how their localization affects αS pathology and where aggregation initiates. A variety of studies has shown that membrane binding and lipid interaction can stimulate but also inhibit αS fibrillation (Narayanan and Scarlata, 2001; Lee et al., 2002a; Jo et al., 2004; Burré et al., 2015; Galvagnion et al., 2016). In line with this controversy it has been observed that SNCA point mutations associated with familial PD are located in the N-terminal lipid binding domain, suggesting that lipid binding may be related to αS acquired toxicity. This happens for some point mutations such as A30P, in which membrane binding is reduced and aggregation is increased, but not for others. For instance, A53T, E46K and H50Q mutations cause a higher fibril formation without affecting lipid binding (Bussell and Eliezer, 2004; Fredenburg et al., 2007; Khalaf et al., 2014); others such as G51D inhibit both membrane binding and aggregation (Fares et al., 2014). Thus, lipid binding and αS aggregation not always correlate directly, but other factors can influence the propensity of the protein toward fibrillation and compensate for aminoacid substitutions, such as intramolecular interaction between the N- and C-terminal or protein binding to the C-terminal (Ulrih et al., 2008; Burré et al., 2010). Moreover, the aforementioned αS post-translational modifications induced by oxidative stress have been shown to increase oligomerization and possibly to influence αS ability to bind vesicle membranes as a monomer or in an oligomer conformation (Binolfi et al., 2006; Xiang et al., 2013; Follmer et al., 2015; Plotegher et al., 2017). In this complex situation, it is clear that interaction with biological membranes leads to modifications not only for αS conformation, but also for the physical properties of the membranes. For instance, it induces changes in melting temperature (Galvagnion et al., 2016) and membrane remodelling (Jiang et al., 2013) such as lateral expansion of membrane lipids and lipid packing modifications (Ouberai et al., 2013). Membranes of specific organelles such as ER, mitochondria, Golgi and synaptic vesicles have been shown to be associated at different extent with αS. After focusing on the physiological aspects, we will now

consider the pathological mechanisms of αS deriving from these subcellular associations.

- ER and Golgi

αS has been found associated with ER and Golgi in mice and human cell cultures. Specifically, microsomes-associated αS was proved to be partially protected from protease K digestion and thus connected with the lumenal side of the microsomes (Colla et al., 2012a). Although no lipid binding involvement has been described yet, αS was found to bind, in αS Tg mice and human cell lines overexpressing αS, to gpr78/BIP, a chaperone bound to the luminal side of the ER, transiently associated with the ER translocon import pore and directly implicated as a sensor of protein misfolding and initiator of the unfolded protein response (Bellucci et al., 2011; Colla et al., 2012b). Additionally, the overexpression of αS impaired the ER-Golgi vesicular trafficking in yeast and other organisms (Cooper et al., 2006), leading to the accumulation of ER proteins with induction of ER stress, Golgi fragmentation and depletion of lysosomal enzymes (Oaks et al., 2013; Mazzulli et al., 2016). Interestingly, this detrimental effect was rescued by overexpressing proteins implicated in vesicle transit from the ER to the cell membrane such as Rab1 (ER-Golgi), Rab8 (Golgi) and Rab3A (post-Golgi) (Gitler et al., 2008) but also from endolysosomal pathway such as Rab-11A (endosomal recycling) (Breda et al., 2015). Another study showed that αS oligomers *in vitro* decrease axonal transport and influence microtubule stability (Prots et al., 2013). These observations have strong implications for a major role of αS in vesicle trafficking and recycling, outside the synapses.

- Mitochondria

Other studies showed that αS can bind the outer and inner membrane of mitochondria (Devi et al., 2008; Nakamura et al., 2008). Since these data were obtained from *in vivo* observations, it is not clear whether the binding depended on lipids, in line with αS preference for cardiolipin, abundant in the mitochondrial membranes, or it was mediated by specific proteins. Interestingly, a translocase of the mitochondrial outer membrane has been described as responsible for the import of αS into the mitochondria and one of its subunits, TOM20, has been shown to bind αS *in vivo* (Di Maio et al., 2016). Additionally, the overexpression of αS was found to promote mitochondrial dysfunction in αS Tg mice (Martin et al., 2006, 2014) and mitochondrial fragmentation in primary neurons. This latter effect was related to the direct interaction of αS with mitochondria, since disruption of αS N-terminal membrane binding domain restored the morphology of the organelles (Nakamura et al., 2011). Particularly toxic to mitochondria are αS oligomers, associated to the inhibition of complex I with subsequent increase of reactive oxygen species and oxidative stress (Cremades et al., 2012; Devi et al., 2008), to the alteration of membrane potential and Ca^{2+} homeostasis, to mitochondrial fragmentation (Nakamura et al., 2011), to mitochondrial protein import impairment (Di Maio et al., 2016), to the externalization of

cardiolipin toward the outer mitochondrial membrane resulting in mitophagy for cellular stress (Ryan et al., 2018).

- Synaptic vesicles

As explained before, αS binds vesicles at the synapse and acts as a molecular chaperone to promote SNARE complex assembly (Burré et al., 2010), which is necessary to regulate docking and neurotransmitter release and reuptake. Following αS overexpression, the SNARE assembly is blocked and the whole process is impaired (Majd et al., 2015).
Other studies based on exogenous administration of large oligomers of recombinant αS at the synapse, showed that αS bound to synaptic vesicles through synaptobrevin-2, leading to inhibition of vesicle docking to the membrane (Choi et al., 2013) and to lower synapsins abundance (Larson et al., 2017). Although direct measurement of ER-Golgi traffic was not assessed in these conditions, it is plausible that accumulation of toxic species of αS might affect the whole protein transport system from the ER to the membrane. Moreover, electrophysiology studies showed that αS oligomers impaired long-term potentiation (Diogenes et al., 2012; Martin et al., 2012) and reduced neuronal excitability (Kaufmann et al., 2016).

Overall it is not clear where αS detrimental effects begin, although it is plausible to hypothesize that the initial pathogenic transition of αS toward a toxic conformation may occur in proximity of the membranes of the subcellular locations described above and then spread to other sites within the neuron.

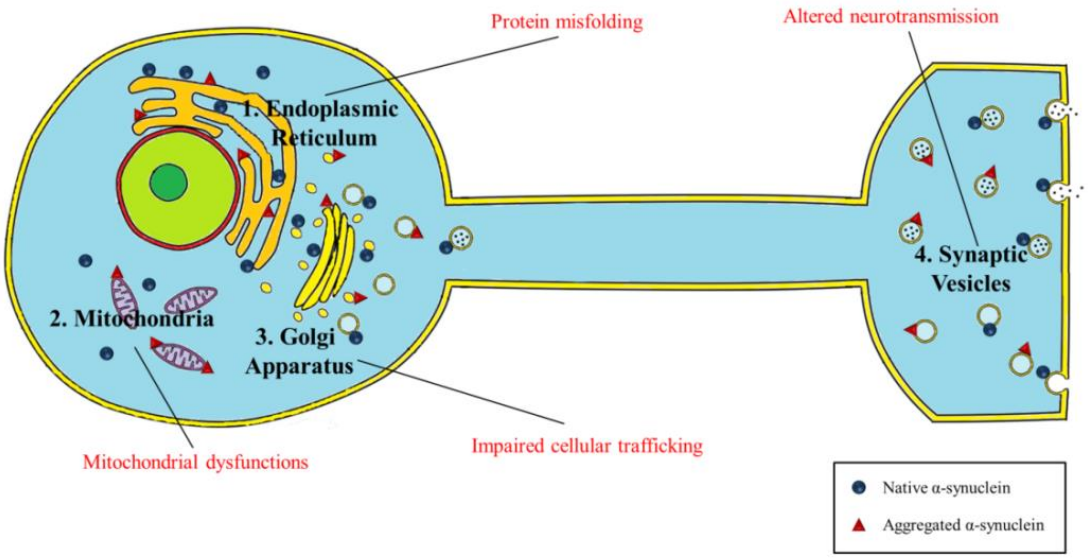

Fig.1.10 Subcellular localization of αS oligomers and aggregates in physiological and pathological conditions. αS capability of binding membranes has been correlated to part of its physiological roles and specifically several studies have shown how this protein can bind to synaptic vesicles, ER/Golgi and mitochondria (Devi et al., 2008; Nakamura et al., 2008; Burré et al., 2010; Colla et al., 2012a). Up to date it is still under debate whether αS association with membranes contrasts or promotes its aggregation, nevertheless it is clear that the accumulation of αS toxic species at these specific subcellular sites leads to precise cellular dysfunctions involving neurotransmission, protein trafficking and mitochondrial respiration (Miraglia et al., 2018).

Lewy pathology in the periphery and Braak model

A turning point for the debated link between PD and GI symptoms occurred in 2003. The finding that LBs and LNs present in the brains of patients (Spillantini et al., 1997) were also present in specific districts of the PNS and specifically in the ENS in PD patients as well as in healthy individuals (Braak et al., 2003a), led to the development of the Braak model. Braak and colleagues suggested that Lewy pathology in PD patients develops following a stereotypic temporal pattern, with a caudo-rostral progression over time. According to this model, the neuropathology can be divided into six stages, accounting both presymptomatic and symptomatic phases (Braak et al., 2003a, 2003b). At the beginning (stage 1), LBs and LNs appear in two sites: the ENS, linked to the dorsal motor nucleus of the vagus nerve (dmX) and the olfactory bulb, in the anterior olfactory nucleus. At stage 2 the pathology is diffused within the medulla (in the gigantocellular reticular nucleus) and the pons (in the lower raphe nuclei and the locus coeruleus). These three nuclei together form the gain setting system, which receives major inputs from components of the limbic and motor systems, such as the central subnucleus of the amygdala.

This system can control the incoming pain signals during stress and ensures that motor neurons are ready for action. The descending fibers of the gain setting system form a sensory control network for both somato and visceromotor efferents, enabling the body for momentary demands. During stage 3, Lewy pathology spreads caudo-rostrally from the brainstem to the mesencephalic tegmentum and basal regions of the prosencephalon. A process of neuronal cell death starts in the central subnucleus of the amygdala and the magnocellular cholinergic nuclei of the basal forebrain. In fact, the central subnucleus of the amygdala projects to the gain setting system and the dmX, and in turn it receives projections from the amygdalar basolateral complex, which receives strong inputs from the magnocellular nuclei of the basal forebrain. Only at stage 4 the patients begin to experience motor dysfunctions, entering the so called symptomatic phase. The pathology hits the SNpc and the temporal mesocortex, which projects all signals from the neocortex to the centers of the limbic circuit (amygdala, hippocampal formation, entohirnal region) and prefrontal cortex. Among the cortical sites, the temporal mesocortex is the most affected in PD. Ultimately (stages 5 and 6) Lewy pathology reaches the neocortex (in the high-order sensory association and prefrontal areas) and the patients develop more severe motor symptoms, together with cognitive dysfunctions. The first order sensory association areas, premotor fields and finally the primary sensory and motor fields become affected.

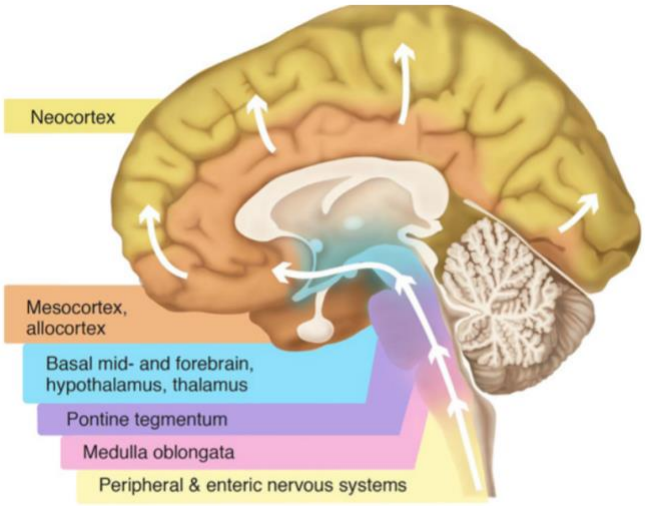

Fig.1.11 Staging of αS pathology in PD according to the Braak model. As summarized in the scheming, Braak and colleagues proposed that the pathological process of αS in PD starts in the PNS and specifically the ENS, gaining access to the CNS through the dmX in the lower brainstem. From here, the pathology spreads upwards through vulnerable regions of the medulla oblongata, pontine tegmentum, midbrain and forebrain, and ultimately reaches the cerebral cortex (Braak et al., 2003a, 2003b; Visanji et al., 2013).

Along with this staging model, Braak and colleagues speculated on the origin of the pathology in the first place, arising the so called dual-hit theory. Based on the location of the first appearances of LBs and LNs, the ENS and the olfactory bulbs, they suggested that idiotpatic PD may start with an infiltration of a neurotropic pathogen at these two sites (hence dual-hit). More precisely, according to this theory, the pathogen would enter the human body through the olfactory pathway, in the respiratory system, and through the gut pathway, by swallowing the saliva containing nasal secretions. The already described olfactory and GI symptoms, which occur very early during the prodromal phase of PD, stand in support of this theory. As previously mentioned, the nasal route is used to explain the early involvement of olfactory structures, although Braak and colleagues do not think this is the starting point for αS pathological spreading within the CNS. In fact, Lewy pathology appears in the anterior olfactory nucleus and olfactory bulb at first and subsequently closely related olfactory areas, but the lesions do not advance further into non olfactory cortical areas. Rather, all patients analyzed show neocortical involvement only after the appearance of lesions in the anteromedial temporal mesocortex. A prerequisite for neocortical affection appears to be that the subcortical lesions have expanded to such an extent that they include the magnocellular nuclei of the basal forebrain. Therefore, the leading predilection sites of the pathological process are located in the lower brainstem. They suggest that the GI tract is the site of departure for the Lewy pathology, where the pathogen is thought to cross the mucosal and epithelial barriers, thus reaching the neuronal structures. The nature of this pathogen is still debated, it has been speculated that it could be a neurotropic virus capable of infecting specific vulnerable neurons, or αS itself (misfolded or fragmented) through a prion-like mechanism (Braak et al., 2003b).

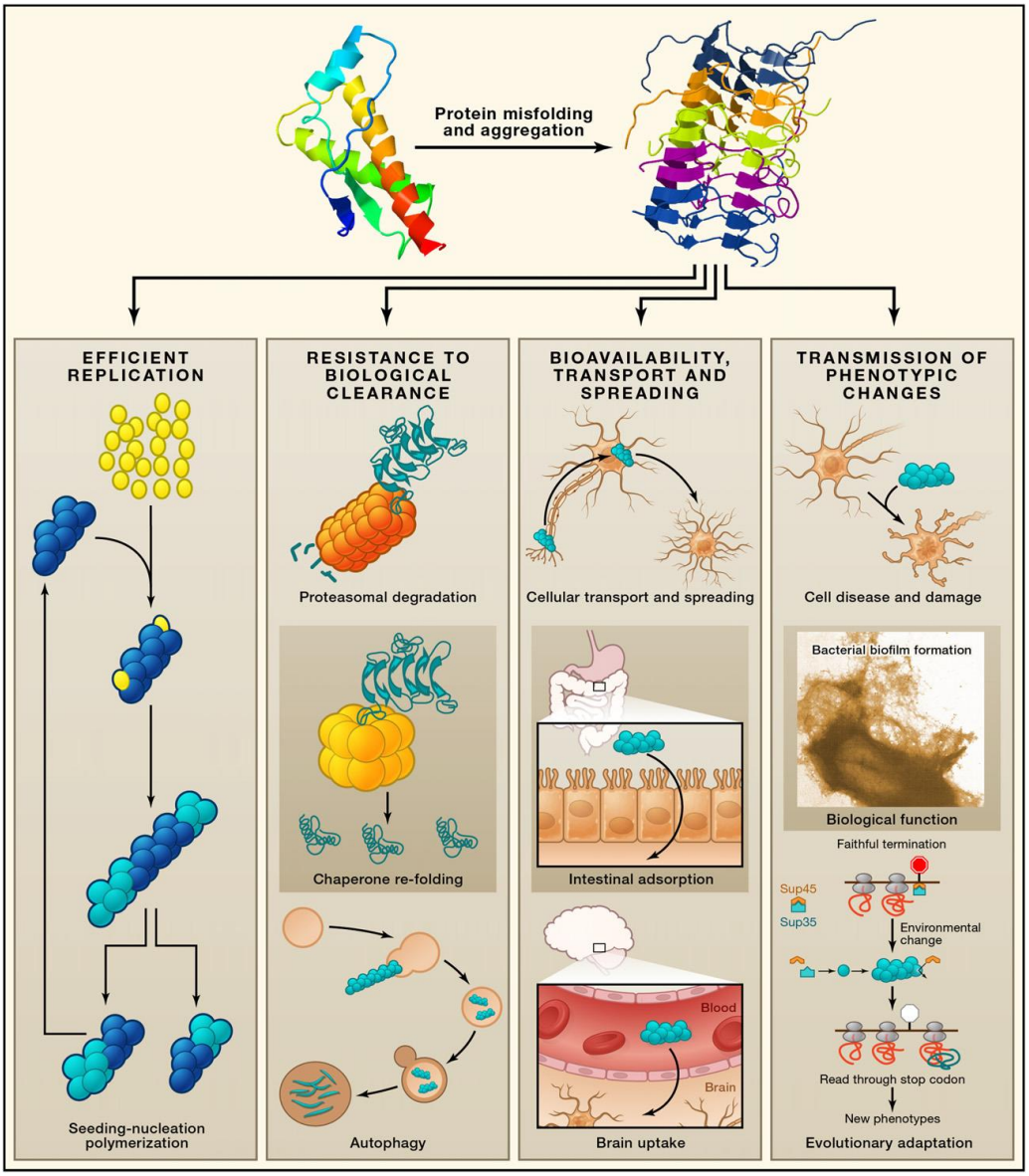

Fig.1.12 Properties required for misfolded proteins to be transmissible. Efficient replication, which occurs thanks to the seeding-nucleation process. Resistance to biological clearance, e.g. proteasomal degradation, chaperone refolding, autophagy. Biovailability (ability to reach the target tissue and cellular location) through cellular transport and spreading, and penetration across the enteric and blood-brain barriers. Transmission of phenotypic changes, where for disease-associated misfolded proteins the changes are cellular damage, tissue dysfunction, and clinical disease; for functional transmissible proteins, the phenotypic change is the modulation of a biological activity or acquisition of a new function (Soto, 2012).

After Braak, different studies have corroborated his hypothesis, by finding LBs and LNs in several districts along the ENS (Lebouvier et al., 2008; Beach et al., 2010; Gelpi et al., 2014). In the meantime, several research groups have implicated αS neuronal transmission and propagation within the nervous system as a mechanism of detrimental spreading of PD pathology, showing

that neuron-to-neuron transfer of pathogenic αS occurs both *in vitro* (Luk et al., 2009; Volpicelli-daley et al., 2012; Colla et al., 2018) and *in vivo*, in human (Kordower et al., 2008a, 2008b) and animal studies (Kordower et al., 2012; Luk et al., 2012; Masuda-Suzukake et al., 2013; Rey et al., 2013; Holmqvist et al., 2014; Recasens et al., 2014; Sacino et al., 2014; Peelaerts et al., 2015), supporting the hypothesis that the accumulation of toxic αS species may originate outside the CNS and later move to the brain using anatomical connections (Braak et al., 2003b; Hawkes et al., 2009). In PD patients, pathological αS has been found in enteric neurons of both submucosal and myenteric plexi along the entire GI tract including the colon (Böttner et al., 2012; Gelpi et al., 2014). Another study found a rostro-caudal gradient of accumulation of pS129-αS within the ENS with a higher incidence of LBs in the lower esophagus and submandibular gland and to a less extent in the colon and rectum (Beach et al., 2010). Although this observation has to be confirmed in a larger population, the involvement of the vagal nerve, which innervates directly the stomach, the small intestine and the ascending colon, as the main dissemination route of toxic αS along the gut-brain axis, has been suggested, based also on the finding of LBs presence in the dmX in prodromal PD (Braak et al., 2003a). However, the high incidence of aggregated αS in the all segments of the spinal cord suggests that other nerves might be implicated in αS propagation (Böttner et al., 2012). Several studies have indicated LBs presence in human colon biopsies as a possible diagnosis method for preclinical PD (Lebouvier et al., 2008; Pouclet et al., 2012; Shannon et al., 2012), although other observations are against this hypothesis (Böttner et al., 2012; Visanji et al., 2015). Overall, detecting pathological αS in the gut as a potential biomarker for PD patients is still challenged by the heterogeneity of antibodies, antigen retrieval methods and GI sites analysed, therefore the discrepancy among these studies should be interpreted cautiously. This is only one example that easly explains why for a great number of human pathologies and in particular neurodegenerative diseases, animal studies are always needed to be carried out, in parallel to clinical studies. Unfortunately, whether there is a direct pathogenic correlation between GI dysfunction and PD or not, to date still remains an open issue, caused in part by the absence of appropriate animal models that recapitulate the chronic and progressive development of PD pathological stages. All the αS Tg mouse lines analyzed for constipation so far showed GI deficit only concurrent with CNS neuropathology (Wang et al., 2008; Kuo et al., 2010; Hallet et al., 2012), while when considering the pharmacologically induced PD models only a small study, based on chronic injections of rotenone at low dosage in rats, showed mild GI abnormalities in absence of CNS αS pathology. Nevertheless, because of the low amount of rotenone used for this purpose, brain pathology and motor symptoms never occurred in these mice (Drolet et al., 2009).

The enteric nervous system

The gut is an extremely complex system responsible for a variety of functions related primarly but not only to digestion, such as absorption, secretion, motility, mucosal maintenance and immunological defense. All these functions require a fine degree of regulation and coordination, provided by the ENS. The ENS is, within the PNS, one of three divisions of the autonomic nervous system, named sympathetic, parasympathetic and enteric (Rao and Gershon, 2016).

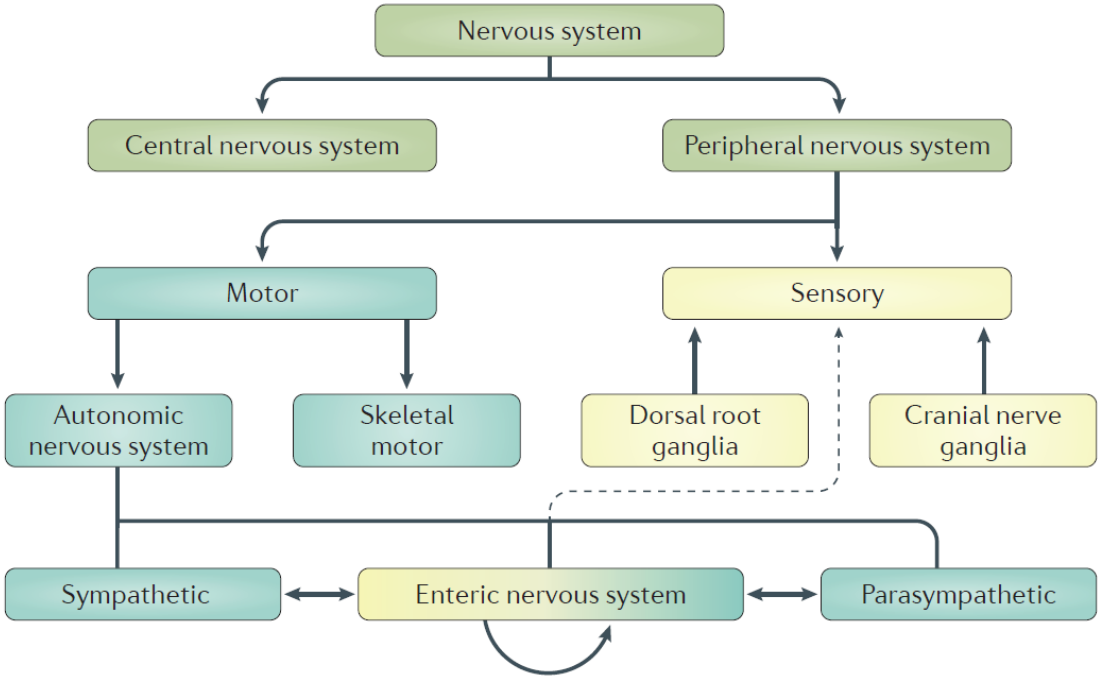

Fig.1.13 Organization of the PNS and the ENS. The nervous system is divided in CNS and PNS (green). Afferent information from the periphery to the CNS is conveyed by neurons located in dorsal root or cranial nerve ganglia, which constitute the sensory division of the PNS (yellow). These inputs integrated by the CNS leads to outputs through the motor division of the PNS (blue). Efferent projections from the CNS target either skeletal muscles or the autonomic nervous system, which is further divided into sympathetic, parasympathetic and enteric. Unlike neurons in sympathetic or parasympathetic ganglia, the majority of enteric neurons do not receive direct innervation from the CNS. In fact, the ENS contains primary afferent neurons able to respond intrinsically to local stimuli, thus integrating information and coordinating motor output independently from the CNS. This gives to the ENS unique sensory and motor properties, although there is still a bidirectional cross-talk between gut and CNS (Rao and Gershon, 2016).

The ENS is responsible for the innervation of the whole digestive tube, from the esophagus to the rectum, and is organized into two plexi. The myenteric plexus (or Auerbach's plexus) is the main player for GI motility, in fact it lies between the longitudinal and circular smooth muscle layers to which it provides motor innervation, with both parasympathetic and sympathetic inputs. The submucosal plexus (or Meissner's plexus) is located in the dense connective tissue of the submucosa just underneath the mucosa, it has only parasympathetic fibers and is the main responsible for GI secrection and absorbtion.

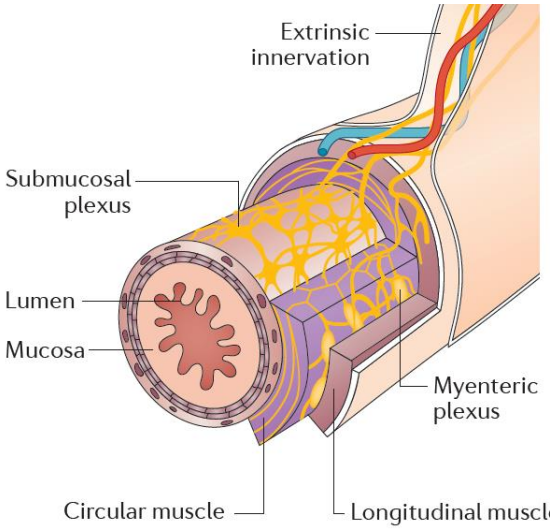

Fig.1.14 The ENS architecture through the gut layers. Schematic view of the intestine illustrating the organization of the ENS and its location within the enteric wall. The myenteric plexus is located between the longitudinal and circular smooth muscle layers, whilst the submucosal plexus is located in the submucosa, underneath the mucosa. There are not nerve fibers entering the lumen or its epithelial lining. The extrinsic innervation reaches the gut through the mesentery together with the vascular system (Rao and Gershon, 2016).

In humans, the ENS accounts more than 100 million neurons, more than the other peripheral ganglia altogether, and at least as many as the spinal cord. Interestingly, with this size the ENS dwarfs the number of efferent vagal fibers projecting to almost all the digestive tract, from the esophagus to the proximal colon. It is important to mention that in addition to the vagus nerve, the splanchnic, mesenteric and pelvic spinal nerves are deputate to the innervation of the abdominal viscera (Furness, 2006; Forsythe et al., 2014). Unlike the rest of the PNS, the enteric division is capable of integrating neuronal activity, that is combining a variety of inputs into coherent behavioural outputs and regulating GI functions independently from CNS inputs. In fact the ENS is organized in microcircuits, with interneurons and intrinsic primary afferent neurons, capable of initiating reflexes (Furness et al., 2014). A great neuronal phenotypic diversity is not prerogative of the CNS, since most of the neurotransmitters active at the central level are also present in the ENS, with few differences (Furness, 2000; Furness et al., 2014). For what concerns peristalsis, the motor activity of the bowel is mainly regulated by the cholinergic and tachykinergic systems for contraction, and by the nitrergic system for relaxation (Mang et al., 2002; Bornstein et al., 2004). Notably, DA contribution to intestinal function in the lower digestive tract is negligible and the presence of DA neurons at this level is highly debated (Bornstein et al., 2004).

Although the ENS is capable of working regardless central inputs, normally the CNS influences GI behaviour, and the gut in turn sends information to the brain. More precisely, 90% of vagal fibers connecting the gut to the brain are afferent, suggesting that the CNS plays more the role of receiver rather than transmitter in this cross-talk. For example, gut-to-brain signalling carries sensations such as nausea, bloating and satiety, although much of this information has a homeostatic nature and does not reach consciousness. Actions such as mastication and swallowing are CNS-dependent instead, and efferent signals brain-to-gut are important for gastric motility control. On the other hand, the movements of the small and large intestine are under the control of the ENS and this is why even if all connections to the CNS are severed, essential motility in these regions of the bowel is not impaired (Forsythe et al., 2014; Furness et al., 2014).

Aim of the project

The aim of this project was to characterize GI function in a mouse model of α-synucleinopathy originally developed to study neurodegeneration in the CNS. Because this model develops αS-induced central dysfunction in adult age (after 9 months) our purpose was to characterize peripheral abnormalities before the onset of central neurodegeneration and overt motor dysfunction, to describe the nature of such alterations and to determine whether this dysfunction was ascribable to αS overexpression or pathology. Ultimately we exploited silenced αS expression in the colon to test whether targeted inhibition of αS could rescue GI dysfunction in this model.

Matherials and methods

Mice

For this research we used Tg mice expressing human A53T αS under the control of the mouse prion protein (PrP) promoter (line G2-3) (Lee et al., 2002b; Martin, 2006). This model develops neurological abnormalities after 9 months of age (with an average peak at ~13 months) that manifest initially with reduced locomotion, wobbling, lack of balance and weakness of the hind limbs. This diseased phenotype becomes progressively more severe culminating into a fatal paralysis within 14-21 days from the first symptoms appearance. Because of the high variability in time of onset (between 9 to 16 months), Tg mice are closely monitored after 9 months of age, being aware that once the first symptoms appear, the animal is committed to develop the full phenotype. Diseased mice show an accumulation of intracellular, phosphorylated (S129) and ubiquitinated αS inclusions, neuroinflammation and neuronal degeneration in the CNS (Lee et al., 2002b). For the purpose of this study, sick Tg mice at 12-14 months, presymptomatic mice at 1, 2, 3, 6, 9 and 12 (if still healthy) months, and age-matched nTg littermate controls were used. All animal studies were approved by and complied in full with the national and international laws for laboratory animal welfare and experimentation (EEC council directive 86/609, 12 December 1987 and Directive 2010/63/EU, 22 September 2010).

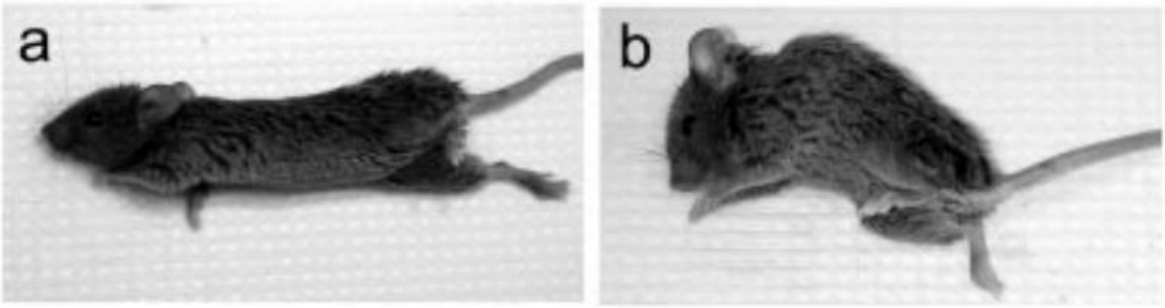

Fig.2.1 Images depicting a Tg mouse during presymptomatic phase, without motor disfunction (A) and a Tg sick mouse, with the typical motor abnormalities in the hind limbs and compromised gait (B) (Lee et al., 2002b).

Behavioral tests and additional parameters

All tests for behavioral and additional parameters were carried out on groups of 20-30 mice, except for gait test, food intake and glycemia where groups consisted of ~10 mice each. Both male and female animals were used. Each trial was performed 1 to 3 times per animal on non consecutive days.

- Gait test

The gait test was assessed in mice after o/n starvation. Each animal's paw was painted with blue washable paint and the mouse was allowed to walk onto a white paper strip, at the end of which a piece of chow was placed as a reward. The footprints were circled and let dry. Stance length, sway distance and stride length were measured for each mouse.

- Whole gut transit time

Whole gut transit time (WGTT) was assessed in mice after oral gavage of 0.05 mL chocolate milk containing 4% of brilliant blue food dye. Post-gavage, the animals were observed until the time of excretion of the first blue stool, which was recorded for each mouse.

- Stool collection

Stool collection assays were performed between 9:00 AM and 11:00 AM on each day. Each animal was removed from its home cage and placed in a clean plastic cage without food or water for 1 h. Stools were collected immediately after expulsion and placed in sealed tubes. At the end of the trial, stools were counted, measured in length and weighted (total weight). After o/n drying at 65 °C stools were weighted again to provide dry weight. Water content was calculated as difference between total weight and dry weight.

- Food intake

Each animal was removed from its home cage and single-housed for 24 h with free access to food and water. Food was weighted before and after the trial and food intake was calculated as difference between the two amounts.

- Glycemia

Glucose levels were assessed using reactive stripes (OneTouch Verio, LifeScan Italia, Milan, Italy) with a single drop sample of blood taken from the tail of each animal. Glucose level was analyzed after o/n food removal (fasted condition) and after the mice were allowed free access to chow for 1 h (fed condition).

Recording of contractile activity from longitudinal and circular muscle preparations of colon and ileum

Contractile activity was recorded from colonic and ileal longitudinal and circular smooth muscles (Antonioli et al., 2014, 2017). Mice were euthanized through CO_2 inhalation. After sacrifice, colon and ileum were removed and placed in cold Krebs solution. Longitudinal and circular muscle strips of the intestine were set up in organ baths containing Krebs solution at 37 °C, bubbled with 95% O_2 + 5% CO_2. The strips were connected to isometric force transducers (2Biological Instruments, Besozzo, Italy). Mechanical activity was recorded as a measure of tension using a BIOPAC MP150 system (2Biological Instruments). A pair of coaxial platinum electrodes was positioned at a distance of 10 mm from the longitudinal axis of each preparation to deliver transmural electrical stimulation (ES) by a BM-ST6 stimulator (Biomedica Mangoni, Pisa, Italy). ES were applied as 10-s single trains consisting of square wave pulses (0.5 ms, 30 mA). To measure muscle contractility of the colon or the ileum, electrically evoked motor responses were recorded from tissue preparations maintained in standard Krebs solution. To measure the neurogenic contribution to muscle contraction, electrically evoked motor responses were recorded after selective stimulation of the nitrergic, cholinergic or NK1-mediated tachykinergic pathway from colonic preparations maintained in Krebs solution containing respectively: guanethidine (10 μM), L-732,138 (10 μM), GR159897 (1 μM), SB218795 (1 μM) and atropine (1 μM) in order to inhibit the noradrenergic, NK-mediated tachykinergic and cholinergic pathways, while recording the nitrergic signal; L-NAME (100 μM), guanethidine (10 μM), GR159897 (1 μM), SB218795 (1 μM) and atropine (1 μM) in order to prevent the recruitment of the nitrergic, noradrenergic, NK2 and NK3-mediated tachykinergic and cholinergic systems, while recording the NK1-mediated tachykinergic pathway; L-NAME, guanethidine, L-732,138, GR159897, SB218795, in order to record the cholinergic response while inhibiting the nitrergic, noradrenergic and tachykinergic signal. To evaluate myogenic contribution to the total contractile activity of the colon, muscle response was evoked by direct pharmacological activation of muscarinic receptors located on smooth muscle cells. For this purpose, colonic preparations were maintained in Krebs solution containing tetrodotoxin (1 μM) and stimulated with carbachol (10 μM). The tension developed by each preparation (g) was normalized by the wet tissue weight (g/g tissue). All the chemical compounds were purchased from Sigma Aldrich (St. Louis, Missouri USA).

Tissue collection and immunoblot analysis

For biochemical analysis mice were euthanized through CO_2 inhalation and the intestine was cut into six segments corresponding to duodenum (D), jejunum (J), proximal ileum (PI), distal ileum (DI), proximal colon (PC) and distal colon (DC), flushed of fecal contents, opened longitudinally, scraped for removing the epithelium and minced. Cold phosphate-buffered saline (PBS), with proteases and phosphatases inhibitors, was used for this procedure. All samples were frozen on dry ice right after collection and stored at -80°C until use. Frozen intestine segments were homogenized using a Potter-Elvehjem Grinder homogenizer on ice in 20% (w/v) TNE lysis buffer (50 mM Tris-HCl pH 7.4, 100 mM NaCl, 0.1 mM EDTA) with proteases and phosphatases inhibitors. Equal volume of TNE buffer containing 2% of NP-40 was added to initial homogenates that were then centrifuged at 10,000 x *g* at 4 °C in order to collect NP-40 soluble and insoluble fractions. Pellets were then washed one time with TNE buffer with 1% of NP-40 and then resuspended in 10% of the original homogenization volume in TNE containing 1% NP-40, 1% SDS, 0.1% DOC. NP-40 insoluble fractions were then sonicated and boiled for 5 min at 95°C.

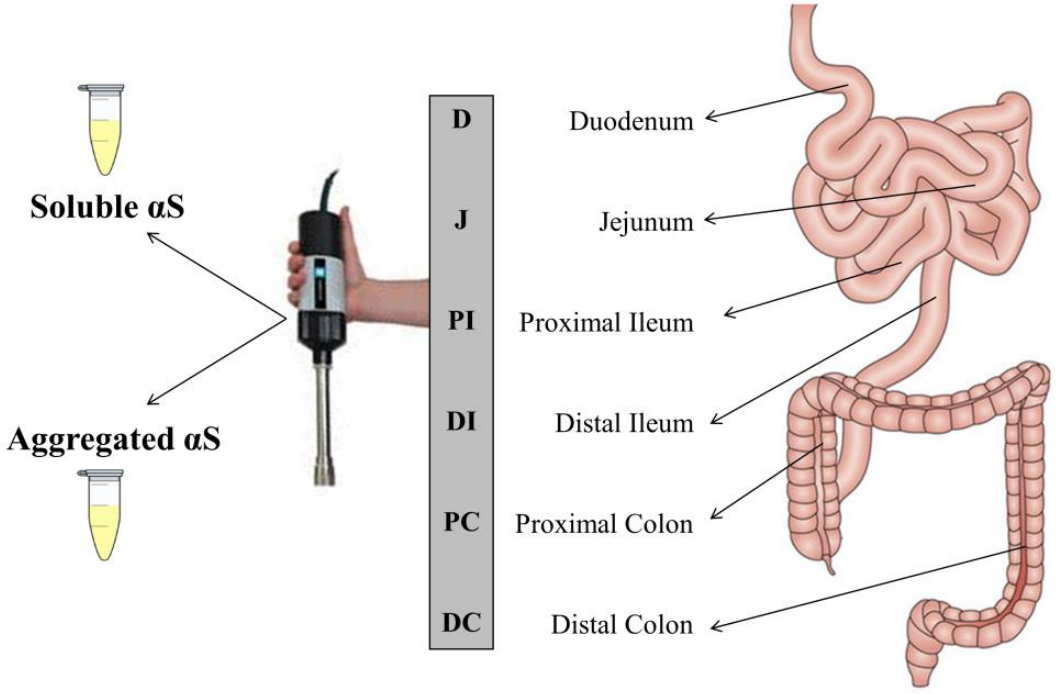

Fig.2.2 Scheming for the harvesting procedure of mice intestine. Six segments corresponding to duodenum (D), jejunum (J), proximal ileum (PI), distal ileum (DI), proximal colon (PC) and distal colon (DC) were collected, homogenized and fractionated into NP-40 soluble and insoluble components, containing respectively soluble and aggregated forms of αS.

Protein amount was determined with BCA. For western blot, protein lysates together with SDS-PAGE sample buffer were run on a 4–20% Criterion™ TGX™ Precast Midi Protein Gel (Bio-Rad, Hercules, CA, USA) and then transferred onto nitrocellulose membrane at 200 mA, o/n at 4°C, using carbonate transfer buffer (10 mM $NaHCO_3$, 3 mM Na_2CO_3, 20% MeOH). Transfer efficiency was controlled by Ponceau staining. For dot blot, 2 µg of protein lysates were spotted directly onto nitrocellulose membrane. Thereafter, for both western blot and dot blot, unspecific binding sites were blocked by 30 min membranes incubation with 5% non fat dry milk (Bio-Rad) in 1X PBS containing 0.01% Tween-20 (PBS-T) at RT. Membranes were then incubated with the specific primary antibody dissolved in 2.5% non fat dry milk in PBS-T, o/n at 4°C. The following antibodies were used: Syn1, pS129-αS, GAPDH, α-Tubulin for western blot and Syn303 for dot blot. Membranes were washed with PBS-T and incubated for 1 h at RT with the appropriate horseradish peroxidase-conjugated secondary antibody in 2.5% non fat milk in PBS-T. Only for pS129-αS detection, 1X Tris-buffered saline containing 0.01% Tween-20 (TBS-T) instead of PBS-T was used for the entire procedure. The chemiluminescent signals were visualized using a CCD-based Bio-Rad Molecular Imager ChemiDoc System (Bio-Rad). Band intensities were analyzed using Quantity One software (Bio-Rad).

Immunofluorescence analysis

For immunofluorescence analysis, mice were perfused with 4% PFA/PBS after 1 mL intraperitoneal injection of 2% w/v Tribromoethanol. Brain and colon (flushed of fecal contents) were collected, post-fixed o/n in 4% PFA/PBS at 4°C and stored in maintenance solution (30% sucrose, 0.1% NaN_2 in PBS) at 4°C. A segment of 2 cm of distal colon was embedded in Tissue-Tek® OCT (Sakura, The Netherlands), cut at the cryostat in serial 12 µm sections and mounted on SuperFrost Plus glass slide (Thermofisher). For one experiment, the whole distal colon was cut longwise and mounted on a toothpick according to the "Swiss roll" technique, before cryosectioning. The slides were washed with PBS and let dry for ~3 h at 37°C before staining. Brains were cut at the microtome in serial 30 µm sections and placed in 24-well plates containing maintenance solution. The slices were washed with PBS before staining. For both colon and brain samples, the sections were incubated with blocking solution [3.5% non fat dry milk, 0.3% Triton X-100 (Tx-100), 6% normal goat serum in PBS] for 1 h at RT and then incubated with primary antibody o/n at RT in blocking buffer. The following antibodies were used: pS129-αS, LB509, β-3-Tubulin, Syn204, Choline Acetyltranferase (ChAT), Tyrosine Hydroxylase (TH), Neurofilament H (NF200), Synaptic Vesicle 2 (SV2). On the next day, the sections were washed twice in PBS and incubated with Alexa Fluor secondary antibodies or Streptavidin (ThermoFisher) in PBS containing 1.5% NGS, 0.3% Tx-100 for 1 h at RT. The sections were counterstained with DAPI and mounted on a glass slide using Fluormount (Sigma-Aldrich).

Antibody	Epitope	Concentration	Isotype	Company	Catalogue number	Molecular analysis
Syn1	NAC αS domain	1:5000	Mouse	BD Biosciences NJ, USA	610787	WB
pS129-αS	Phosphorylated αS at S129	1:2000 WB 1:5000 IF	Rabbit	Abcam MA, USA	51253	WB, IF
GAPDH	GAPDH	1:5000	Mouse	Fitzgerald Industries International MA, USA	10RG109a	WB
α-Tubulin	α-Tubulin	1:5000	Mouse	Sigma-Aldrich MISS, USA	T5168	WB
LB509	Human αS AA 115-122	1:500	Mouse	Abcam MA, USA	27766	IF
β-3-Tubulin	Human β-3-Tubulin C term	1:100	Rabbit	Cell Signaling Technology MA, USA	5568S	IF
Syn204	Human αS	1:100	Mouse	Cell Signaling Technology MA, USA	2647	IF
ChAT	Choline Acetyltransferase	1:100	Goat	Millipore MA, USA	144P	IF
TH	Tyrosine Hydroxylase	1:500	Rabbit	Millipore MA, USA	152	IF
NF200	Neurofilament H	1:500	Mouse	Millipore MA, USA	5539	IF
SV2	Synaptic vesicle glycoprotein 2A	1:250	Mouse	Developmental Studies Hybridoma Bank IA, USA	2315387	IF
Syn303	Oligomers of αS	1:1000	Mouse	Biolegend CA, USA	MMS5085	DB
Mouse αS	Mouse αS	1:1000	Rabbit	Cell Signaling Technology MA, USA	4179	WB

Tab.2.3 List of antibodies employed for western blot (WB), dot blot (DB) and immunofluorescence (IF) analyses, with the specifics referred to the experiments in this study.

Antisense oligonucleotides

The antisense oligonucleotides (ASOs) were synthesized and provided by Eurogentec (Liege, Belgium) and Integrated DNA Technologies (San Jose, CA, USA). Each ASO was a sequence of 20-base pairs with a phosphorothioate backbone. Following a gapmer design, a 2'-O-methoxyethyl (2'-MOE) modification was added on the sugar of the first and the last 5 nucleotides, leaving the middle 10 nucleotides unmodified at the 2'-sugar position. For the experiment *in vitro*, 1 scramble ASO control and 3 ASOs against αS were used (ASO 1, 2, 3), the first two targeting human A53T αS, the last one targeting both human A53T and mouse αS. For the experiment *in vivo*, only the ASO 2 was used, with the addition of a Biotin-TEG at its 5' position.

Cell treatment

SH-SY5Y human neuroblastoma cells were plated in 6-well culture plates and maintained using Dulbecco's Modified Eagle's Medium F12 (DMEM-F12; Sigma-Aldrich, St. Louis, USA) with 10% FBS, 0.1 mg/ml of streptomycin and 100 U/ml of penicillin. When cells were confluent, a double transfection was performed, using Opti-MEM as medium and Lipofectamine 2000 as transfection reagent. The first transfection was done with 4 µg of DNA (human A53T or mouse αS, both in vector pcDNA3.1) and 10 µL of Lipofectamine in a total volume of 500 µL of Opti-MEM. After 24 h, cells medium was removed and a second transfection was performed with no material (negative control) or 2 µL of 500 nM antisense oligonucleotide (Scramble, ASO 1, ASO 2 or ASO 3) and 10 µL of Lipofectamine in a total volume of 500 µL of Opti-MEM.

Cell lysis and western blot analysis

24 hours after the second transfection, cells were washed twice with PBS and lysed on ice in 200 µL lysis buffer (1X PBS, 1% Tx-100, 1% SDS) with proteases and phosphatases inhibitors. Lysed cells were scraped onto 6-well culture plates and then collected in tubes. The total lysates collected were sonicated and boiled for 5 min at 95°C. Protein amount was determined with BCA. Western blot analysis was performed as previously described for tissues in this section.

Mice treatment

10 weeks old Tg mice received biotinylated ASO 2 (50 µg per day) or the same volume of PBS as control, via rectal administration or through osmotic pumps (ALZET, CA, USA). Rectal administration was performed on the mouse under anesthesia with oxygen and isofluorane, using

a small-gauge soft flexible tubing and a 0.5 mL syringe. The tubing was gently inserted through the anus for ~3 cm and 300 µL of solution were administred. As for the osmotic pumps, one pump was inserted for each mouse under anesthesia with oxygen and isofluorane, after surgically opening the abdomen, and positioned with its flow-moderator next to the distal colon. The mouse was then stiched up with surgical clips and left undisturbed in its originary cage. For a preliminary evaluation of the ASO distribution, Tg mice received one single 50 µg dose of ASO rectally and were sacrificed after 6 h, or 150 µg of ASO distributed in 3 days of continuous diffusion by osmotic pump, model 1003D (100 µL). For the actual experiment, rectal administration was repeated every day for 7 days, and the pump model 2001 (200 µL) was used for 7 days of continuous delivery (Fig.2.4). Before and at the end of the 7 days treatment, Tg mice were assessed for WGTT; at the end of both experiments, the mice were sacrificed for tissues collection.

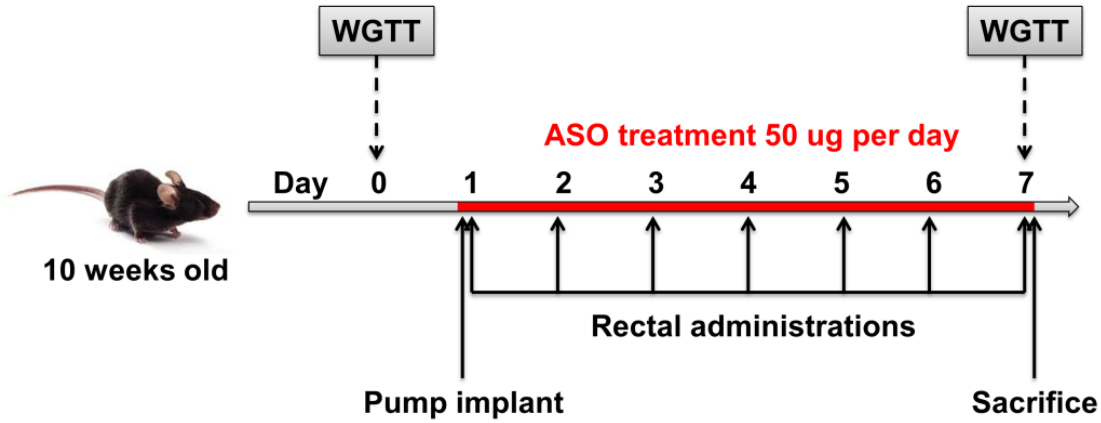

Fig.2.4 Experimental design for mice treatment. 10 weeks old Tg mice received as treatment ASO 2 in the dose of 50 µg per day, or the same volume of PBS as control. The administration was rectal or through osmotic pump. For the rectal group, 7 administrations were performed for 7 consecutive days (day 1 to day 7). For the pump group, the implant was done on day 1, and the drug or vehicle diffusion was constant from day 1 to day 7. WGTT was assessed at day 0 and at day 7. On day 7 all mice were sacrificed for tissues collection.

Statistical analysis

All values are expressed as the mean ± SEM. Differences between means were evaluated by two-way ANOVA, followed by Fisher's LSD post-hoc test, or by one-way ANOVA in case the comparison was between two groups only (Prism, Graph Pad Software, San Diego, CA).

Results

Constipation in PrP A53T αS Tg mice is already present at 3 months of age in absence of overt motor dysfunction and accumulation of αS CNS inclusions

To determine whether PrP A53T αS Tg mice can be used as a suitable model to study constipation as it occurs in the prodromal phase of PD, we first analyzed motor deficit and correlated accumulation of αS-positive inclusions in the CNS, two typical features of this model, in young and adult presymptomatic mice, to exclude that subtle changes in the αS-driven phenotype were already present at young age before the appearance of full-blown motor dysfunctions. In the presymptomatic stage these mice did not show any gross motor abnormalities, maintained normal gait (Fig.3.1a, b, c, d) and balance (Lee et al., 2002b), while presence of phosphorylated (S129) αS inclusions in medulla (Fig.3.1g, h, i, j) and spinal cord (Colla et al., 2018) of sick Tg animals but not 9 months old presymptomatic (Fig.3.1e, f) was found, confirming that the appearance of αS-driven pathology in the CNS is closely linked and concomitant with onset of motor dysfunction and neurodegeneration. Additionally, presymptomatic mice up to 9 months of age do not show signs of neuronal dysfunction in the CNS including the appearance of ER stress markers, ER stress-induced cell death and accumulation of microsomes-associated and ubiquitinated αS species (Colla et al., 2012a).

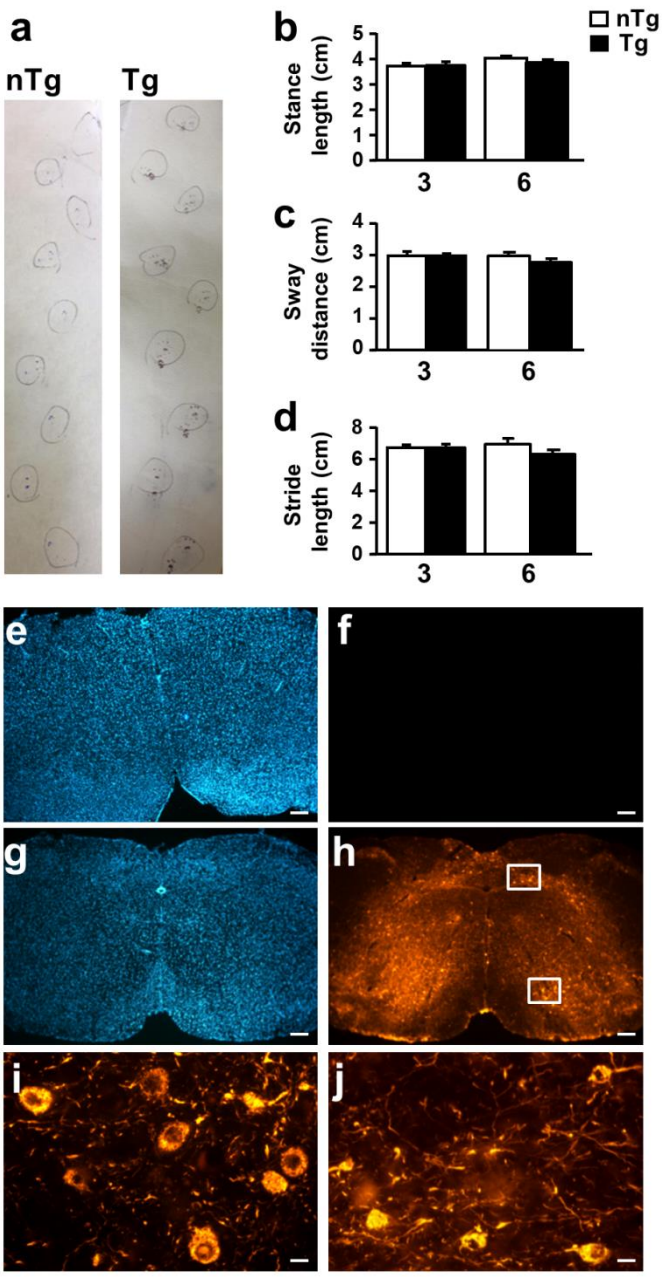

Fig.3.1 αS Tg presymptomatic mice do not display motor deficits nor αS pathology in the CNS. αS Tg mice were evaluated for αS-driven pathology and motor abnormalities. During the gait test presymptomatic 3 and 6 months old mice were allowed to walk on a white paper strip with painted paws and stance length, sway distance and stride length were measured. The walking pattern in 3 and 6 months old Tg and nTg mice remained unchanged. a) Representative walking patterns of a presymptomatic 6 months Tg and its nTg littermate do not show differences in stride and stance length and sway distance. b, c, d) Graphs of gait parameters analyzed in 3 and 6 months old mice. Values on graphs are expressed as raw data and are given as the mean ± SEM (n=5/10 per group), two-way ANOVA followed by Fischer's LSD test. e, f, g, h, i, j) Immunofluorescence analysis of medulla in 9 months presymptomatic (e, f) or sick (g, h, i, j) αS Tg mice stained with pS129-αS antibody (f, h, i, j) or DAPI (e, g). Phosphorylated pathological αS was found only in sick Tg mice after the onset of neurodegeneration, indicating the lack of αS-driven pathology in the CNS of adult presymptomatic animals. i, j) Magnifications of image h for lateral reticular nucleus, magnocellular part (i) and nucleus of the solitary tract (j). Images were acquired with Nikon epifluorescence microscope, objective 4x, scale bar = 100 µm (e, f, g, h) or objective 40x, scale bar = 30 µm (i, j).

Once confirmed that αS Tg mice are free of αS pathology in the CNS at least until 9 months of age, we started to analyze GI functionality by evaluating the WGTT, that is the time it takes for an edible dye to travel through the GI tract and to be excreted. At 3 months of age, the average transit time was 5.919 ± 0.2768 h for αS Tg mice and 4.117 ± 0.2751 h for nTg littermates, indicating that αS Tg mice had a transit delay of almost 2 h when compared to controls ($p<0.0001$). This difference increased over time, reaching a plateau at 6 months of age (the average transit time was 7.680 ± 0.242 h for αS Tg mice and 4.555 ± 0.174 h for nTg mice, $p<0.0001$), with a delay of more than 3 h compared to nTg littermates that was maintained later with aging (Fig. 3.2a). To see whether constipation was present before 3 months of age or it could be based on gender differences, we assessed this parameter also in 1 and 2 months old mice and we analyzed males and females data separately. In both gender groups, no significant differences between Tgs and nTgs were observed for WGTT until 3 months of age. Tg females displayed a slower average transit compared to Tg males, of about 45 min at 2 months and of about 1 h from 6 months (Fig.3.2b, c). Overall, despite these differences, WGTT trends resulted comparable in the two Tg groups. Since such a slowed transit time can affect the amount of pellets expelled, we measured the stool total weight and water content in young and adult mice. To our surprise, stool weight recorded in 1 h period (Fig.3.3a) and related water content (Fig.3.3c) remained unchanged between Tgs and nTgs at all time points considered. Likewise, mice growth measured through body weight and food intake was comparable between the two groups up to 9 months of age. No food malabsorption, episodes of vomit or diarrhea, nor hyperglycemia were observed (Fig.3.3d, e, f), suggesting that the marked delay in transit time was more likely to be related to GI dysmotility rather than digestive abnormality. In agreement with this, when stool output frequency for each single animal was measured in 1 h trial, αS Tgs at 3 months of age showed already a 40% reduction in stool number (2.243 ± 0.221 for αS Tgs versus 3.670 ± 0.346 for nTgs, p value=0.00048) and a correlated 1.4-fold increase in stool length (7.864 ± 0.477 for αS Tgs versus 5.599 ± 0.242 for nTgs, ($p<0.0001$) (Fig. 3.2d, e, f). This difference was maintained in presymptomatic 6 months old mice but not at 9 months, suggesting that at 9 months other pathological processes might have affected directly or indirectly GI functionality in Tg animals and some mice might have been already committed to develop shortly αS-driven neuronal pathology in the brain. In line with this hypothesis, from 9 months of age αS Tgs showed a slight reduction in body weight and food intake consistent with changes in feeding behavior typical of motor symptoms onset (Fig.3.3d, e). Thus, young Tg mice showed signs of constipation and GI abnormalities in presymptomatic conditions that largely anticipate the appearance of αS pathology in the CNS. In addition, the drastic increase in WGTT in young αS Tg mice did not translate into a decrease of total amount of stools but rather affected the number and length of single pellets excreted, suggesting a defect in propulsive and contractile bowel movements from an early age.

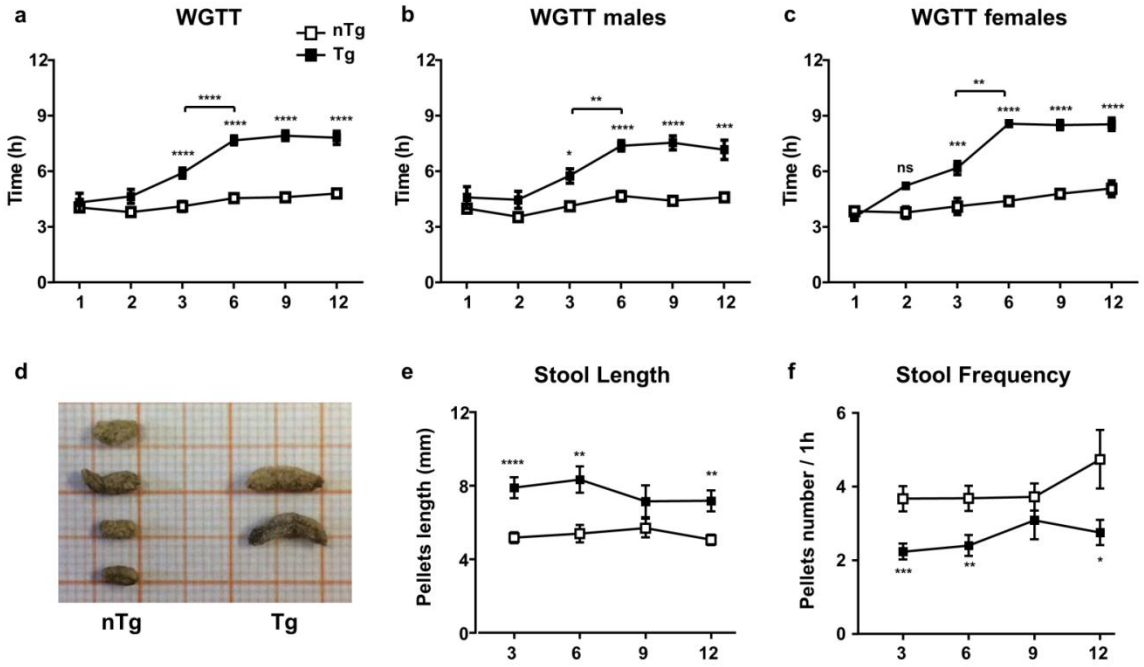

Fig.3.2 GI dysfunction in presymptomatic αS Tg mice is present starting from 3 months of age. GI functionality was evaluated through behavioral tests in presymptomatic 1, 2, 3, 6, 9 and 12 (if healthy) months old αS Tg mice and nTg littermates. Each trial was performed 1 to 3 times per animal on non consecutive days. Groups comprised 20-30 mice with similar presence of females and males. GI behavioral analysis showed significant constipation in young and adult Tg animals and nTg age-matched littermates. a, b, c) WGTT was recorded as the time for a non absorbable dye to travel through the GI tract. a) The transit time is increased in presymptomatic αS Tg mice versus controls starting from 3 months and exacerbates with age, reaching an average 3 h 12 min delay in Tg animals by 6 months of age. b, c) A comparable result was obtained when considering males and females separately. Notably, Tg females have a slower transit time compared to males, starting from 2 months of age. d, e, f) Presymptomatic αS Tg mice excreted a reduced number of stools but with an increased length compared to controls already at 3 months. d) Representative image of stools collected in 1 h trial from a 6 month old αS Tg mouse and littermate. Notably, pellets from young Tg mice are longer but less abundant. e, f) Pellets from each mouse were collected in 1 h trail. Stools from Tg mice were consistently longer and less abundant compared to controls. Values on graphs are expressed as raw data and are given as the mean ± SEM (n=20-30 per group). * $p<0.05$; ** $p<0.01$; *** $p<0.001$, **** $p<0.0001$, two-way ANOVA followed by Fischer's LSD test.

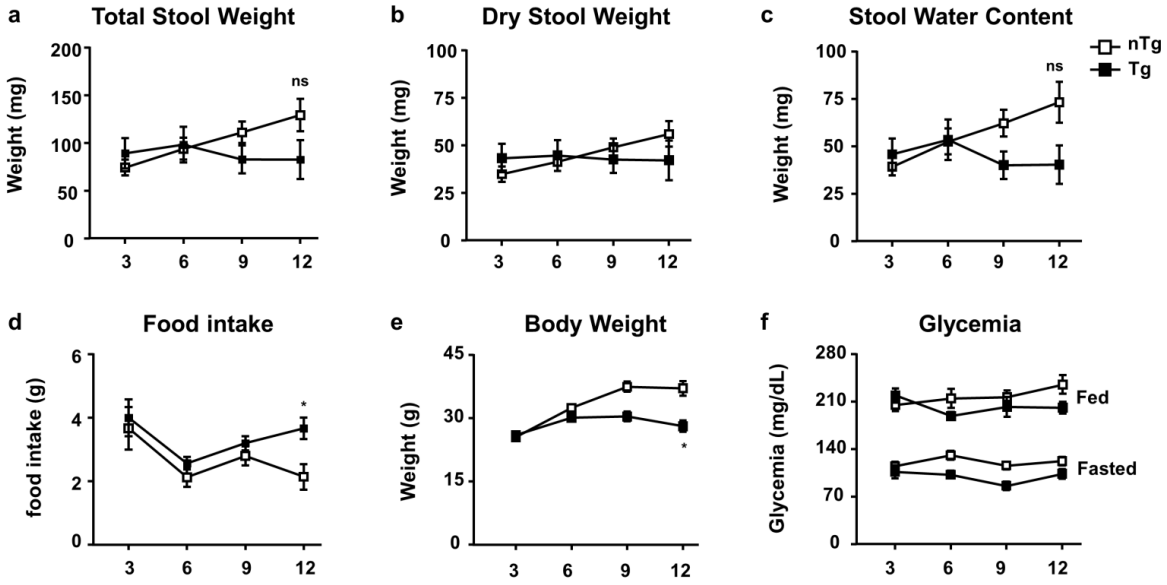

Fig.3.3 GI dysfunction in presymptomatic Tg mice. Stool weight, feeding behavior, body growth and glycemic levels are not affected in presymptomatic αS Tg mice. Additional parameters related to GI functionality were evaluated through behavioral tests in presymptomatic αS Tg mice and nTg littermates. Each trial was performed 1 to 3 times per animal on non consecutive days. Groups comprised 20-30 mice for stool tests and body weight, or 10 mice for glycemic tests, with similar presence of males and females. a, b, c) Pellets from each mouse were weighted for total stool weight, then let dry o/n at 65 °C and weighted again to measure dry stool weight and water content. No difference in total (a), dry stool weight (b) nor water content (c) of pellets was found between Tgs and controls at any time point. d) Food intake was measured in a 24 h trial. No significant difference was found between the two groups in the amount of chow ingested until 9 months of age, indicating that GI dysfunction was not due to erratic food consumption. e) Body weight of the animals remained comparable between the two groups until 12 months of age, a time in which surviving Tg mice may have been already committed to develop shortly the full motor phenotype. Maybe for a compensation at this time point close to central pathology, 12 months old Tgs appear to increase their food intake compared to controls (d). f) Glycemic levels were measured under fasted and fed conditions. No variations were noticed between the two groups, nor diabetes-like signs were present at any time. Values on graphs are expressed as raw data and are given as the mean ± SEM. * $p<0.05$, two-way ANOVA followed by Fischer's LSD test.

Presymptomatic αS Tg mice show a reduced electrically evoked motor response of the colonic muscle layers from 3 months of age

Since constipation is correlated with a deficit in bowel motility, we recorded colonic and ileal contractility of longitudinal and circular muscles in young and adult αS Tg mice. Electrical stimulation of the colon from αS Tg mice showed a clear reduction in the magnitude of motor response of both muscle layers compared to controls, that was already present in 3 months old Tgs. In particular, the circular muscle seemed more affected since its response to stimulation was increasingly reduced with aging in αS Tg mice (Fig.3.4a). By contrast, in control animals, electrically evoked contractions showed consistently similar patterns of magnitude at all ages analyzed. To establish whether the reduced motor response in the colon of αS Tg animals was due to an impairment of a specific system within the ENS, we recorded the contractile response after selective stimulation of the nitrergic, cholinergic or tachykinergic system, pharmacologically isolated by using specific inhibitors (Fig.3.4b, c, d). Remarkably, only the excitatory cholinergic component was consistently impaired in Tgs compared to age-matched littermates at all ages analyzed, as shown by the decrease of the electrically evoked motor response, whilst the other systems appeared not affected. This deficit in cholinergic transmission indicates that the increase in WGTT with concomitant alteration in stool formation is mainly due to a decrease in colon muscle contraction, rather than a dysfunction in muscle relaxation, which is mainly modulated in mice by the nitrergic system (Mang et al., 2002). Furthermore, in order to understand whether this deficit was myogenic or neurogenic, we evoked colonic contractions by direct pharmacological activation of muscarinic receptors located on smooth muscle cells, by using tetrodotoxin and carbachol (Fig.3.4e). Interestingly, in this case the motor response was comparable between Tgs and controls at all ages analyzed, indicating that the observed colonic dysmotility of Tg animals was mainly related to a deficit in the neural component. In addition, since WGTT is a measure of the transit time for the whole GI tract, electrical stimulation of ileal preparations from presymptomatic mice at 3 and 12 months was performed (Fig.3.4f). To our surprise, motor response in the ileum was comparable between Tg and nTg animals for both time points, indicating that the deficit in contraction seen in young Tg mice was specific for the colon. Thus, the reduced contractility of the colon in presymptomatic mice, due to an altered cholinergic transmission, contributes to their abnormal formation of stools and delayed GI transit time.

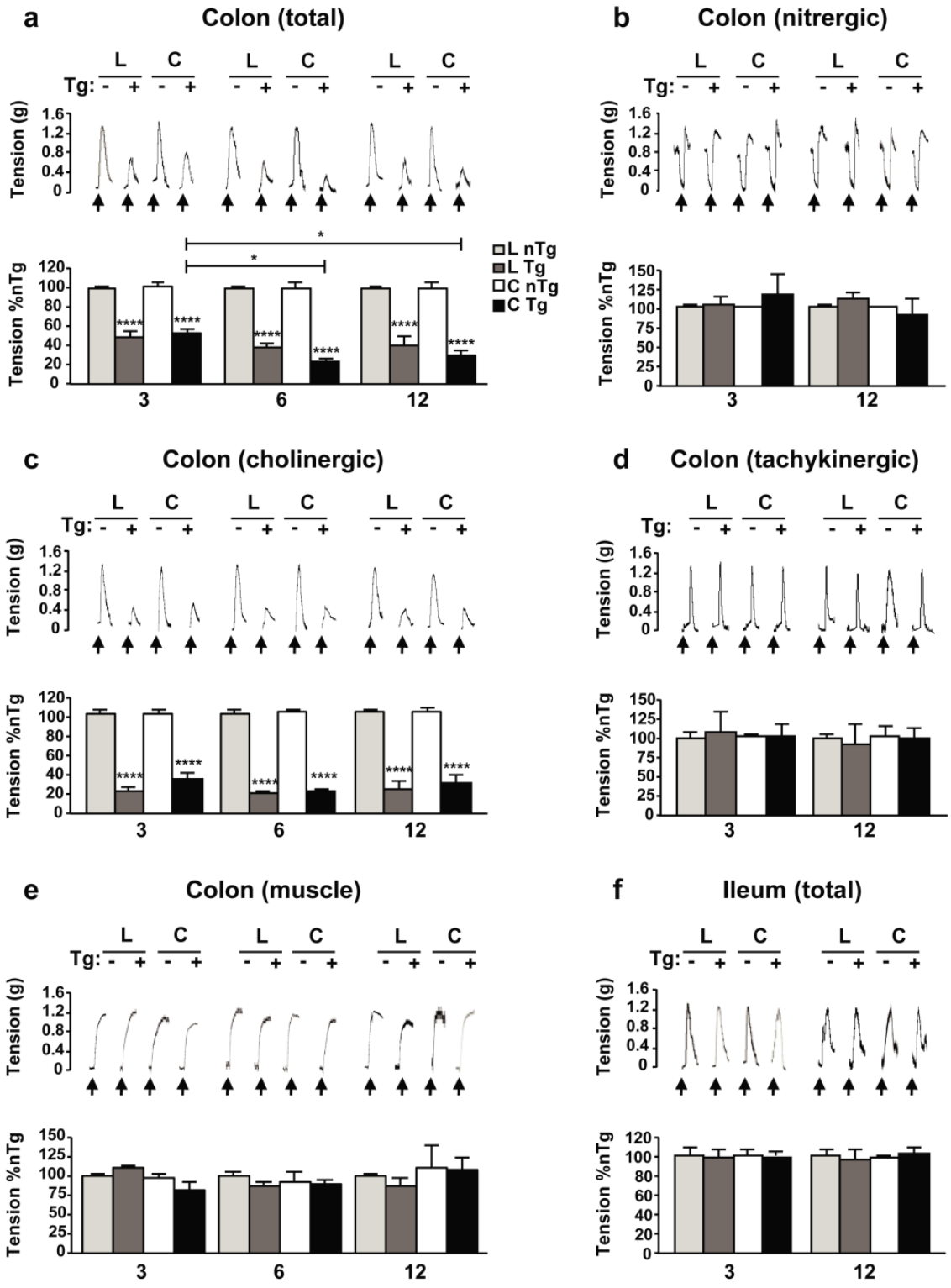

Fig.3.4 Colonic contractile activity is impaired in presymptomatic αS Tg mice from 3 months of age. Electrical stimulation (ES) of intestinal tissues shows a reduced response of longitudinal (L) and circular (C) smooth muscles in Tg mice already at 3 months, in the colon but not the ileum. The reduced contraction was mainly due to a decreased cholinergic transmission and exacerbated with age. Recordings were performed in αS Tg mice and nTg littermate controls in colon (a, b, c, d, e) and ileum (f). a, f) Effect of ES (↑=ES, 10 Hz) on the contractile activity of colonic (a) or ileal (f) preparations maintained in standard

Krebs solution in order to register the overall response. b) Effect of selective ES (↑=ES, 10 Hz) of the inhibitory nitrergic pathway on the activity of colonic muscles in order to record nitrergic-induced response. Colonic preparations were maintained in Krebs solution containing guanethidine, L-732,138, GR159897, SB218795 and atropine. c) Effect of selective ES (↑=ES, 10 Hz) of the excitatory cholinergic system on the activity of colonic muscles in order to record cholinergic-induced contractions. Colonic sections were maintained in Krebs solution containing L-NAME, guanethidine, L-732,138, GR159897, and SB218795. d) Effect of selective ES (↑=ES, 10 Hz) of the excitatory tachykinergic pathway on the activity of colonic muscles to record NK1-mediated tachykinergic contractions. Colonic preparations were maintained in Krebs solution containing L-NAME, guanethidine, GR159897, SB218795, atropine. e) Effects of carbachol (↑=Cch; 10 μM) stimulation on the activity of colonic preparations in order to record the myogenic response in absence of neurogenic stimulation. Colonic preparations were maintained in Krebs solution containing tetrodotoxin. Tracings in the inset on the top of each panel display the contractile responses to ES, as raw data. Values on graphs are expressed as % relative to controls and are given as the mean ± SEM (n=8 per group). * $p<0.05$; **** $p<0.0001$, two-way ANOVA followed by Fischer's LSD test.

Accumulation of αS soluble and insoluble HMW species in the colon increases over time in presymptomatic αS Tg mice

In order to investigate whether the expression of αS could be related to the GI deficits that we observed, we performed immunoblot analysis on the intestine of young and diseased animals to check for peripheral distribution of αS. The whole length of the intestine was examined from the pylorus to the rectum, divided into six segments corresponding to duodenum, jejunum, proximal and distal ileum, proximal colon and distal colon. Western blot assays showed that αS monomer was present at low level in all fractions analyzed, with the exception of the colon where αS transgene expression reached a ~60-fold increase, compared to the small intestine, in presymptomatic 3 months old Tg animals (Fig.3.5). Very interestingly, when NP-40 insoluble fraction was run, 3 months old presymptomatic αS Tg mice already showed accumulation in the colon (mainly in the distal segment) of aggregated HMW species of αS. In diseased mice, after CNS neuronal degeneration onset, αS distribution was similar to that found in 3 months old mice, although the level of HMW αS was higher, suggesting a possible increase in αS inclusions formation with age.

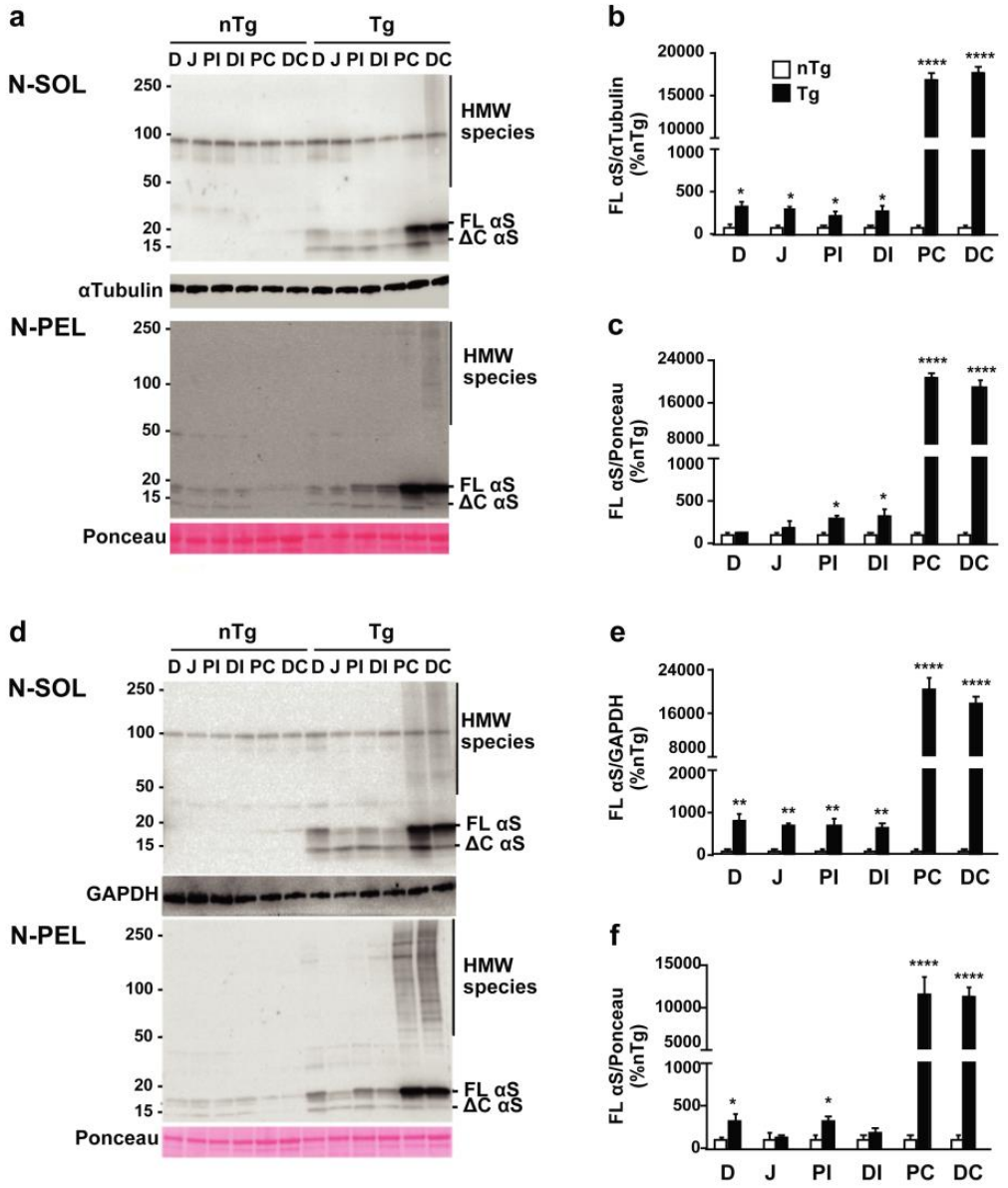

Fig.3.5 Intestinal αS distribution in presymptomatic and diseased αS Tg mice. Distribution of αS transgene expression was assessed in young presymptomatic (3 months old) and diseased Tg mice. Fresh mouse intestinal tract was divided into six segments corresponding to anatomical distinct areas: duodenum (D), jejunum (J), proximal ileum (PI), distal ileum (DI), proximal colon (PC), distal colon (DC). NP-40 soluble (N-SOL) and insoluble (N-PEL) fractions were loaded on a SDS-PAGE and blotted for Syn1 and α-Tubulin or GAPDH antibodies. αS expression was more abundant in the colon of both 3 months old presymptomatic (a) and sick αS Tg (d) mice, compared to the small intestine ($p<0.0001$) or nTg age-matched littermates lysates, although it was present at minimal level in all fractions examined in Tg mice. Notably, insoluble and more surprisingly soluble fraction contained HMW αS species. FL αS, full length αS, ΔC αS, truncated αS. b, c, e, f) Relative density of αS monomer in soluble (b, e) or insoluble (c, f) fractions. Values on graphs are expressed as % relative to nTg and are given as the mean ± SEM (n=3-4 per group). * $p<0.05$; **** $p<0.0001$, two-way ANOVA followed by Fischer's LSD test.

In fact, when the proximal and distal colon from different ages were specifically analyzed for αS aggregates, we found an increased accumulation of insoluble and aggregated species of αS over time for both segments, although the distal colon appeared more affected, that peaked at 6 months and remained stable at later time points (Fig.3.5d, e, f) whereas αS monomer level did not change (Fig.3.6).

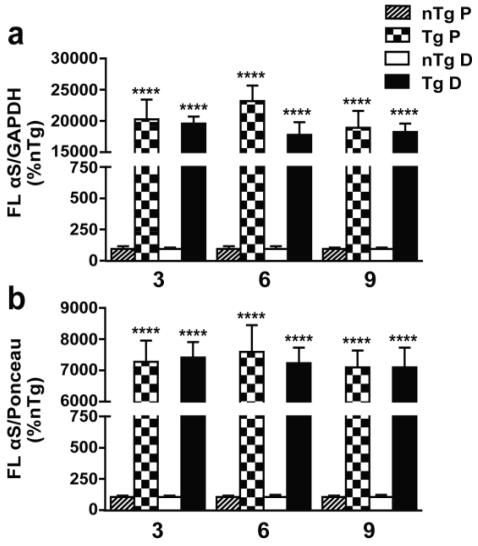

Fig.3.6 Distribution of αS monomer in the colon of presymptomatic Tg mice. Relative density of αS monomer in the proximal (P) and distal (D) colon of Tg mice and age-matched controls at various age shows that αS monomer level does not change with age. Quantitative analysis of immunoblots of soluble (a) and insoluble (b) fractions presented in Fig.3.7. FL αS, full length αS. Values on graphs are expressed as % relative to nTg and are given as the mean ± SEM (n=3/4 per group). **** $p<0.0001$; two-way ANOVA followed by Fischer's LSD test.

Notably, also the soluble fraction of the proximal and distal colon contained soluble HMW oligomers of αS, the amount of which increased with aging and paralleled the trend seen for αS insoluble aggregates (Fig.3.5a, b, c). In addition, phosphorylated αS at S129 was also detected in both insoluble and, more surprisingly, soluble fractions of the colon (Fig.3.5c, f), a unique condition of the ENS, since phospho-αS species accumulate in the CNS of this line only after neurodegeneration onset and mainly in non ionic detergent-insoluble pellet (Fig.3.1) (Colla et al., 2012a, 2012b, 2018). Thus, accumulation of phosphorylated αS inclusions in the colon of αS Tg mice largely precedes brain neuropathology, mimicking behavior and physiology data. Moreover, soluble αS is already phosphorylated at 3 months of age and forms stable, but still soluble, HMW oligomers, suggesting that the pathobiology of αS may differ between the CNS and the ENS.

It is also interesting to notice that truncated αS is present at all ages in proximal and distal colon. Although we have not focused on this specific aspect yet, it may be possible that two different truncated forms are present in proximal and distal colon respectively, as it appears from the blots at least at 3 and 9 months of age for Tg presymptomatic mice. It would be interesting to further characterize this issue and be able to compare the truncation pattern in the ENS of Tg mice with the CNS data published from our group (Li et al., 2005; Colla et al., 2018). Based on our observations, we demonstrated that the accumulation of specific αS truncated species in the CNS varies bewtween presymptomatic and diseased Tg mice, when analyzing different subcellular districts of neurons.

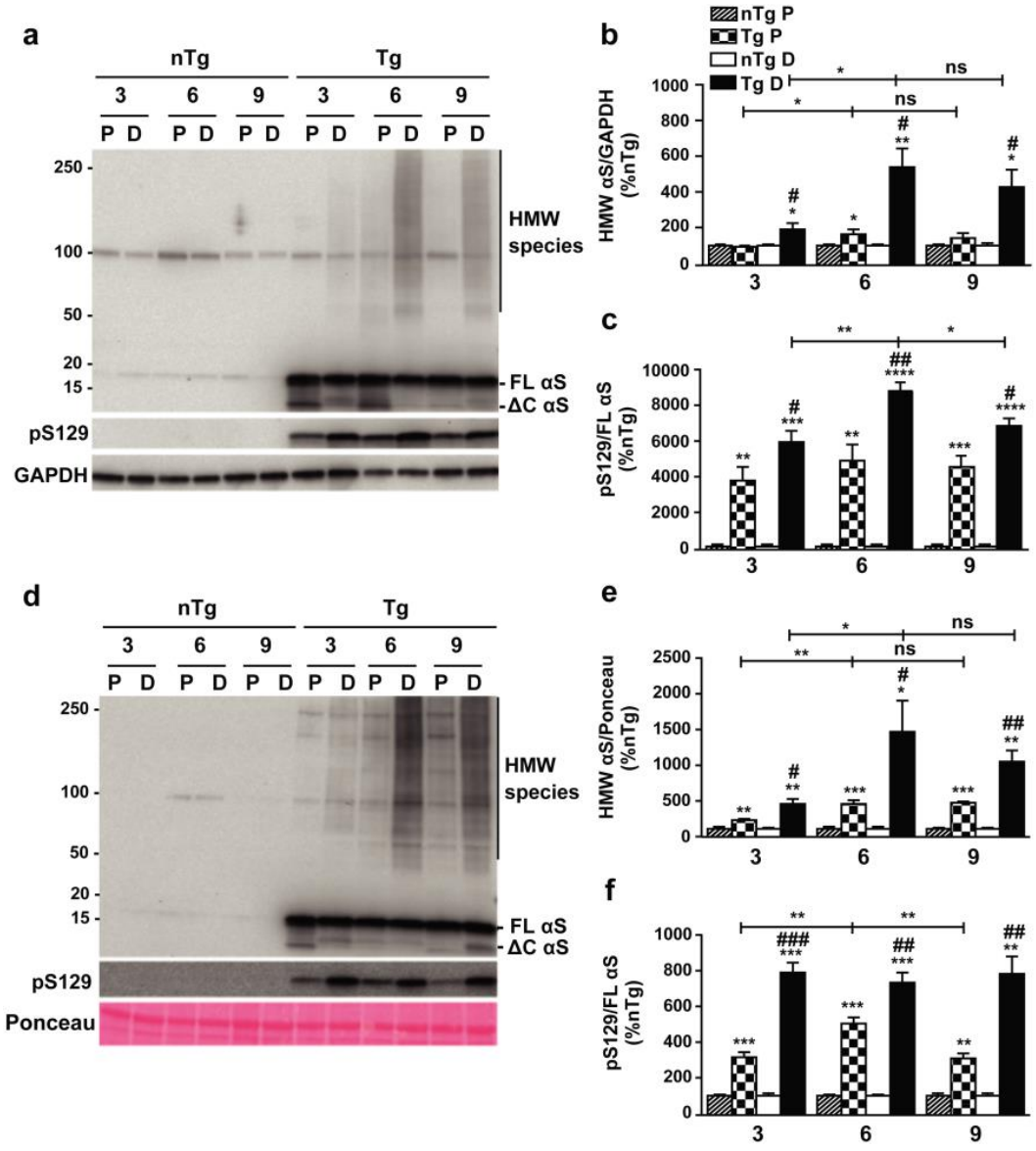

Fig.3.7 αS soluble and insoluble HMW species in the colon increase with age in presymptomatic mice. Time course analysis of soluble and insoluble fractions obtained from the proximal (P) and distal (D) colon of presymptomatic Tg mice at different age shows an increase in the accumulation of αS HMW species. NP-40 soluble (a) and insoluble (d) lysates of proximal and distal colon were isolated from presymptomatic Tg mice and nTg littermates at different age, run on a SDS-PAGE and blotted with Syn1, pS129-αS and GAPDH antibodies. Soluble and insoluble phospho-αS HMW species were already abundantly present in Tg mice at 3 months of age and their level exacerbated with age, reaching a plateau at 6 months. The distal colon appears to be the intestinal region with the highest presence of αS HMW species. b, c, e, f) Graphs showing relative density of HMW αS (b, e) or phospho-αS (c, f) in all fractions analyzed. Values on graphs are expressed as % relative to nTg and are given as the mean ± SEM (n=3-4 per group). * $p<0.05$; ** $p<0.01$; *** $p<0.001$; **** $p<0.0001$, # $p<0.05$; ## $p<0.01$; ### $p<0.001$; #### $p<0.0001$, where * refers to comparisons between Tgs and their nTg age-matched controls, while # refers to comparisons between distal and proximal colon of Tgs; two-way ANOVA followed by Fischer's LSD test.

By using a specific antibody that can detect oxidated and aggregated αS forms in dot blot but not western blot assays (due to the necessity of not denaturate such aggregates), we were able to further characterize the nature of the HMW species found in the insoluble fraction of colon lysates. With a similar trend of the previous time course data, the dot blot performed on proximal and distal colon of Tg and control mice at all time points, confirmed an accumulation of aggregated species in Tgs in both segments of the colon already at 3 months of age, with higher levels in the distal part and a peak at 6 months (Fig.3.8)

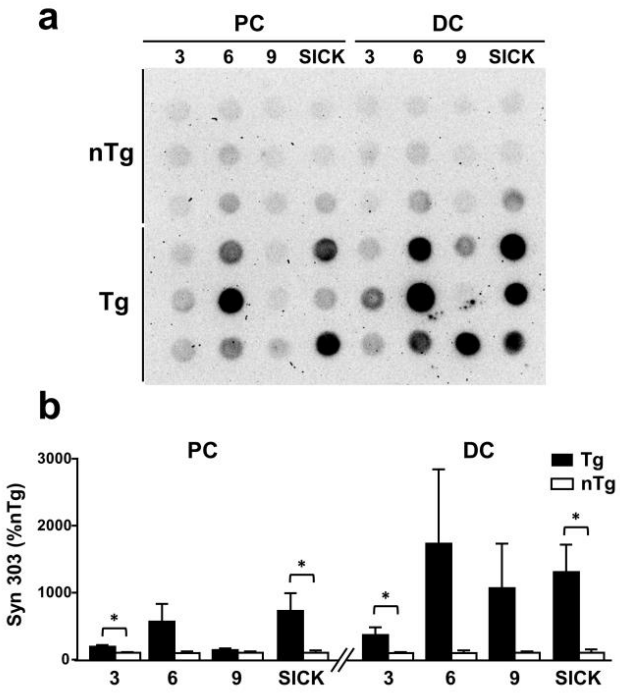

Fig.3.8 Time course of αS insoluble oligomers in the colon of presymptomatic and diseased Tg mice. a) NP-40 insoluble fractions from proximal (PC) and distal (DC) segments of the colon of presymptomatic and sick αS Tg mice and controls were blotted with an antibody specific for oxidated and aggregated αS, Syn303. b) Dot blot values in the graph are expressed as % of age-matched nTg mice and given as the mean ± SEM (n=3 per group). * $p<0.05$, one-way ANOVA.

Pathological αS in presymptomatic and diseased αS Tg mice is found in ChAT-positive and TH-positive enteric neurons of the colon

In order to further investigate the distribution of pathological αS in the colon of Tg mice, we performed immunofluorescence analysis on frozen sections of the distal colon in 3 months old presymptomatic and sick Tg mice. Colocalization with β-3-Tubulin, a pan-neuronal marker, showed that αS aggregates were present only in neurons, mainly in the soma, of both myenteric and submucosal plexi of the ENS of Tg animals (Fig.3.9a, b, c). A further double immunostaining was carried out with specific neuronal type markers to assess whether αS was associated with specific neuronal populations. αS was found in ChAT-positive neurons (Fig.3.9e, f) and in TH-positive neurons (Fig.3.9h, i) of both enteric plexi. Interestingly, not all ChAT-positive and TH-positive neurons stained for αS, which was concomitantly seen in other neuronal populations. This suggests a dynamic progression in the spreading and/or accumulation of toxic αS in the ENS. Thus, accumulation of αS aggregates in colonic enteric neurons in both plexi is associated with the onset of constipation and GI transit abnormalities that manifest in αS Tg mice in presymptomatic conditions without overt neurodegeneration in the CNS.

Fig.3.9 Accumulation of pathological αS in enteric neurons of presymptomatic and sick αS Tg mice. Immunocolocalization with neuronal markers shows accumulation of αS toxic species only in enteric neurons, including ChAT-positive and TH-positive types, in both the submucosal and myenteric plexi in Tg mice but not in controls. Distal colon frozen sections from 3 months old presymptomatic (b, e, h) and sick αS Tgs (c, f, i) and nTg littermates (a, d, g) were stained with LB509 and β-3-Tubulin (a, b, c); ChAT and pS129-αS (d, e, f); Syn204 and TH (g, h, i). Sections were counterstained with DAPI. Notably, within the same section and concurrently with double labeled neurons (full arrow heads), we found healthy neurons without accumulation of toxic αS (empty arrow heads) or neurons with accumulation of toxic αS that belonged to other neuronal populations beyond the ChAT-positive or TH-positive (*), suggesting that different enteric neurons may be distinctively susceptible to αS spreading. Images were acquired with Leica microscope SP2 system, objective 63x. Scale bars = 40μm.

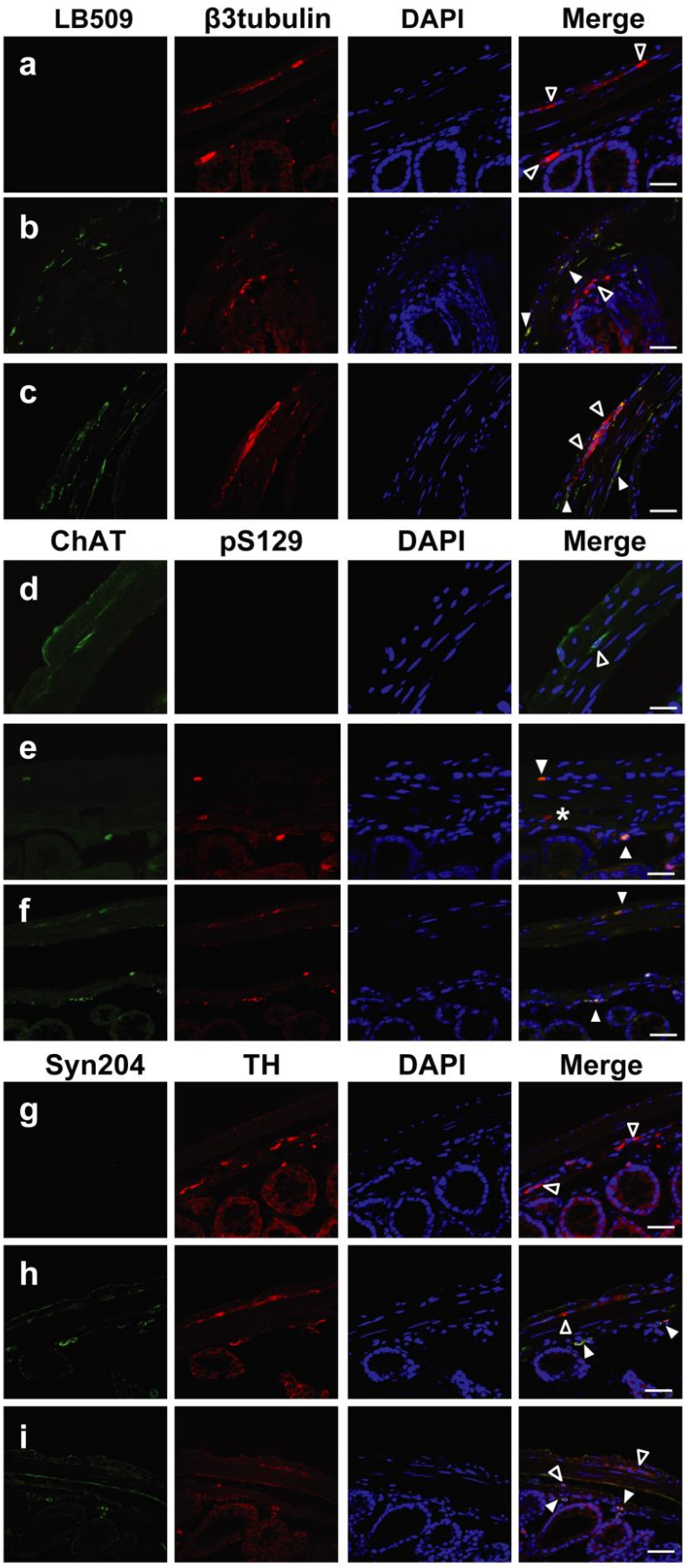
LB509
β3tubulin
DAPI
Merge
a
b
c
ChAT
pS129
DAPI
Merge
d
e
f
Syn204
TH
DAPI
Merge
g
h
i

Antisense oligonucleotide treatment

After a detailed characterization of PrP A53T αS Tg mice line G2-3 from an enteric point of view and with a peculiar focus on the prodromal phase, we proceeded our research toward a disease modifying direction, through therapeutic intervention. Our strategy was to use an ASO directed to the periphery, in presymptomatic 10 weeks old Tg mice.

ASOs are small, single-stranded sequences of nucleic acids, between 8 to 50 nucleotides in length, able to bind to a complementary target mRNA through standard Watson-Crick base pairing. This specific matching results in the alteration of the original function of the target RNA, through different mechanisms, which largely depend on the chemical structure of the ASO itself. One frequent mechanism is the recruitment of RNase H, an endogenous enzyme that recognizes RNA/DNA heteroduplexes and degrades the target RNA after its binding with the ASO. The destruction of the mRNA prevents its translation into protein, yielding a decrease of the intended target. This approach is useful for pathologies characterized by the accumulation of specific proteins, such as αS in PD, and many other neurodegenerative disorders (DeVos and Miller, 2013). In order to be able to recruit RNAse H, the ASO needs to have a phosphorothioate (PS) backbone, a very common modification which consists in replacing the oxygen atom in the phosphodiester linkage with a sulfur atom. Besides allowing the RNAse H mechanism, the PS backbone improves the ASO pharmacokinetics, by increasing its resistance against nucleases degradation and its binding to plasma proteins, which ultimately lead to a higher concentration and a more efficient cellular uptake (Schoch and Miller, 2017). Another largely used modification involves the sugar moiety at the position 2' and consists in the addition of a 2'-O-methoxyethyl (MOE) group. This leads to a higher binding affinity of the ASO to the target RNA and it helps overcoming some disadvantageous immunostimolatory properties of the PS backbone, thus reducing the ASO toxicity (Evers et al., 2015). However, ASOs made of fully modified 2'-sugar moieties lose the ability of recruiting RNAse H, and this is why in order to exploit the advantages of both modifications it is necessary to further manipulate the sequence with a gapmer design. A gapmer ASO has a central region with unmodified sugars, flanked by two shorter regions with modified sugars. It is important to point out that a gapmer 2'-MOE PS ASO was the first to be used in a clinical trial for a neurodegenerative disease, with a positive outcome in terms of safety and tolerability (Miller et al., 2013).

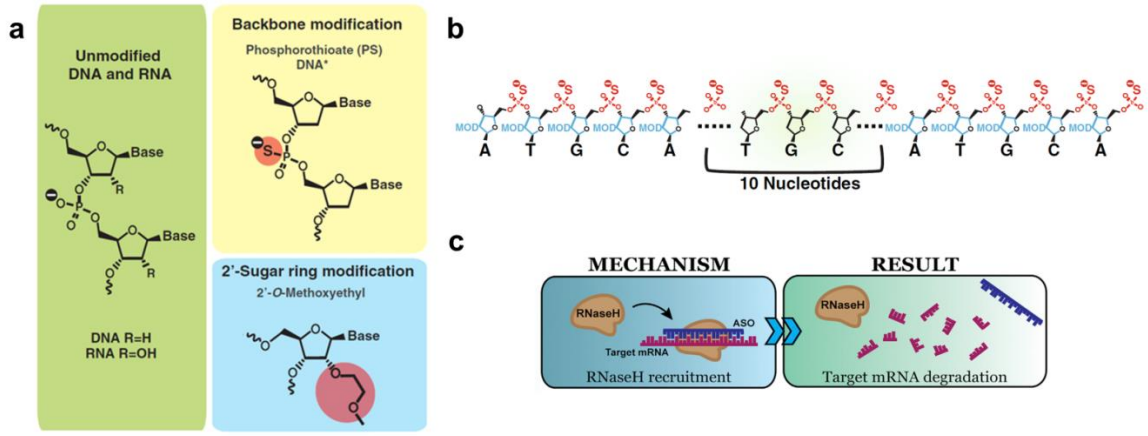

Fig.3.10 Schematic representation of structure and mechanism of action of a gapmer 2'MOE PS ASO. a) Panel depicting the two most common modifications for ASOs at the backbone and 2'sugar ring, which are the phosphorothioate (PS) modification (in yellow) and the 2'-O-Methoxyethyl (MOE) modification (in blue) respectively. b) Example of a 20-mer PS ASO (PS group in red) with a gapmer design, consisting in a central region of 10 nucleotides with unmodified sugars, flanked by two regions of 5 nucleotides each, with modified sugars (MOD, in blue). The gapmer design allows a PS 2'-MOE modified ASO to maintain its ability of RNAse H recruitment, otherwise lost with a full 2'-MOE modification for its entire length. This RNAse H mechanism of action (c) is possible thanks to the specific matching of the ASO to a target mRNA and results in the mRNA degradation. This approach is particularly useful for neurodegenerative diseases, in which reducing the levels of a specific toxic protein would contrast the development of the pathology (DeVos and Miller, 2013).

ASO treatment reduces selectively human A53T αS expression in SH-SY5Y cells

In line with this strategy, we designed three gapmer 2'-MOE PS ASOs directed against αS and one scramble ASO with a random non matching sequence to be used as negative control. ASO 1 and ASO 2 matched with the human A53T αS, whilst ASO 3 matched with both human A53T and murine αS. In a first experiment we tested the efficiency of all three ASOs against human A53T αS. Cells were transfected first with human A53T αS and then with the ASO to be evaluated. Immunoblots of cell lysates showed comparable levels of inhibition in αS expression (Fig.3.11). Because of this, we chose ASO 2 for further characterization. In order to confirm that ASO 2 does not inhibit murine αS expression, a critical issue to be evaluated in view of a treatment in mice, we repeated the experiment transfecting SH-SY5Y cells with human A53T or mouse αS. As expected, this ASO reduced significantly human A53T αS but not mouse αS levels (Fig.3.12). Thus, ASO 2 was chosen to be suitable for the *in vivo* experiment.

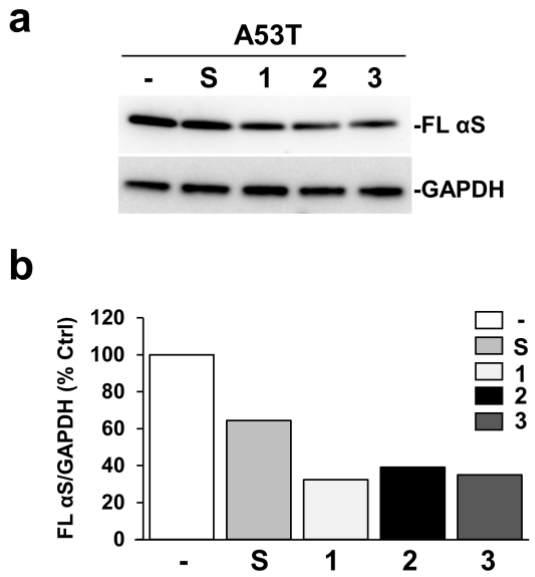

Fig.3.11 ASOs against αS tested in SH-SY5Y cells expressing A53T αS. a) Expression of αS measured in SH-SY5Y cell line lisates after a first transfection with A53T human Tg αS and second transfection with no material (negative control) or ASO scramble (S, control), ASO 1, 2, 3. b) Quantification of αS/GAPDH levels for each ASO, relative to the negative control.

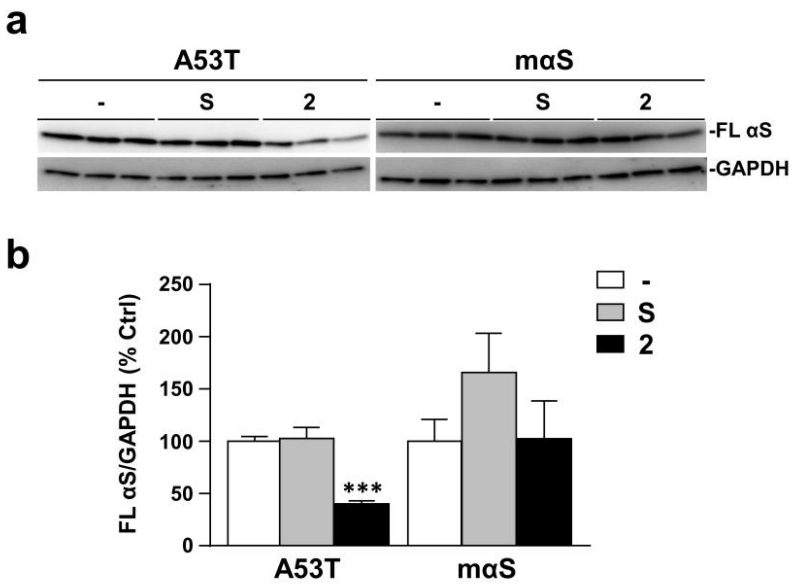

Fig.3.12 ASO 2 tested in SH-SY5Y cells expressing human Tg A53T or mouse αS. a) Expression of αS measured in SH-SY5Y cell line lisates after a first transfection with A53T human Tg or mouse αS, and second transfection with no material (-, negative control), antisense oligonucleotides scramble (S, control) or ASO 2, in triplicates. b) Quantification of αS/GAPDH levels for A53T and mouse αS. Values on graphs are expressed as % relative to negative control and are given as the mean ± SEM (n=3 per group). *** $p<0.001$, one-way ANOVA.

ASO is uptaken at the colon following rectal or osmotic pump delivery in mice

Before testing ASO 2 inhibitory effect *in vivo*, we performed a preliminary experiment to verify how its distribution takes place in the colon of mice. In order to make the ASO detectable in tissues an additional 3' biotin TEG was added to the original ASO 2 sequence. Since we demonstrated that αS pathology in this mouse model affects both submucosal and myenteric neurons of the colon, we decided to use two different delivery routes, rectal or osmotic pumps, in order to reach both plexi. Rectal administration is less expensive, but probably more stressful for the animal, as it requires to be repeated several times by the operator, and maybe for this reason it was also related to a higher mortality. Osmotic pumps implant requires one single surgical intervention, which is more invasive but less problematic for the mouse in a long-term perspective. None of the implanted mice died following the procedure, but did so for the rectal route during the second experiment. Although rectal administration might seem easier in terms of expertise, both techniques require a good command of surgical skills and animal handling. To check the ASO distribution, Tg mice received ASO 2 or PBS for 3 days in the case of osmotic pump implant or in one single dose in the case of the rectal route. Mice were sacrificed after 3 days of diffusion (pumps) or 6 h after administration (rectal) and serial frozen sections of the colon were stained using a Streptavidin antibody that recognizes the 3' biotin TEG cap in the ASO 2 sequence. Despite detecting the ASO in tissues was not simple, as some of the amount was probably degraded or reached undesired areas, ASO specific immunofluorescent signal was detected in samples from both administration routes in proximity of neuronal and non neuronal cell types (Fig.3.13).

Fig.3.13 ASO distribution after colonic administration in presymptomatic αS Tg mice. Immunocolocalization with neuronal markers shows the presence of biotinylated ASO in the colon of ASO treated mice but not in PBS treated controls. Frozen sections of distal colon mounted according to the "Swiss roll" procedure from presymptomatic 3 months old Tgs were stained with Streptavidin for detecting biotinylated ASO, and SV2 together with NF200 for peripheral neurons. Sections were counterstained with DAPI. The mice received the treatment rectally (a, b, e) or through osmotic pumps (c, d, f), containing ASO (b, d, e, f) or PBS as control (a, c). The tissues were collected 6 h after one rectal administration (a, b, e) or 3 days after pumps implant (c, d, f). The images below (e, f) represent a magnification of b, d merges respectively, from the selected area. As expected, no Streptavidin-positive signal was detected in PBS treated mice (a, c), whilst it was found in ASO treated mice (b, d, e, f). In both rectal (b, e) and pump (d, f) routes group, the ASO signal was detected in proximity of neurons (full arrow heads) and in proximity of other enteric cell types (empty arrow heads). Images were acquired with ZEISS Apotome.2 semiconfocal microscope, objective 20x. Scale bars = 50μm.

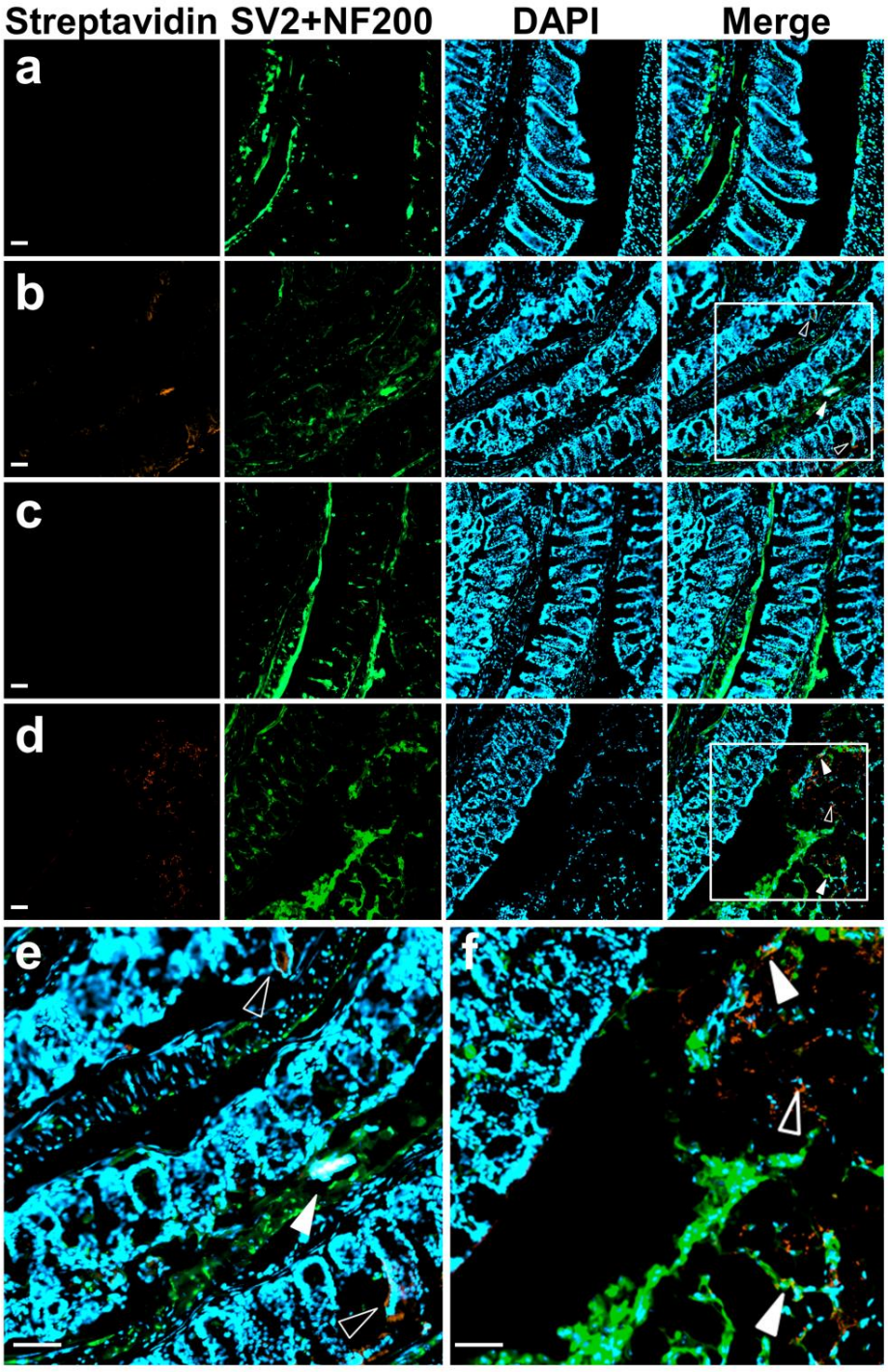
Streptavidin
SV2+NF200
DAPI
Merge
a
b
c
d
e
f

ASO treatment targeting the colon rescues the impaired transit time in young αS Tg mice

Once confirmed the uptake of ASO at the level of the desired target, we performed a treatment of young Tg mice for 7 days, with a dose of 50 µg per animal per day, distributed in 7 administrations for the rectal group every day at the same time, or through a continuous diffusion following the implant for the osmotic pump group. The ideal time to start the ASO treatment in our model would be before the onset of constipation, that means well before before 3 months of age. Because of the limitation in the use of osmotic pumps in young animals, which depends on body size, we chose to initiate the treatment at 10 weeks and to use an all-male group of mice for osmotic pumps, due to their larger size compared to females. Additionally, during the practice for rectal administration, females resulted easier to manipulate compared to males. Thus, we used an all-female group for this route. Tg mice were analyzed for WGTT before (Day 0) and after receiving the ASO for 7 days (Day 7). All mice were then sacrificed and the expression of total αS in the colon was assessed. At the end of a 7 days treatment, Tg mice which received the ASO displayed a significant reduction in their WGTT compared to controls which received PBS only and compared to the time point before starting the treatment, for both routes of administration. Specifically, within the rectal group the average transit time of Tg mice was 6.267 ± 0.081 h at Day 0 and 4.267 ± 0.185 h at Day 7 ($p<0.0001$), meaning 2 h of decrease, whereas for the pumps group it was 4.933 ± 0.376 h at time point 0 and 3.528 ± 0.2037 h after 7 days of ASO treatment ($p=0.0004$), which is about 1.5 h of decrease. The difference in the baseline of WGTT at Day 0 between females and males was known before starting the analysis as we have previously discussed and showed in Fig.3.2.

Moreover, compared to the respective PBS group at Day 7, ASO treatment resulted in a significant decrease in transit time for both routes of administration, with a WGTT of 4.266 ± 0.185 h vs 5.083 ± 0.417 h for the rectal group ($p=0.0362$) and 3.527 ± 0.204 h vs 4.418 ± 0.108 h for the pumps group ($p=0.0495$), which is about 50 min of decrease for both cases. To notice, for rectal administration, we observed a reduction in WGTT at Day 7 also for PBS treated Tg mice, although less pronounced with respect to the ASO treated group. We believe this was the result of repeated rectal administrations, consisting every time in 300 µL of liquid entering the distal colon, thus stimulating bowel movements for evacuation. For future experiments, one way to avoid this unwanted effect might be reducing the amount of solution given for each administration (Fig.3.14).

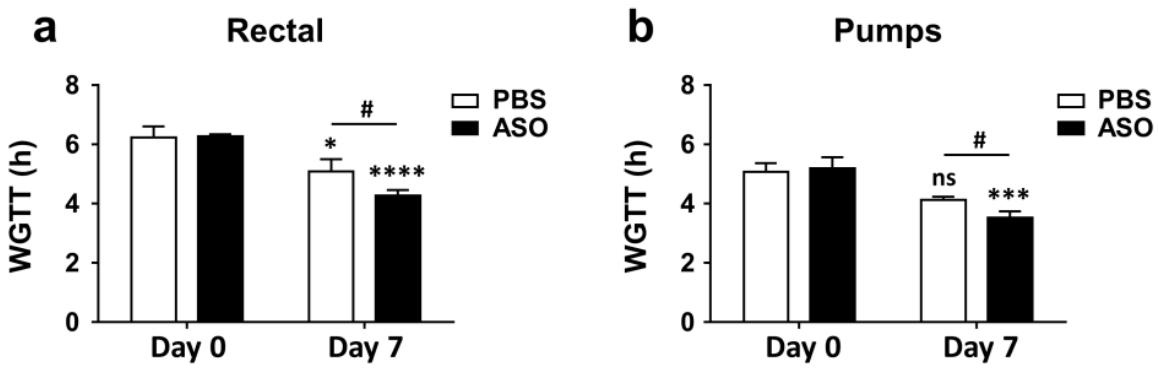

Fig.3.14 WGTT in young Tg mice ameliorated after 7 days of ASO treatment. WGTT was measured before starting the treatment (Day 0) and after 7 days of ASO treatment (Day 7), which was administred rectally (a) or through osmotic pumps (b). In both cases, 10 weeks old Tg mice received 50 µg of ASO per day or PBS for the control groups. Values on graphs are expressed as raw data and are given as the mean ± SEM (n=3-6 per group) . * $p<0.05$; *** $p<0.001$; # $p<0.05$, where * refers to comparisons between the same group at Day 7 versus Day 0, while # refers to comparisons between PBS and ASO group at Day 7; two-way ANOVA followed by Fischer's LSD test.

After WGTT measurement, mice were sacrificed and tissues were collected for further analysis. In order to investigate whether the ASO treatment reduced αS protein expression in the colon of Tg mice, in correlation with the changes observed for transit time, we performed immunoblot analysis on proximal and distal colon and checked for αS levels. Western blot assay showed that total αS level was reduced, although not significantly, of about 35% and 50% in rectally and pumps ASO treated mice compared to PBS controls only in the distal colon, but remained unchanged in the proximal colon (Fig.3.15).

Thus, this reduction in αS protein level in the colon after ASO treatment was sufficient to improve constipation in young Tg mice. We believe that repeating the experiment with a more congruous number of animals, increasing the ASO dosage and/or prolonging the treatment to 2 weeks or more may result in a significant inhibition of αS expression and possibly a better improvement in constipation.

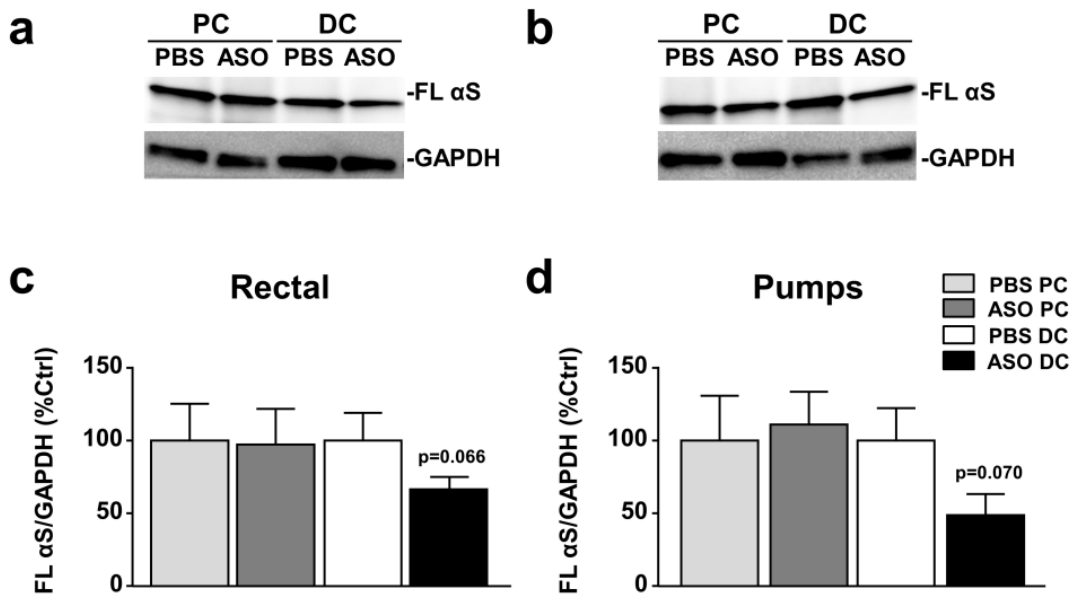

Fig.3.15 αS levels in the colon of young Tg mice after 7 days of ASO treatment. a, b) Immunoblot for αS in NP-40 soluble lisates from proximal colon (PC) and distal colon (DC) of Tg mice treated with PBS or ASO, rectally (a) or through osmotic pumps (b), for 7 days. c, d) Quantification of FL αS/GAPDH levels for rectal (c) or pumps (d) group. Although not significant, there is a reduction of αS monomer in both rectal (a, c) and pumps (b, d) treated mice in the distal colon and no change in the proximal colon. Values on graphs are expressed as % relative to PBS control and are given as the mean ± SEM (n=2/3 per group). one-way ANOVA.

Discussion

This research demonstrates that the PrP A53T αS Tg mice line G2-3 can be an extremely valuable model and to the best of our knowledge the only one at present, for studying constipation as it occurs in the prodromal phase of PD, meaning in absence of overt motor abnormalities and CNS neurodegeneration (Rota et al., 2019). This mouse model developed in 2002 (Lee et al., 2002b) is defined as a model of α-synucleinopathy, since it shows a non significant decrease of DA in the SN and no signs of dopaminergic neurodegeneration in the SN, two pathophysiological elements relevant for PD definition, probably because the central pathology develops so fast that the animal dies before the expected neurodegenerative process takes place. Concomitant with typical motor dysfunctions upon which diagnosis is still mainly made, PD patients experience a plethora of non motor symptoms affecting both the CNS and the PNS (Schapira et al., 2017). Among these, GI symptoms and specifically constipation represent an important feature of the prodromal phase of the pathology, since GI abnormalities can appear even decades before the onset of motor signs (Cersosimo et al., 2013). The relevance of studying constipation is also attributable to the fact that it affects 80% of PD patients, and after being diagnosed with constipation there is almost a 3-fold increased risk of developing PD (Abbott et al., 2001). Nevertheless, whether there is a direct pathogenic correlation between GI dysfunction and PD, still remains an open issue, in part because of the absence of appropriate animal models able to recapitulate the chronic and progressive evolution of PD pathological stages. In the G2-3 line constipation and GI deficits precede motor dysfunction and neurodegeneration in the CNS by at least 6 months. In fact from an early age (3 months), when the CNS is free of αS-driven neuropathology, these mice exhibit significant GI dysfunction, as here documented by a strong delay in GI transit time and concurrent abnormalities in stool formation, which result in the production of longer but less frequent fecal pellets. Because of the similarities in feces consistency, food intake ration, body size and stool weight between Tgs and age-matched nTg littermates, which allow us to exclude issues related to chow malabsorption, the transit delay observed in young Tg mice could underlie dysfunctional bowel movements which in turn could affect the processes of formation, propagation and expulsion of stools.

Consistently with this hypothesis, we found a reduced ability in contraction of longitudinal and circular muscle layers of the colon in young Tg mice, mainly dictated by a decreased neuronal transmission. In fact, while the colon muscles in Tg animals still contract normally when stimulated directly, the neuronal pathway supplying for such muscles was found to be deficient. Moreover, at 6 months of age this abnormal behavior progressively worsens, reaching a delay in GI transit time of more than 3 hours that was parallel to a further decrease in colon contractility, still in absence of any sign of CNS neurodegeneration.

As previously explained, the motor activity of the bowel in mice is mainly regulated by the cholinergic and tachykinergic systems for contraction, while the nitrergic system is the main regulator of gut muscle relaxation (Mang et al., 2002; Bornstein et al., 2004). When considering only the recruitment of postganglionic cholinergic motor neurons, electrically evoked contractions resulted decreased in αS Tg compared to nTg mice in both muscle layers (Fig. 3.4b). On the other hand, when stimulating specifically the nitrergic or the tachykinergic system, the muscle response was unchanged between the two groups, at all ages, confirming that GI delay in transit was mainly ascribable to a deficit in cholinergic-evoked muscle contractions and not to an excess of the relaxant response.

In line with this view, a more accurate immunofluorescence analysis revealed toxic αS accumulated in enteric neurons, including ChAT-positive and TH-positive types, of both myenteric and submucosal plexi in presymptomatic and diseased animals. Notably, in the same section, not all the neurons stained for αS aggregates, suggesting that accumulation of toxic αS is a progressive process in which not all neuronal populations present the same degree of susceptibility to αS insults, especially in the gut where neuronal biodiversity is remarkable (Furness, 2000). Besides the renowned central DA dysfunction linked to the classical parkinsonian motor features (Blesa and Przedborski, 2014), other neuronal systems are affected in PD and have been related to both motor and non motor dysfunctions, within and outside the CNS. In particular, the cholinergic system has been implicated in PD progression in relation to the occurrence of typical motor symptoms such as postural instability and gait disturbances (Karachi et al., 2010), but also to non motor symptoms such as dementia and cognitive deficits (Hilker et al., 2005; Bohnen et al., 2006), or REM sleep behavior disorder (Kotagal et al., 2012), hyposmia (Versace et al., 2017) and possibly dysphagia (Lee et al., 2015), which can all arise during preclinical PD. Interestingly, selective accumulation of LBs in cholinergic neurons within the nucleus basalis of Meynert, located in the basal forebrain, has been described to occur concomitantly with DA neuronal loss in the SN (Braak et al., 2003a). Also, treatment with cholinesterase inhibitors in PD patients appears to improve constipation and GI motility, supporting the importance of the cholinergic system in PD (Lepkowsky, 2018). In addition, DA exerts a negligible control of intestinal motility at the level of the lower digestive tract in humans (Bornstein et al., 2004), strongly suggesting the implication of other neurotransmitters for the development of GI dysfunction in PD. Hence, our observation of αS accumulating in TH-positive neurons has to be interpreted cautiously before considering these as DA neurons, since DA at this level could be a precursor for the other monoamines biosynthesis and its presence does not necessarly mean that the neuron in question uses DA as main neurotransmitter.

Furthermore, in the present study we demonstrate that the bowel dysfunctions shown by behavioral data and electrical recordings in Tg mice are supported by a robust biochemical basis since immunoblot analysis of the whole intestine revealed that young presymptomatic Tg mice

predominantly express αS transgene only in the colon with consequent selective accumulation in this tract of insoluble and phosphorylated HMW aggregates already at 3 months of age. Remarkably, while the distribution of αS transgene expression did not change with age, including after the onset of central pathology, the amount of insoluble aggregates increased over time, reaching a peak at 6 months of age, temporally matching the increased delay in GI transit and reduction of gut motility, and at the same time providing a strong molecular basis for the behavioral and functional GI abnormalities observed. This strong correlation between αS Tg expression and LB-like αS aggregates in the colon with bowel dysfunction is also confirmed by the absence of GI dysmotility in the ileum of Tg mice, where αS expression is minimal. Therefore αS inclusions, neuronal deficit and dysmotility at the level of the colon in this mouse model are tightly connected to αS overexpression in this site and represent an early sign of αS-driven dysfunction, without CNS involvement.

In PD patients, αS and LBs have been found in enteric neurons of both submucosal and myenteric plexi along the whole GI tract, including the colon (Böttner et al., 2012; Gelpi et al., 2014). An investigation led by Beach and coworkers found a rostro-caudal gradient for the accumulation of pS129-αS within the ENS with a higher incidence of LBs in the lower esophagus and submandibular gland, and lower in the colon and rectum (Beach et al., 2010). As previously mentioned, the involvement of the vagus nerve has been suggested as dissemination route of toxic αS along the gut-brain axis (Braak et al., 2003a). Nevertheless, the high incidence of aggregated αS in all the segments of the spinal cord suggests that other nerves may be implicated in αS propagation (Böttner et al., 2012; Pan-Montojo et al., 2012). In addition, several studies have indicated LBs presence in human colon biopsies as a possible diagnosis method for preclinical PD (Lebouvier et al., 2008; Pouclet et al., 2012; Shannon et al., 2012). Thus, whilst the expression of Tg αS at the gastric level still remains to be investigated in our mouse model, the early accumulation of toxic αS in the large intestine is sufficient in these mice to recapitulate distinctive features of GI dysfunction of human PD, making the G2-3 line an optimal paradigm to study constipation in premotor PD.

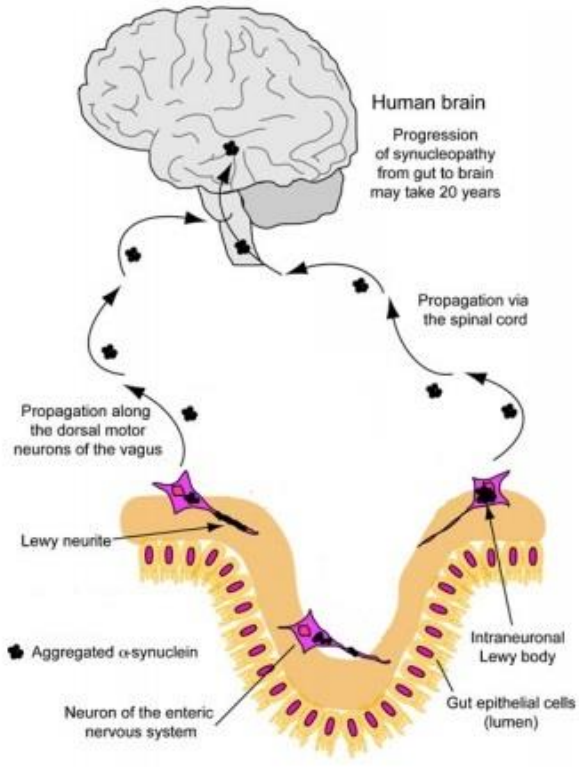

Fig.4.1 Putative spreading routes of α-synucleinopathy from the ENS to the brain in PD. Following a variety of possible exogenous and/or endogenous causes, αS accumulates in enteric neurons. This occurs in concomitance to the alteration of gut activity, which is observable by abnormal intestinal motility and constipation. Aggregated αS might be progressively released by damaged neurons, generating a cell-to-cell transmission responsible for the progression of the pathology, from the ENS toward the brain, along nuclei in vagus nerve and the spinal cord (Tomé et al., 2013).

In addition, and surprisingly, detergent-stable soluble oligomers of αS were also found in presymptomatic young 3 months old Tg mice and their accumulation increased over time. This represents a striking difference compared to the CNS, where αS soluble oligomers are only found at low level in adult (after 9 months) or diseased mice and are mainly associated with the microsomal vesicles fraction (Colla et al., 2012b, 2018). Furthermore, level of pS129-αS in the soluble fraction was also abundant, suggesting that αS pathobiology might differ between brain and gut, where modified HMW αS remains soluble for a longer period of time, instead of being promptly confined in insoluble inclusions.

Notably, truncated αS was present at all ages in the colon of Tg mice and it may be possible that two different truncated forms are present in the proximal and distal colon. Based on other recent data we published for the CNS, the accumulation of specific αS truncated species varies bewtween presymptomatic and diseased Tg mice (Colla et al., 2018). While the toxicity remains to be investigated, increased solubility of αS toxic species, either phosphorylated or truncated, may facilitate their spreading and tissue propagation. It would be interesting to compare the phosphorylation and truncation patterns in the ENS with the CNS of these mice.

Following this accurate characterization of PrP A53T αS Tg mice from a GI perspective and with a specific focus at the prodromal phase, our research moved toward a disease modifying approach. The therapeutic intervention was designed to be applied during the favorable time window we had identified, when Tg mice start showing an altered but not yet consistent transit time and in absence of any other sign at the central level. We used an ASO, administred to Tg mice at 10 weeks of age, for a continuous period of 7 days. As previously explained, ASOs are small, single-stranded sequences of nucleic acids able to bind to a complementary target mRNA, this binding causes the recruitment of RNase H enzyme (in our specific case) that in turn degrades the target RNA, thus preventing its translation into protein. This approach has been proven successful in preclinical trials for a variety of neurodegenerative diseases, characterized by the accumulation of specific proteins, such as αS in PD (DeVos and Miller, 2013). Several empiric data revealed a widespread distribution through brain and spinal cord following intraventricular or intrathecal administration followed by positive phenotypic effects, in mice (Devos et al., 2013; Lagier-tourenne et al., 2013), rats (Smith et al., 2006) and non human primates (Kordasiewicz et al., 2012; Rigo et al., 2014). Thanks to these results, ASOs made it to clinical trials in which intrathecal delivery led to positive outcomes in terms of safety and tolerability for patients affected by amyotrophic lateral sclerosis (Miller et al., 2013) and spinal muscular atrophy (Chiriboga et al., 2016). Very recently two ASOs finally received FDA approval, Nusinersen for spinal muscular atrophy (Aartsma-Rus, 2017) and Eteplirsen for Duchenne muscolar distorphy (Lim et al., 2017), representing the first cases of disease modifying therapy for neurodegenerative diseases. Other clinical trials are ongoing for Huntington's disease and spinocerebellar ataxias (Scoles and Pulst, 2018). It is important to underline that the therapeutic use of ASOs, especially for neurodegenerative diseases, is often based on the target of the whole protein level and not exclusively its toxic form. The overload of certain proteins plays a pivotal role for these pathologies both in their native and toxic forms (strictly interdependent), thus reducing the total amount of a protein can re-establish its altered homeostasis in a broader manner.

Although CNS-directed administration routes have been well tolerated so far, they remain quite invasive and for this reason researchers are pointing toward novel peripheral delivery methods for ASOs still utimately aimed at the nervous system, such as subcutaneous, oral and intranasal routes (Schoch and Miller, 2017). A number of studies carried out in mice showed that the peripheral administration (intraperitoneal or tail vein injection) of ASOs resulted in a positive effect at the neuronal level, in the PNS (Bogdanik et al., 2015) and in the CNS (Erickson et al., 2012; Farr et al., 2014), meaning that the ASOs were able to cross both the blood nerve barrier (BNB) and the blood brain barrier (BBB). Another study was able to individuate a saturable system (termed oligonucleotide transport system-1) which facilitates the transport of ASOs across the BBB in mice, following intravenous administration (Banks et al., 2001). The BNB, despite some differences in composition compared to the BBB, plays a similar role and can be equally effective

in excluding specific molecules from the neural parenchyma *in vivo* (Choi and Kim, 2008; Kanda, 2013), thus it is possible that they share also similar transport systems. Additionally, it is important to take into account that neurodegenerative diseases are often characterized by neuroinflammation and disruption of the vascular barriers (Tomkins et al., 2007; Winkler et al., 2014; Sweeney et al., 2018), including PD (Kortekaas et al., 2005; Shi et al., 2014). Such alterations might further facilitate the ASO crossing of neural barriers, in animal models and in human subjects. In order to extert its effects on the target mRNA an ASO has to overcome membrane barriers outside and inside the cell. Although the details of these mechanisms may differ across cell types and still require further investigations, it has been recently explained how the process of ASOs entering into cells requires the inclusion in lysosomal or endosomal compartments and the trafficking inside the cell (Geary et al., 2015).

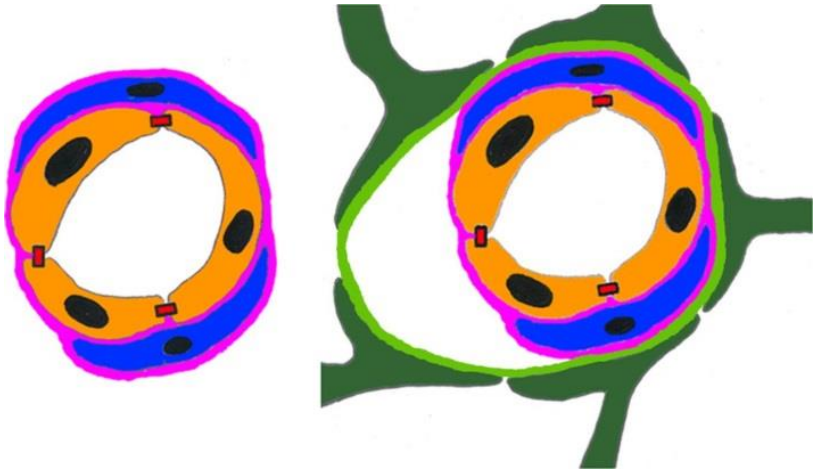

Fig.4.2 Schematic representation of BNB and BBB in radial section. Although the BNB (left) differs from the BBB (right) in some components, they both exert a similar function in controlling the passage of molecules aimed to protect the nerves and the brain, respectively. In both cases, endothelial cells (orange) are connected by tight junctions (red rectangles) and embedded in a single basement membrane (pink) with surrounding pericytes (blue). Only in the BBB, a second glial membrane (light green) wraps the just mentioned structures, still leaving a so called perivascular space, and an astrocytic endfoot layer (dark green) surrounds the outer surface (Kanda, 2013).

All this considered, we decided to perform rectal and intraperitoneal administration, the latter exploiting a continous drug diffusion through osmotic pumps, in order to target the colonic ENS with an ASO against αS, chosen among others following an *in vitro* evaluation. Since αS pathology in these mice is found in both submucosal and myenteric plexi, we speculated that we might have the chance to reach both by means of two routes. As expected, with both delivery methods the ASO reached neuronal and non neuronal cell types at the level of the colon, 6 h after rectal administration or 3 days after osmotic pump implant, indicating that it was absorbed by the tissue already at early time points. After this confirmation, we performed a 1 week ASO treatment in 10 weeks old Tgs, to evaluate whether local inhibition of αS protein expression could improve the deficit in GI transit. Very surprisingly, after only 7 days of treatment, Tg mice which received the ASO displayed a significant reduction in their WGTT compared to the values before starting the treatment and to the PBS control group, for both administration routes. Concomitant with the improvement in constipation, ASO treatment induced a reduction, although not significant, in the total level of αS in the distal colon but not in the proximal colon, for both delivery methods. The lack of inhibitory effect in the initial tract of the large intestine was not surprising, since the osmotic pump was positioned close to the distal colon and the rectal administration was not such invasive to reach consistently the upper tract of the colon. Nevertheless, since the distal colon in this mouse model is more affected in terms of αS deposition compared to the proximal segment, targeting this area appeared to be sufficient to obtain, directly or indirectly, an improvement of WGTT. The results obtained highlight the necessity to repeat the experiment on a larger sized group of mice. Nonetheless, our data positively support the correlation between GI behavior and αS levels in this PD mouse model. Although we cannot rule out the possibility of a CNS involvement since we have not measured the ASO levels in blood or cerebrospinal fluid, these data still indicate that reducing the total level of αS locally is associated with an improvement of GI transit time.

Thus, our study supports the hypothesis that lowering the total level of aggregation-prone proteins can be a successful disease modifying therapy against neurodegenerative diseases. We strongly believe that ASO therapy will make a difference for such disorders and that a peripheral approach not only is possible but also necessary, if we want to fully comprehend PD and analogous pathologies.

Conclusions and future directions

The overexpression of αS in the ENS of the PrP human A53T αS Tg mouse model line G2-3 causes constipation and colon contractile deficits. This enteric dysfunction represents an early symptom of α-synucleinopathy that occurs at least 6 months before motor symptoms and neurodegeneration in the CNS. From a biochemical point of view, such pathology is evident in the colon of these mice, where αS accumulates abnormally in different neuronal types of the ENS, in a time dependent manner. Thanks to the net spatio-temporal separation of the two αS-driven pathologies first in the colon and then in the CNS, this mouse line is a unique model to investigate the gut-brain connection in PD progression and to study GI dysfunction in prodromal PD. Promising results arised from targeting the colon through a brief ASO treatment, in terms of GI phenotype recovery and disease modifying therapy. Additional experiments are required in order to verify whether the putative positive effects of a longer ASO treatment may slow or halt the enteric α-synucleinopathy from reaching the brain. In parallel, ongoing research is investigating the state of inflammation and permeability of the colon in A53T αS Tg presymptomatic mice, in order to evaluate the possible impact of a peripheral proinflammatory condition on αS behavior in the ENS.

Acknowledgments

I thank the Morelli-Rotary Fundation of Bergamo which funded all the experiments with antisense oligonucleotides *in vitro* and *in vivo*. I thank Prof. Farah for his hospitality at Johns Hopkins School of Medicine. I thank Prof. Blandizzi and his team from University of Pisa for the experiments on electrical recording. I thank Prof. Capsoni from University of Ferrara for her suggestions on behavioral analysis.

References

Aartsma-Rus A (2017) FDA Approval of Nusinersen for Spinal Muscular Atrophy Makes 2016 the Year of Splice. Nucleic Acid Ther 27:67–69.

Abbott R, Petrovitch H, White L, Masaki K, Tanner C, Curb J, Grandinetti A, Blanchette P, Popper J, Ross G (2001) Frequency of bowel movements and the future risk of Parkinson's disease. Neurology 57:456–462.

Abeliovich A, Schmitz Y, Fariñas I, Choi-Lundberg D, Ho WH, Castillo PE, Shinsky N, Verdugo JM, Armanini M, Ryan A, Hynes M, Phillips H, Sulzer D, Rosenthal A (2000) Mice lacking α-synuclein display functional deficits in the nigrostriatal dopamine system. Neuron 25:239–252.

Anderson JP et al. (2006) Phosphorylation of Ser-129 is the dominant pathological modification of alpha-synuclein in familial and sporadic lewy body disease. J Biol Chem 281:29739–29752.

Andrews CN, Storr M (2011) The pathophysiology of chronic constipation. Can J Gastroenterol 25 Suppl B:16B–21B.

Antonioli L, Giron MC, Colucci R, Pellegrini C, Sacco D, Caputi V, Orso G, Tuccori M, Scarpignato C, Blandizzi C, Fornai M (2014) Involvement of the P2X7 purinergic receptor in colonic motor dysfunction associated with bowel inflammation in rats. PLoS One 9:1–20.

Antonioli L, Pellegrini C, Fornai M, Tirotta E, Gentile D, Benvenuti L, Giron MC, Caputi V, Marsilio I, Orso G, Bernardini N, Segnani C, Ippolito C, Csóka B, Németh ZH, Haskó G, Scarpignato C, Blandizzi C, Colucci R (2017) Colonic motor dysfunctions in a mouse model of high-fat diet-induced obesity: an involvement of A2Badenosine receptors. Purinergic Signal 13:497–510.

Appel-Cresswell S, Vilarino-Guell C, Encarnacion M, Sherman H, Yu I, Shah B, Weir D, Thompson C, Szu-Tu C, Trinh J, Aasly JO, Rajput A, Rajput AH, Jon Stoessl A, Farrer MJ (2013) Alpha-synuclein p.H50Q, a novel pathogenic mutation for Parkinson's disease. Mov Disord 28:811–813.

Arima K (1999) Cellular co-localization of phosphorylated tau and NACP/alpha-synuclein epitopes in Lewy bodies in sporadic Parkinson's disease and in dementia with Lewy bodies. Brain Res:53–61.

Asi YT, Simpson JE, Heath PR, Wharton SB, Lees AJ, Revesz T, Houlden H, Holton JL (2014) Alpha-synuclein mRNA expression in oligodendrocytes in MSA. Glia 62:964–970.

Banks WA, Farr SA, Butt W, Kumar VB, Franko MW, Morley JE (2001) Delivery across the Blood-Brain Barrier of Antisense Directed against Amyloid Beta: Reversal of Learning and Memory Deficits in Mice Overexpressing Amyloid Precursor Protein. J Pharmacol Exp Ther 297:1113–1121.

Barbeau (1969) L-Dopa Therapy in Parkinson's Disease: A Critical Review of Nine Years' Experience. Can Med Assoc J 101:59–68.

Barrett PJ, Timothy Greenamyre J (2015) Post-translational modification of α-synuclein in Parkinson's disease. Brain Res 1628:247–253.

Bartels T, Choi JG, Selkoe DJ (2011) Alpha-Synuclein occurs physiologically as a helically folded tetramer that resists aggregation. Nature 477:107–110.

Bartels T, Kim NC, Luth ES, Selkoe DJ (2014) N-alpha-acetylation of α-synuclein increases its helical folding propensity, GM1 binding specificity and resistance to aggregation. PLoS One 9:1–10.

Beach TG, Adler CH, Sue LI, Vedders L, Lue LF, White CL, Akiyama H, Caviness JN, Shill HA, Sabbagh MN, Walker DG (2010) Multi-organ distribution of phosphorylated alpha-synuclein histopathology in subjects with Lewy body disorders. Acta Neuropathol 119:689–702.

Bellucci A, Navarria L, Zaltieri M, Falarti E, Bodei S, Sigala S, Battistin L, Spillantini M, Missale C, Spano P (2011) Induction of the unfolded protein response by α-synuclein in experimental models of Parkinson's disease: α-Synuclein accumulation induces the UPR. J Neurochem 116:588–605.

Bendor J, Logan T, Edwards RH (2014) The Function of α-Synuclein. Neuron 79.

Berardelli A et al. (2013) EFNS/MDS-ES recommendations for the diagnosis of Parkinson's disease. Eur J Neurol 20:16–34.

Beyer K, Ariza A (2013) α-Synuclein posttranslational modification and alternative splicing as a trigger for neurodegeneration. Mol Neurobiol 47:509–524.

Binolfi A, Rasia RM, Bertoncini CW, Ceolin M, Zweckstetter M, Griesinger C, Jovin TM, Fernández CO (2006) Interaction of α-Synuclein with Divalent Metal Ions Reveals Key Differences: A Link between Structure, Binding Specificity and Fibrillation Enhancement. J Am Chem Soc 128:9893–9901.

Blandini F, Nappi G, Tassorelli C, Martignoni E (2000) Functional changes of the basal ganglia circuitry in Parkinson's disease. Prog Neurobiol 62:63–88.

Blesa J, Przedborski S (2014) Parkinson's disease: animal models and dopaminergic cell vulnerability. Front Neuroanat 8:1–12.

Bogdanik LP, Osborne MA, Davis C, Martin WP, Austin A, Rigo F, Bennett CF, Lutz CM (2015) Systemic, postsymptomatic antisense oligonucleotide rescues motor unit maturation delay in a new mouse model for type II/III spinal muscular atrophy. Proc Natl Acad Sci 112:5863–5872.

Bohnen N, Albin R (2011) The Cholinergic System in Parkinson's Disease. Behav Brain Res 221:564–573.

Bohnen NI, Kaufer DI, Hendrickson R, Ivanco LS, Lopresti BJ, Constantine GM, Mathis CA, Davis JG, Moore RY, DeKosky ST (2006) Cognitive correlates of cortical cholinergic denervation in Parkinson's disease and parkinsonian dementia. J Neurol 253:242–247.

Bornstein JC, Costa M, Grider JR (2004) Enteric motor and interneuronal circuits controlling motility. Neurogastroenterol Motil 16:34–38.

Böttner M, Zorenkov D, Hellwig I, Barrenschee M, Harde J, Fricke T, Deuschl G, Egberts J-H, Becker T, Fritscher-Ravens A, Arlt A, Wedel T (2012) Expression pattern and localization of alpha-synuclein in the human enteric nervous system. Neurobiol Dis 48:474–480.

Bousset L, Pieri L, Ruiz-Arlandis G, Gath J, Jensen PH, Habenstein B, Madiona K, Olieric V, Böckmann A, Meier BH, Melki R (2013) Structural and functional characterization of two alpha-synuclein strains. Nat Commun 4.

Braak H, Del Tredici K, Rüb U, De Vos RAI, Jansen Steur ENH, Braak E (2003a) Staging of brain pathology related to sporadic Parkinson's disease. Neurobiol Aging 24:197–211.

Braak H, Rüb U, Gai WP, Del Tredici K (2003b) Idiopathic Parkinson's disease: possible routes by which vulnerable neuronal types may be subject to neuroinvasion by an unknown pathogen. J Neural Transm 110:517–536.

Breda C, Nugent ML, Estranero JG, Kyriacou CP, Outeiro TF, Steinert JR, Giorgini F (2015) Rab11 modulates α-synuclein-mediated defects in synaptic transmission and behaviour. Hum Mol Genet 24:1077–1091.

Buell AK, Galvagnion C, Gaspar R, Sparr E, Vendruscolo M, Knowles TPJ, Linse S, Dobson CM (2014) Solution conditions determine the relative importance of nucleation and growth processes in α-synuclein aggregation. Proc Natl Acad Sci 111:7671–7676.

Burai R, Ait-bouziad N, Chiki A, Lashuel H (2015) Elucidating the role of site-specific nitration of alpha-

synuclein in the pathogenesis of Parkinson's disease via protein semisynthesis and mutagenesis. J Am Chem Soc 137:5041–5052.

Burré J, Sharma M, Sudhof TC (2015) Definition of a Molecular Pathway Mediating α-Synuclein Neurotoxicity. J Neurosci 35:5221–5232.

Burré J, Sharma M, Südhof TC (2014) α-Synuclein assembles into higher-order multimers upon membrane binding to promote SNARE complex formation. Proc Natl Acad Sci 111:E4274–E4283.

Burré J, Sharma M, Tsetsenis T, Buchman V, Etherton MR, Sudhof TC (2010) Alpha-Synuclein Promotes SNARE-Complex Assembly in Vivo and in Vitro. Science 329:1663–1667.

Burré J, Vivona S, Diao J, Sharma M, Brunger AT, Südhof TC (2013) Properties of native brain alpha-synuclein. Nature 498:4–6.

Bussell R, Eliezer D (2004) Effects of Parkinson's disease-linked mutations on the structure of lipid-associated α-synuclein. Biochemistry 43:4810–4818.

Cartelli D, Aliverti A, Barbiroli A, Santambrogio C et al. (2016) α-Synuclein is a Novel Microtubule Dynamase. Sci Rep 6:33289.

Cersosimo MG, Raina GB, Pecci C, Pellene A, Calandra CR, Gutiérrez C, Micheli FE, Benarroch EE (2013) Gastrointestinal manifestations in Parkinson's disease: Prevalence and occurrence before motor symptoms. J Neurol 260:1332–1338.

Chen L, Periquet M, Wang X, Negro A, McLean PJ, Hyman BT, Feany MB (2009) Tyrosine and serine phosphorylation of alpha-synuclein have opposing effects on neurotoxicity and soluble oligomer formation. J Clin Invest 119:3257–3265.

Chen SW, Drakulic S, Deas E, Ouberai M, Aprile FA, Arranz R, Ness S, Roodveldt C, Guilliams T, De-Genst EJ, Klenerman D, Wood NW, Knowles TPJ, Alfonso C, Rivas G, Abramov AY, Valpuesta JM, Dobson CM, Cremades N (2015) Structural characterization of toxic oligomers that are kinetically trapped during α-synuclein fibril formation. Proc Natl Acad Sci 112:E1994–E2003.

Chiriboga CA, Swoboda KJ, Darras BT, Iannaccone ST, Montes J, De Vivo DC, Norris DA, Bennett CF, Bishop KM (2016) Results from a phase 1 study of nusinersen (ISIS-SMN Rx) in children with spinal muscular atrophy. Neurology 890–897.

Choi B-K, Choi M-G, Kim J-Y, Yang Y, Lai Y, Kweon D-H, Lee NK, Shin Y-K (2013) Large α-synuclein oligomers inhibit neuronal SNARE-mediated vesicle docking. Proc Natl Acad Sci 110:4087–4092.

Choi YK, Kim K (2008) Blood-neural barrier: its diversity and coordinated cell-to-cell communication. BMB Rep 41:345–352.

Chung CY, Khurana V, Auluck P et al. (2013) Identification and Rescue of α-Synuclein Toxicity in Parkinson Patient-Derived Neurons. Science 342: 983–987.

Colla E, Coune P, Liu Y, Pletnikova O, Troncoso JC, Iwatsubo T, Schneider BL, Lee MK (2012a) Endoplasmic Reticulum Stress Is Important for the Manifestations of Alpha-Synucleinopathy In Vivo. J Neurosci 32:3306–3320.

Colla E, Jensen PH, Pletnikova O, Troncoso JC, Glabe C, Lee MK (2012b) Accumulation of Toxic Alpha-Synuclein Oligomer within Endoplasmic Reticulum Occurs in Alpha-Synucleinopathy In Vivo. J Neurosci 32:3301–3305.

Colla E, Panattoni G, Ricci A, Rizzi C, Rota L, Carucci N, Valvano V, Gobbo F, Capsoni S, Lee MK, Cattaneo A (2018) Toxic properties of microsome-associated alpha-synuclein species in mouse primary neurons. Neurobiol Dis 111:36–47.

Cooper AA, Gitler AD, Cashikar A, Haynes CM, Hill KJ, Bhullar B, Liu K, Xu K, Strathearn KE, Liu F, Cao S, Caldwell KA, Caldwell GA, Marsischky G, Kolodner RD, Labaer J, Rochet J-C, Bonini NM, Lindquist S (2006) Alpha-synuclein blocks ER-Golgi traffic and Rab1 rescues neuron loss in Parkinson's models. Science 313:324–328.

Cremades N, Cohen SIA, Deas E, Abramov AY, Chen AY, Orte A, Sandal M, Clarke RW, Dunne P, Aprile FA, Bertoncini CW, Wood NW, Knowles TPJ, Dobson CM, Klenerman D (2012) Direct Observation of the Interconversion of Normal and Toxic Forms of α-Synuclein. Cell 149:1048–1059.

Danzer KM, Haasen D, Karow AR, Moussaud S, Habeck M, Giese A, Kretzschmar H, Hengerer B, Kostka M (2007) Different Species of α-Synuclein Oligomers Induce Calcium Influx and Seeding. J Neurosci 27:9220–9232.

de Lau LML, Breteler MMB (2006) Epidemiology of Parkinson's disease. Lancet Neurol 5:525–535.

de Rijk M, Breteler M, Graveland G, Ott A, Grobbee D, van der Meché F, Hofman A (1995) Prevalence of Parkinson's disease in the elderly: the Rotterdam Study. Neurology 45:2143–2146.

Dettmer U, Newman AJ, Soldner F, Luth ES, Kim NC, von Saucken VE, Sanderson JB, Jaenisch R, Bartels T, Selkoe D (2015a) Parkinson-causing alpha-synuclein missense mutations shift native tetramers to monomers as a mechanism for disease initiation. Nat Commun 6:7314.

Dettmer U, Newman AJ, von Saucken VE, Bartels T, Selkoe D (2015b) KTKEGV repeat motifs are key mediators of normal alpha-synuclein tetramerization: their mutation causes excess monomers and neurotoxicity. Proc Natl Acad Sci 112:9596–9601.

Devi L, Raghavendran V, Prabhu BM, Avadhani NG, Anandatheerthavarada HK (2008) Mitochondrial Import and Accumulation of α-Synuclein Impair Complex I in Human Dopaminergic Neuronal Cultures and Parkinson Disease Brain. J Biol Chem 283:9089–9100.

Devos SL, Goncharoff DK, Chen G, Kebodeaux CS, Yamada K, Stewart FR, Schuler DR, Maloney SE, Wozniak DF, Rigo F, Bennett CF, Cirrito JR, Holtzman DM, Miller TM (2013) Antisense Reduction of Tau in Adult Mice Protects against Seizures. Neurobiol Dis 33:12887–12897.

DeVos SL, Miller TM (2013) Antisense Oligonucleotides: Treating Neurodegeneration at the Level of RNA. Neurotherapeutics 10:486–497.

Di Maio R, Barrett PJ, Hoffman EK, Barrett CW, Zharikov A, Borah A, Hu X, McCoy J, Chu CT, Burton EA, Hastings TG, Greenamyre JT (2016) α-Synuclein binds to TOM20 and inhibits mitochondrial protein import in Parkinson's disease. Sci Transl Med 8(342):78.

Diao J, Burré J, Vivona S, Cipriano DJ, Sharma M, Kyoung M, Südhof TC, Brunger AT (2013) Native alpha-synuclein induces clustering of synaptic-vesicle mimics via binding to phospholipids and synaptobrevin-2/VAMP2. Elife 2.

Diogenes MJ, Dias RB, Rombo DM, Vicente Miranda H, Maiolino F, Guerreiro P, Nasstrom T, Franquelim HG, Oliveira LMA, Castanho MARB, Lannfelt L, Bergstrom J, Ingelsson M, Quintas A, Sebastiao AM, Lopes LV, Outeiro TF (2012) Extracellular α-Synuclein Oligomers Modulate Synaptic Transmission and Impair LTP Via NMDA-Receptor Activation. J Neurosci 32:11750–11762.

Drolet RE, Cannon JR, Montero L, Greenamyre JT (2009) Chronic rotenone exposure reproduces Parkinson's disease gastrointestinal neuropathology. Neurobiol Dis 36:96–102.

Duda JE, Giasson BI, Chen Q, Gur TL, Hurtig HI, Stern MB, Gollomp SM, Ischiropoulos H, Lee VMY, Trojanowski JQ (2000) Widespread nitration of pathological inclusions in neurodegenerative synucleinopathies. Am J Pathol 157:1439–1445.

El-Agnaf OM, Bodles AM, Guthrie DJ, Harriott P, Irvine GB (1998) The N-terminal region of non-A beta component of Alzheimer's disease amyloid is responsible for its tendency to assume beta-sheet and aggregate to form fibrils. Eur J Biochem 258:157–163.

Erickson MA, Niehoffc ML, Farr SA, Morley JE, Dillman LA, Lynch MK, Banks WA (2012) Peripheral Administration of Antisense Oligonucleotides Targeting the Amyloid-beta Protein Precursor Reverses AbetaPP and LRP-1 Overexpression in the Aged SAMP8 Mouse Brain. J Alzheimers Dis 28:951–960.

Erro R, Picillo M, Vitale C, Amboni M, Moccia M, Longo K, Cozzolino A, Giordano F, De Rosa A, De Michele G, Pellecchia MT, Barone P (2013) Non-motor symptoms in early Parkinson's disease: a 2-year follow-up study on previously untreated patients. J Neurol Neurosurg Psychiatry 84:14–17.

Evers MM, Toonen LJA, van Roon-Mom WMC (2015) Antisense oligonucleotides in therapy for neurodegenerative disorders. Adv Drug Deliv Rev 87:90–103.

Fares M-B, Ait-Bouziad N, Dikiy I, Mbefo MK, Jovi i A, Kiely A, Holton JL, Lee S-J, Gitler AD, Eliezer D, Lashuel HA (2014) The novel Parkinson's disease linked mutation G51D attenuates in vitro aggregation and membrane binding of α-synuclein, and enhances its secretion and nuclear localization in cells. Hum Mol Genet 23:4491–4509.

Farr SA, Erickson MA, Niehoffb ML, Banks WA, Morley JE (2014) Central and Peripheral Administration of Antisense Oligonucleotide Targeting Amyloid Precursor Protein Improves Learning and Memory and Reduces Neuroinflammatory Cytokines in Tg2576 (APPswe) Mice. J Alzheimers Dis 40:1005–1016.

Fasano A, Visanji NP, Liu LWC, Lang AE, Pfeiffer RF (2015) Gastrointestinal dysfunction in Parkinson's disease. Lancet Neurol 14:625–639.

Fauvet B, Mbefo MK, Fares M-B, Desobry C, Michael S, Ardah MT, Tsika E, Coune P, Prudent M, Lion N, Eliezer D, Moore DJ, Schneider B, Aebischer P, El-Agnaf OM, Masliah E, Lashuel HA (2012) Alpha-Synuclein in Central Nervous System and from Erythrocytes, Mammalian Cells, and Escherichia coli Exists Predominantly as Disordered Monomer. J Biol Chem 287:15345–15364.

Feany MB, Bender WW (2000) A Drosophila model of Parkinson's disease. Nature 404:394–398.

Follmer C, Coelho-Cerqueira E, Yatabe-Franco DY, Araujo GDT, Pinheiro AS, Domont GB, Eliezer D (2015) Oligomerization and Membrane-binding Properties of Covalent Adducts Formed by the Interaction of α-Synuclein with the Toxic Dopamine Metabolite 3,4-Dihydroxyphenylacetaldehyde (DOPAL). J Biol Chem 290:27660–27679.

Forsythe P, Bienenstock J, Kunze WA (2014) Vagal Pathways for Microbiome-Brain-Gut Axis Communication. Adv Exp Med Biol 817:115–133.

Fortin DL (2004) Lipid Rafts Mediate the Synaptic Localization of Alpha-Synuclein. J Neurosci 24:6715–6723.

Fredenburg RA, Rospigliosi C, Meray RK, Kessler JC, Lashuel HA, Eliezer D, Lansbury PT (2007) The Impact of the E46K Mutation on the Properties of α-Synuclein in Its Monomeric and Oligomeric States. Biochemistry 46:7107–7118.

Fujiwara H, Hasegawa M, Dohmae N, Kawashima A, Masliah E, Goldberg MS, Shen J, Takio K, Iwatsubo T (2002) Alpha-Synuclein Is Phosphorylated in Synucleinopathy Lesions. Nat Cell Biol 4:160–164.

Furness JB (2000) Types of neurons in the enteric nervous system. J Auton Nerv Syst 81:87–96.

Furness JB (2006) Novel gut afferents: Intrinsic afferent neurons and intestinofugal neurons. Aut Neurosci 125:81–85.

Furness JB, Callaghan BP, Rivera LR, Cho H (2014) The Enteric Nervous System and Gastrointestinal Innervation: Integrated Local and Central Control. Adv Exp Med Biol 817:39–71.

Fusco G, Chen SW, Williamson PTF, Cascella R, Perni M, Jarvis JA, Cecchi C, Vendruscolo M, Chiti F,

Cremades N, Ying L, Dobson CM, De Simone A (2017) Structural basis of membrane disruption and cellular toxicity by α-synuclein oligomers. Science 358:1440–1443.

Galvagnion C, Brown JWP, Ouberai MM, Flagmeier P, Vendruscolo M, Buell AK, Sparr E, Dobson CM (2016) Chemical properties of lipids strongly affect the kinetics of the membrane-induced aggregation of alpha-synuclein. Proc Natl Acad Sci 113:7065–7070.

Gardai SJ et al. (2013) Elevated Alpha-Synuclein Impairs Innate Immune Cell Function and Provides a Potential Peripheral Biomarker for Parkinson's Disease. PLoS One 8:1–21.

Geary RS, Norris D, Yu R, Bennett CF (2015) Pharmacokinetics, biodistribution and cell uptake of antisense oligonucleotides. Adv Drug Deliv Rev 87:46–51.

Gelpi E, Navarro-Otano J, Tolosa E, Gaig C, Compta Y, Rey MJ, Martí MJ, Hernández I, Valldeoriola F, Reñé R, Ribalta T (2014) Multiple organ involvement by alpha-synuclein pathology in lewy body disorders. Mov Disord 29.

George JM, Jin H, Woods WS, Clayton DF (1995) Characterization of a novel protein regulated during the critical period for song learning in the zebra finch. Neuron 15:361–372.

Giasson BI, Duda JE, Murray I V, Chen Q, Souza JM, Hurtig HI, Ischiropoulos H, Trojanowski JQ, Lee VM (2000) Oxidative damage linked to neurodegeneration by selective alpha-synuclein nitration in synucleinopathy lesions. Science 290:985–989.

Gitler AD, Bevis BJ, Shorter J, Strathearn KE, Hamamichi S, Su LJ, Caldwell KA, Caldwell GA, Rochet J-C, McCaffery JM, Barlowe C, Lindquist S (2008) The Parkinson's disease protein alpha-synuclein disrupts cellular Rab homeostasis. Proc Natl Acad Sci U S A 105:145–150.

Goedert M, Spillantini MG, Del Tredici K, Braak H (2013) 100 years of Lewy pathology. Nat Rev Neurol 9:13–24.

Goldman JG, Goetz CG (2007) History of Parkinson's disease. Handb Clin Neurol 83:107–128.

Guo JL, Covell DJ, Daniels JP, Iba M, Stieber A, Zhang B, Riddle DM, Kwong LK, Xu Y, Trojanowski JQ, Lee VMY (2013) Distinct α-Synuclein Strains Differentially Promote Tau Inclusions in Neurons. Cell 154:103–117.

Hallet PJ, McLean JR, Kartunen A, Langston JW, Isacson O (2012) Alpha-synuclein overexpressing transgenic mice show internal organ pathology and autonomic deficits. Neurobiol Dis 47:258–267.

Hawkes CH, Del Tredici K, Braak H (2009) Parkinson's disease: The dual hit theory revisited. Ann N Y Acad Sci 1170:615–622.

Hilker R, Thomas A V., Klein JC, Weisenbach S, Kalbe E, Burghaus L, Jacobs AH, Herholz K, Heiss WD (2005) Dementia in Parkinson disease: Functional imaging of cholinergic and dopaminergic pathways. Neurology 65:1716–1722.

Holmqvist S, Chutna O, Bousset L, Aldrin-Kirk P, Li W, Björklund T, Wang ZY, Roybon L, Melki R, Li JY (2014) Direct evidence of Parkinson pathology spread from the gastrointestinal tract to the brain in rats. Acta Neuropathol 128:805–820.

Ibáñez P, Bonnet A-M, Débarges B, Lohmann E, Tison F, Agid Y, Dürr A, Brice A, Pollak P (2004) Causal relation between alpha-synuclein locus duplication as a cause of familial Parkinson's disease. Lancet 364:1169–1171.

Jensen MB, Bhatia VK, Jao CC, Rasmussen JE, Pedersen SL, Jensen KJ, Langen R, Stamou D (2011) Membrane curvature sensing by amphipathic helices: A single liposome study using α-synuclein and annexin B12. J Biol Chem 286:42603–42614.

Jiang Z, de Messieres M, Lee JC (2013) Membrane Remodeling by α-Synuclein and Effects on Amyloid Formation. J Am Chem Soc 135:15970–15973.

Jo E, Darabie AA, Han K, Tandon A, Fraser PE, McLaurin J (2004) α-Synuclein-synaptosomal membrane interactions: Implications for fibrillogenesis. Eur J Biochem 271:3180–3189.

Kalia L V., Lang AE (2015) Parkinson's disease. Lancet 386:896–912.

Kanda T (2013) Biology of the blood-nerve barrier and its alteration in immune mediated neuropathies. J Neurol Neurosurg Psychiatry 84:208–212.

Karachi C, Grabli D, Bernard FA, Tandé D, Wattiez N, Belaid H, Bardinet E, Prigent A, Nothacker HP, Hunot S, Hartmann A, Lehéricy S, Hirsch EC, François C (2010) Cholinergic mesencephalic neurons are involved in gait and postural disorders in Parkinson disease. J Clin Invest 120:2745–2754.

Kaufmann H, Norcliffe-Kaufmann L, Palma J-A, Biaggioni I, Low PA, Singer W, Goldstein DS, Peltier AC, Shibao CA, Gibbons CH, Freeman R, Robertson D (2017) The Natural History of Pure Autonomic Failure: a U.S. Prospective Cohort. Ann Neurol 81:287–297.

Kaufmann TJ, Harrison PM, Richardson MJE, Pinheiro TJT, Wall MJ (2016) Intracellular soluble α-synuclein oligomers reduce pyramidal cell excitability: Impact of α synuclein on neocortical neurons. J Physiol 594:2751–2772.

Khalaf O, Fauvet B, Oueslati A, Dikiy I, Mahul-Mellier AL, Ruggeri FS, Mbefo MK, Vercruysse F, Dietler G, Lee SJ, Eliezer D, Lashuel HA (2014) The H50Q mutation enhances alpha-synuclein aggregation, secretion, and toxicity. J Biol Chem 289:21856–21876.

Klein C, and Westernberger A (2012) Genetics of Parkinson's disease. Cold Spring Harb Perspect Med 2:1–15.

Kordasiewicz HB, Stanek LM, Wancewicz E V, Mazur C, Melissa M, Pytel K a, Artates JW, Weiss A, Cheng SH, Shihabuddin LS, Hung G, Bennett CF, Cleveland DW (2012) Sustained Therapeutic Reversal of Huntington's Disease by Transient Repression of Huntingtin Synthesis. Neuron 74:1031–1044.

Kordower JH, Chu Y, Hauser RA, Freeman TB, Olanow CW (2008a) Lewy body-like pathology in long-term embryonic nigral transplants in Parkinson's disease. Nat Med 14:504–506.

Kordower JH, Chu Y, Hauser RA, Olanow CW, Freeman TB (2008b) Transplanted dopaminergic neurons develop PD pathologic changes: a second case report. Mov Disord 23:2303–2306.

Kordower JH, Dodiya HB, Kordower AM, Terpstra B, Madhavan L, Sortwell C, Steece-collier K, Timothy J (2012) Transfer of host-derived alpha-synuclein to grafted dopaminergic neurons in rat. Neurobiol Dis 43:552–557.

Kortekaas R, Leenders KL, Oostrom JCH Van, Vaalburg W, Bart J, Willemsen ATM, Hendrikse NH (2005) Blood-Brain Barrier Dysfunction in Parkinsonian Midbrain In Vivo. Ann Neurol 57:176–179.

Kotagal V, Albin RL, Müller MLTM, Koeppe RA, Chervin RD, Frey KA, Bohnen NI (2012) Symptoms of Rapid Eye Movement Sleep Behavior Disorder are Associated with Cholinergic Denervation in Parkinson Disease. Ann Neurol 71:560–568.

Kravitz A V, Freeze BS, Parker PRL, Kay K, Myo T, Deisseroth K, Kreitzer AC (2013) Regulation of parkinsonian motor behaviors by optogenetic control of basal ganglia circuity. Nature 466:622–626.

Krüger R, Kuhn W, Müller T, Woitalla D, Graeber M, Kösel S, Przuntek H, Epplen JT, Schöls L, Riess O (1998) Ala30Pro mutation in the gene encoding alpha-synuclein in Parkinson's disease. Nat Genet 18:106–108.

Krumova P, Meulmeester E, Garrido M, Tirard M, Hsiao HH, Bossis G, Urlaub H, Zweckstetter M, Kügler S, Melchior F, Bähr M, Weishaupt JH (2011) Sumoylation inhibits alpha-synuclein aggregation and toxicity. J Cell Biol 194:49–60.

Kunadt M et al. (2015) Extracellular vesicle sorting of α-Synuclein is regulated by sumoylation. Acta Neuropathol 129:695–713.

Kuo YM, Li Z, Jiao Y, Gaborit N, Pani AK, Orrison BM, Bruneau BG, Giasson BI, Smeyne RJ, Gershon MD, Nussbaum RL (2010) Extensive enteric nervous system abnormalities in mice transgenic for artificial chromosomes containing Parkinson disease-associated alpha-synuclein gene mutations precede central nervous system changes. Hum Mol Genet 19:1633–1650.

Lagier-tourenne C, Baughn M, Rigo F, Sun S, Liu P, Li H, Jiang J (2013) Targeted degradation of sense and antisense C9orf72 RNA foci as therapy for ALS and frontotemporal degeneration. Proc Natl Acad Sci U S A 110:1–10.

Lakso M, Vartiainen S, Moilanen A-M, Sirviö J, Thomas JH, Nass R, Blakely RD, Wong G (2003) Dopaminergic neuronal loss and motor deficits in Caenorhabditis elegans overexpressing human α-synuclein. J Neurochem 86:165–172.

Larsen KE, Schmitz Y, Troyer MD, Mosharov E, Dietrich P, Quazi AZ, Savalle M, Nemani V, Chaudhry FA, Edwards RH, Stefanis L, Sulzer D (2006) Alpha-Synuclein Overexpression in PC12 and Chromaffin Cells Impairs Catecholamine Release by Interfering with a Late Step in Exocytosis. J Neurosci 26:11915–11922.

Larson ME, Greimel SJ, Amar F, LaCroix M, Boyle G, Sherman MA, Schley H, Miel C, Schneider JA, Kayed R, Benfenati F, Lee MK, Bennett DA, Lesné SE (2017) Selective lowering of synapsins induced by oligomeric α-synuclein exacerbates memory deficits. Proc Natl Acad Sci 114:4648-4657.

Lashuel HA, Overk CR, Oueslati A, Masliah E (2013) The many faces of α-synuclein: from structure and toxicity to therapeutic target. Nat Rev Neurosci 14:38–48.

Lashuel HA, Petre BM, Wall J, Simon M, Nowak RJ, Walz T, Lansbury PT (2002) α-Synuclein, Especially the Parkinson's Disease-associated Mutants, Forms Pore-like Annular and Tubular Protofibrils. J Mol Biol 322:1089–1102.

Lebouvier L, Chaumette T, Damier P, Coron E, Touchefeu Y, Vrignaud S, Naveilhan P, Galmiche J, Bruley des Varannes S, Derkinderen P, Neunlist M (2008) Pathological lesions in colonic biopsies during Parkinson's disease. Gut 57:1741–1743.

Lee H-J (2005) Intravesicular Localization and Exocytosis of α-Synuclein and its Aggregates. J Neurosci 25:6016–6024.

Lee H-J, Choi C, Lee S-J (2002a) Membrane-bound Alpha-Synuclein Has a High Aggregation Propensity and the Ability to Seed the Aggregation of the Cytosolic Form. J Biol Chem 277:671–678.

Lee KD, Koo JH, Song SH, Jo KD, Lee MK, Jang W (2015) Central cholinergic dysfunction could be associated with oropharyngeal dysphagia in early Parkinson's disease. J Neural Transm 122:1553–1561.

Lee MK, Stirling W, Xu Y, Xu X, Qui D, Mandir AS, Dawson TM, Copeland NG, Jenkins NA, Price DL (2002b) Human alpha-synuclein-harboring familial Parkinson's disease-linked Ala53Thr mutation causes neurodegenerative disease with alpha-synuclein aggregation in transgenic mice. Proc Natl Acad Sci U S A 99:8968–8973.

Lepkowsky C (2018) Prevalence and Treatment of Constipation in Patients with Alpha-Synuclein Pathology. Intech Open:1–23.

Lesage S, Anheim M, Letournel F, Bousset L, Honoré A, Rozas N, Pieri L, Madiona K, Dürr A, Melki R, Verny C, Brice A (2013) G51D α-synuclein mutation causes a novel Parkinsonian-pyramidal

syndrome. Ann Neurol 73:459–471.

Lewis KA, Su Y, Jou O, Ritchie C, Foong C, Hynan LS, White CL, Thomas PJ, Hatanpaa KJ (2010) Abnormal neurites containing C-terminally truncated alpha-synuclein are present in Alzheimer's disease without conventional lewy body pathology. Am J Pathol 177:3037–3050.

Li W, West N, Colla E, Pletnikova O, Troncoso JC, Marsh L, Dawson TM, Jäkälä P, Hartmann T, Price DL, Lee MK (2005) Aggregation promoting C-terminal truncation of alpha-synuclein is a normal cellular process and is enhanced by the familial Parkinson's disease-linked mutations. Proc Natl Acad Sci U S A 102:2162–2167.

Lill CM (2016) Genetics of Parkinson's disease. Mol Cell Probes 30:386–396.

Lim KRQ, Maruyama R, Yokota T (2017) Eteplirsen in the treatment of Duchenne muscular dystrophy. Drug Des Devel Ther:533–545.

Liu CW, Giasson BI, Lewis KA, Lee VM, DeMartino GN, Thomas PJ (2005) A precipitating role for truncated alpha-synuclein and the proteasome in alpha-synuclein aggregation: Implications for pathogenesis of parkinson disease. J Biol Chem 280:22670–22678.

Liu Y, Qiang M, Wei Y, He R (2011) A novel molecular mechanism for nitrated alpha-synuclein-induced cell death. J Mol Cell Biol 3:239–249.

Luk KC, Kehm V, Carroll J, Zhang B, Brien PO, John Q, Lee VM (2012) Pathological Alpha-Synuclein Transmission Initiates Parkinson-like Neurodegeneration in Non-transgenic Mice. Science 338:949–953.

Luk KC, Song C, O'Brien P, Stieber A, Branch JR, Brunden KR, Trojanowski JQ, Lee VM-Y (2009) Exogenous alpha-synuclein fibrils seed the formation of Lewy body-like intracellular inclusions in cultured cells. Proc Natl Acad Sci 106:20051–20056.

Lundby A, Lage K, Weinert BT, Bekker-Jensen DB, Secher A, Skovgaard T, Kelstrup CD, Dmytriyev A, Choudhary C, Lundby C, Olsen J V. (2012) Proteomic Analysis of Lysine Acetylation Sites in Rat Tissues Reveals Organ Specificity and Subcellular Patterns. Cell Rep 2:419–431.

Majd S, Power JH, Grantham HJM (2015) Neuronal response in Alzheimer's and Parkinson's disease: The effect of toxic proteins on intracellular pathways. BMC Neurosci 16:1–13.

Mang CF, Truempler S, Erbelding D, Kilbinger H (2002) Modulation by NO of acetylcholine release in the ileum of wild-type and NOS gene knockout mice. Am J Physiol Gastrointest Liver Physiol 283:G1132–G1138.

Maroteaux L, Campanelli JT, Scheller RH (1988) Synuclein: a neuron-specific protein localized to the nucleus and presynaptic nerve terminal. J Neurosci 8:2804–2815.

Martin LJ, Pan Y, Price AC, Sterling W, Copeland NG, Jenkins NA, Price DL, Lee MK (2006) Parkinson's disease alpha-synuclein transgenic mice develop neuronal mitochondrial degeneration and cell death. J Neurosci 26:41–50.

Martin LJ, Semenkow S, Hanaford A, Wong M (2014) The mitochondrial permeability transition pore regulates Parkinson's disease development in mutant α-synuclein transgenic mice. Neurobiol Aging 35:1132–1152.

Martin ZS, Neugebauer V, Dineley KT, Kayed R, Zhang W, Reese LC, Taglialatela G (2012) α-Synuclein oligomers oppose long-term potentiation and impair memory through a calcineurin-dependent mechanism: relevance to human synucleopathic diseases. J Neurochem 120:440–452.

Martinez-Martin P, Rodriguez-Blazquez C, Kurtis MM, Chaudhuri KR (2011) The impact of non-motor symptoms on health-related quality of life of patients with Parkinson's disease. Mov Disord 26:399–

406.

Masliah E (2000) Dopaminergic Loss and Inclusion Body Formation in α-Synuclein Mice: Implications for Neurodegenerative Disorders. Science (80-) 287:1265–1269.

Masuda-Suzukake M, Nonaka T, Hosokawa M, Oikawa T, Arai T, Akiyama H, Mann DMA, Hasegawa M (2013) Prion-like spreading of pathological alpha-synuclein in brain. Brain 136:1128–1138.

Mazzulli JR, Zunke F, Isacson O, Studer L, Krainc D (2016) α-Synuclein–induced lysosomal dysfunction occurs through disruptions in protein trafficking in human midbrain synucleinopathy models. Proc Natl Acad Sci 113:1931–1936.

Miller T et al. (2013) A Phase I, Randomised, First-in-Human Study of an Antisense Oligonucleotide Directed Against SOD1 Delivered Intrathecally in SOD1-Familial ALS Patients. Lancet Neurol 12:435–442.

Mink JW (1996) The basal ganglia: Focused selection and inhibition of competing motor programs. Prog Neurobiol 50:381–425.

Miraglia F, Ricci A, Rota L, Colla E (2018) Subcellular localization of alpha-synuclein aggregates and their interaction with membranes. Neural Regen Res 13:1136–1144.

Nakai M, Fujita M, Waragai M, Sugama S, Wei J, Akatsu H, Ohtaka-Maruyama C, Okado H, Hashimoto M (2007) Expression of alpha-synuclein, a presynaptic protein implicated in Parkinson's disease, in erythropoietic lineage. Biochem Biophys Res Commun 358:104–110.

Nakamura K, Nemani VM, Azarbal F, Skibinski G, Levy JM, Egami K, Munishkina L, Zhang J, Gardner B, Wakabayashi J, Sesaki H, Cheng Y, Finkbeiner S, Nussbaum RL, Masliah E, Edwards RH (2011) Direct Membrane Association Drives Mitochondrial Fission by the Parkinson Disease-associated Protein α-Synuclein. J Biol Chem 286:20710–20726.

Nakamura K, Nemani VM, Wallender EK, Kaehlcke K, Ott M, Edwards RH (2008) Optical Reporters for the Conformation of α-Synuclein Reveal a Specific Interaction with Mitochondria. J Neurosci 28:12305–12317.

Narayanan V, Scarlata S (2001) Membrane binding and self-association of α-synucleins. Biochemistry 40:9927–9934.

Nemani VM, Lu W, Berge V, Nakamura K, Onoa B, Lee MK, Chaudhry FA, Nicoll RA, Edwards RH (2010) Increased Expression of α-Synuclein Reduces Neurotransmitter Release by Inhibiting Synaptic Vesicle Reclustering after Endocytosis. Neuron 65:66–79.

Nonaka T, Iwatsubo T, Hasegawa M (2005) Ubiquitination of Alpha-Synuclein. Biochemistry 44:361–368.

Oaks AW, Marsh-Armstrong N, Jones JM, Credle JJ, Sidhu A (2013) Synucleins Antagonize Endoplasmic Reticulum Function to Modulate Dopamine Transporter Trafficking. PLoS One 8:e70872.

Obeso JA et al. (2017) Past, Present and Future of Parkinson's Disease: A Special Essay on the 200th Anniversary of the Shaking Palsy. Mov Disord 32:1264–1310.

Obeso JA, Rodriguez-Oroz MC, Rodriguez M, Lanciego JL, Artieda J, Gonzalo N, Olanow CW (2000) Pathophysiology of the basal ganglia in Parkinson's disease. Trends Neurosci 23.

Ouberai MM, Wang J, Swann MJ, Galvagnion C, Guilliams T, Dobson CM, Welland ME (2013) Alpha-Synuclein Senses Lipid Packing Defects and Induces Lateral Expansion of Lipids Leading to Membrane Remodeling. J Biol Chem 288:20883–20895.

Paleologou KE, Oueslati A, Shakked G, Rospigliosi CC, Kim H-Y, Lamberto GR, Fernandez CO, Schmid A, Chegini F, Gai WP, Chiappe D, Moniatte M, Schneider BL, Aebischer P, Eliezer D, Zweckstetter

M, Masliah E, Lashuel HA (2010) Phosphorylation at S87 Is Enhanced in Synucleinopathies, Inhibits Alpha-Synuclein Oligomerization and Influences Synuclein-Membrane Interactions. J Neurosci 30:3184–3198.

Paleologou KE, Schmid AW, Rospigliosi CC, Kim HY, Lamberto GR, Fredenburg RA, Lansbury PT, Fernandez CO, Eliezer D, Zweckstetter M, Lashuel HA (2008) Phosphorylation at Ser-129 but not the phosphomimics S129E/D inhibits the fibrillation of alpha-synuclein. J Biol Chem 283:16895–16905.

Pan-Montojo F, Schwarz M, Winkler C, Arnhold M, O'Sullivan GA, Pal A, Said J, Marsico G, Verbavatz JM, Rodrigo-Angulo M, Gille G, Funk RHW, Reichmann H (2012) Environmental toxins trigger PD-like progression via increased alpha-synuclein release from enteric neurons in mice. Sci Rep 2:1–12.

Pasanen P, Myllykangas L, Siitonen M, Raunio A, Kaakkola S, Lyytinen J, Tienari PJ, Pöyhönen M, Paetau A (2014) A novel alpha-synuclein mutation A53E associated with atypical multiple system atrophy and Parkinson's disease-type pathology. Neurobiol Aging 35:1–5.

Peelaerts W, Bousset L, Baekelandt V, Melki R (2018) α-Synuclein strains and seeding in Parkinson's disease, incidental Lewy body disease, dementia with Lewy bodies and multiple system atrophy: similarities and differences. Cell Tissue Res 373:195–212.

Peelaerts W, Bousset L, Van Der Perren A, Moskalyuk A, Pulizzi R, Giugliano M, Van Den Haute C, Melki R, Baekelandt V (2015) Alpha-Synuclein strains cause distinct synucleinopathies after local and systemic administration. Nature 522:340–344.

Petrucelli L, Farrell CO, Lockhart PJ, Baptista M, Kehoe K, Vink L, Choi P, Wolozin B, Farrer M, Hardy J, Cookson MR (2002) Parkin Protects against the Toxicity Associated with Mutant Alpha-Synuclein: Proteasome Dysfunction Selectively Affects Catecholaminergic Neurons. Neuron 36:1007–1019.

Pillon B, Dubois B, Cusimano G, Bonnet AM, Lhermitte F, Agid Y (1989) Does cognitive impairment in Parkinson's disease result from non-dopaminergic lesions? J Neurol Neurosurg Psychiatry 52:201–206.

Plotegher N, Berti G, Ferrari E, Tessari I, Zanetti M, Lunelli L, Greggio E, Bisaglia M, Veronesi M, Girotto S, Dalla Serra M, Perego C, Casella L, Bubacco L (2017) DOPAL derived α-synuclein oligomers impair synaptic vesicles physiological function. Sci Rep 7:40699.

Polito L, Greco A, Seripa D (2016) Genetic Profile, Environmental Exposure and Their Interaction in Parkinson's Disease. Park Dis 2016:6465793.

Polymeropoulos MH (1997) Mutation in the α-Synuclein Gene Identified in Families with Parkinson's Disease. Science 276:2045–2047.

Polymeropoulos MH et al. (1997) Mutation in the Alpha-Synuclein Gene Identified in Families with Parkinson's Disease Mutation in the Alpha-Synuclein Gene Identified in Families with Parkinson's Disease. Science 276:2045–2047.

Pouclet H, Lebouvier T, Coron E, Bruley des Varannes S, Rouaud T, Roy M, Neunlist M, Derkinderen P (2012) A comparison between rectal and colonic biopsies to detect Lewy pathology in Parkinson's disease. Neurobiol Dis 45:305–309.

Prots I, Veber V, Brey S, Campioni S, Buder K, Riek R, Böhm KJ, Winner B (2013) α-Synuclein Oligomers Impair Neuronal Microtubule-Kinesin Interplay. J Biol Chem 288:21742–21754.

Proukakis C, Dudzik CG, Brier T, MacKay DS, Cooper JM, Millhauser GL, Houlden H, Schapira AH (2013) A novel alpha-synuclein missense mutation in Parkinson disease. Neurology 80:1062–1064.

Rana HQ, Balwani M, Bier L, Alcalay RN (2013) Age-specific Parkinson disease risk in GBA mutation carriers: Information for genetic counseling. Genet Med 15:146–149.

Rao M, Gershon MD (2016) The bowel and beyond: The enteric nervous system in neurological disorders. Nat Rev Gastroenterol Hepatol 13.

Recasens A, Dehay B, Bové J, Carballo-Carbajal I, Dovero S, Pérez-Villalba A, Fernagut PO, Blesa J, Parent A, Perier C, Fariñas I, Obeso JA, Bezard E, Vila M (2014) Lewy body extracts from Parkinson disease brains trigger alpha-synuclein pathology and neurodegeneration in mice and monkeys. Ann Neurol 75.

Rey NL, Petit GH, Bousset L, Melki R, Brundin P (2013) Transfer of human alpha-synuclein from the olfactory bulb to interconnected brain regions in mice. Acta Neuropathol 126:555–573.

Rigo F, Chun SJ, Norris DA, Hung G, Lee S, Matson J, Fey RA, Gaus H, Hua Y, Grundy JS, Krainer AR, Henry SP, Bennett CF (2014) Pharmacology of a Central Nervous System Delivered 2'-O-Methoxyethyl-Modified Survival of Motor Neuron Splicing Oligonucleotide in Mice and Nonhuman Primates. J Pharmacol Exp Ther 350:46–55.

Rota L, Pellegrini C, Benvenuti L, Antonioli L, Fornai M, Blandizzi C, Cattaneo A, Colla E (2019) Constipation, deficit in colon contractions and alpha-synuclein inclusions within the colon precede motor abnormalities and neurodegeneration in the central nervous system in a mouse model of alpha-synucleinopathy. Transl Neurodegener 8:1–15.

Rott R, Szargel R, Haskin J, Shani V, Shainskaya A, Manov I, Liani E, Avraham E, Engelender S (2008) Monoubiquitylation of α-Synuclein by seven in absentia homolog (SIAH) promotes its aggregation in dopaminergic cells. J Biol Chem 283:3316–3328.

Rott R, Szargel R, Shani V, Bisharat S, Engelender S (2014) α-Synuclein Ubiquitination and Novel Therapeutic Targets for Parkinson's Disease. CNS Neurol Disord Drug Targets 13:630–637.

Ryan T, Bamm V V., Stykel MG, Coackley CL, Humphries KM, Jamieson-Williams R, Ambasudhan R, Mosser DD, Lipton SA, Harauz G, Ryan SD (2018) Cardiolipin exposure on the outer mitochondrial membrane modulates α-synuclein. Nat Commun 9:817.

Sacino AN, Brooks M, Thomas MA, McKinney AB, Lee S, Regenhardt RW, McGarvey NH, Ayers JI, Notterpek L, Borchelt DR, Golde TE, Giasson BI (2014) Intramuscular injection of alpha-synuclein induces CNS alpha-synuclein pathology and a rapid-onset motor phenotype in transgenic mice. Proc Natl Acad Sci 111:10732–10737.

Sampathu DM, Giasson BI, Pawlyk AC, Trojanowski JQ, Lee VM-Y (2003) Ubiquitination of alpha-synuclein is not required for formation of pathological inclusions in alpha-synucleinopathies. Am J Pathol 163:91–100.

Sato H, Arawaka S, Hara S, Fukushima S, Koga K, Koyama S, Kato T (2011) Authentically Phosphorylated Alpha-Synuclein at Ser129 Accelerates Neurodegeneration in a Rat Model of Familial Parkinson's Disease. J Neurosci 31:16884–16894

Savica R, Cannon-Albright LA, Pulst S (2016) Familial aggregation of Parkinson disease in Utah: A population-based analysis using death certificates. Neurol Genet 2:65.

Schapira AHV, Chaudhuri KR, Jenner P (2017) Non-motor features of Parkinson disease. Nat Rev Neurosci 18:435–450.

Schlossmacher MG, Frosch MP, Forno L, Ochiishi T, Shimura H, Sharon R, Hattori N, Langston JW, Mizuno Y, Hyman BT, Selkoe DJ, Kosik KS (2002) Parkin Localizes to the Lewy Bodies of Parkinson Disease and Dementia with Lewy Bodies. Am J Pathol 160:1655–1667.

Schmid AW, Chiappe D, Pignat V, Grimminger V, Hang I, Moniatte M, Lashuel HA (2009) Dissecting the mechanisms of tissue transglutaminase-induced cross-linking of alpha-synuclein: Implications for the pathogenesis of Parkinson disease. J Biol Chem 284:13128–13142.

Schneider SA, Alcalay RN (2017) Neuropathology of genetic synucleinopathies with parkinsonism: Review

of the literature. Mov Disord 32:1504–1523.

Schoch KM, Miller TM (2017) Antisense Oligonucleotides: Translation from Mouse Models to Human Neurodegenerative Diseases. Neuron 94:1056–1070.

Scoles DR, Pulst SM (2018) Oligonucleotide therapeutics in neurodegenerative diseases. RNA Biol 15:707–714.

Shannon KM, Keshavarzian A, Dodiya HB, Jakate S, Kordower JH (2012) Is alpha-synuclein in the colon a biomarker for premotor Parkinson's Disease? Evidence from 3 cases. Mov Disord 27:716–719.

Shi M, Liu C, Cook TJ, Bullock KM, Zhao Y, Li Y, Aro P, Dator R, He C, Hipp MJ, Cyrus P, Peskind ER, Hu S, Quinn JF, Douglas R (2014) Plasma exosomal α-synuclein is likely CNS-derived and increased in Parkinson's disease. Acta Neuropathol 128:639–650.

Shults CW (2006) Lewy bodies. Proc Natl Acad Sci 103:1661–1668.

Singleton a B et al. (2003) Alpha-Synuclein Locus Triplication Causes Parkinson's Disease. Science 302:841.

Smith RA, Bennett CF, Cleveland DW, Smith RA, Miller TM, Yamanaka K, Monia BP, Condon TP, Hung G, Lobsiger CS, Ward CM, Mcalonis-downes M, Wei H, Wancewicz E V, Bennett CF, Cleveland DW (2006) Antisense oligonucleotide therapy for neurodegenerative disease. J Clin Invest 116:2290–2296.

Song J, Lu J, Liu L, Chen L, Sundara S, Durairajan K, Yue Z, Zhang H, Li M (2014) HMGB1 is involved in autophagy inhibition caused by SNCA/α-synuclein overexpression: A process modulated by the natural autophagy inducer corynoxine B. Autophagy 10:144–154.

Soto C (2012) Perspective Transmissible Proteins: Expanding the Prion Heresy. Cell 149:968–977.

Špica V, Pekmezović T, Svetel M, Kostić VS (2013) Prevalence of non-motor symptoms in young-onset versus late-onset Parkinson's disease. J Neurol 260:131–137.

Spillantini MG, Schmidt ML, Lee VM-Y, Trojanowski JQ, Jakes R, Goedert M (1997a) Alpha-Synuclein in Lewy bodies. Nature 388:839–840.

Stirpe P, Hoffman M, Badiali D, Colosimo C (2016) Constipation: an emerging risk factor for Parkinson's disease? Eur J Neurol 23:1606–1613.

Sveinbjornsdottir S, Hicks A, Jonsson T, Petursson H, Gugmundsson G, Frigge M, Kong A, Gulcher J, Stefansson K (2000) Familial aggregation of Parkinson's disease in Iceland. N Engl J Med 343:1765–1770.

Sweeney MD, Sagare AP, Zlokovic B V, Angeles L (2018) Blood-brain barrier breakdown in Alzheimer's disease and other neurodegenerative disorders. Nat Rev Neurol 14:133–150.

Tetzlaff JE, Putcha P, Outeiro TF, Ivanov A, Berezovska O, Hyman BT, Mclean PJ (2008) CHIP Targets Toxic α-Synuclein Oligomers for Degradation Bradley. J Biol Chem 283:17962–17968.

Thayanidhi N, Helm JR, Nycz DC, Bentley M, Liang Y, Hay JC (2010) Alpha-Synuclein Delays Endoplasmic Reticulum (ER)-to-Golgi Transport in Mammalian Cells by Antagonizing ER/Golgi SNAREs. Mol Biol Cell 21:1850–1863.

Theillet F-X, Binolfi A, Bekei B, Martorana A, Rose HM, Stuiver M, Verzini S, Lorenz D, van Rossum M, Goldfarb D, Selenko P (2016) Structural disorder of monomeric α-synuclein persists in mammalian cells. Nature 530:45–50.

Tofaris GK, Razzaq A, Ghetti B, Lilley KS, Spillantini MG (2003) Ubiquitination of Alpha-Synuclein in

Lewy Bodies Is a Pathological Event Not Associated with Impairment of Proteasome Function. J Biol Chem 278:44405–44411.

Tomé CML, Tyson T, Rey NL, Grathwohl S, Britschgi M, Brundin P (2013) Inflammation and α-Synuclein's Prion-like Behavior in Parkinson's Disease: Is There a Link? Mol Neurobiol 47:561–574.

Tomkins O, Friedman O, Ivens S, Reiffurth C, Major S, Dreier JP, Heinemann U, Friedman A (2007) Blood-brain barrier disruption results in delayed functional and structural alterations in the rat neocortex. Neurobiol Dis 25:367–377.

Tuttle MD, Comellas G, Nieuwkoop AJ, Covell DJ, Berthold DA, Kloepper KD, Courtney JM, Kim JK, Barclay AM, Kendall A, Wan W, Stubbs G, Schwieters CD, Lee VMY, George JM, Rienstra CM (2016) Solid-state NMR structure of a pathogenic fibril of full-length human α-synuclein. Nat Struct Mol Biol 23:409–415.

Tysnes OB, Storstein A (2017) Epidemiology of Parkinson's disease. J Neural Transm 124:901–905.

Ulrih NP, Barry CH, Fink AL (2008) Impact of Tyr to Ala mutations on α-synuclein fibrillation and structural properties. Biochim Biophys Acta 1782:581–585.

Valente EM et al. (2004) Hereditary Early-Onset Parkinson's Disease Caused by Mutations in PINK1. Science 304:1158–1161.

Versace V, Langthaler PB, Sebastianelli L, Höller Y, Brigo F, Orioli A, Saltuari L, Nardone R (2017) Impaired cholinergic transmission in patients with Parkinson's disease and olfactory dysfunction. J Neurol Sci 377:55–61.

Vilar M, Chou H-T, Luhrs T, Maji SK, Riek-Loher D, Verel R, Manning G, Stahlberg H, Riek R (2008) The fold of α-synuclein fibrils. Proc Natl Acad Sci 105:8637–8642.

Visanji NP, Brooks PL, Hazrati L, Lang AE (2013) The prion hypothesis in Parkinson's disease: Braak to the future. Acta Neuropathol Commun 8:1–12.

Visanji NP, Marras C, Kern DS, Al Dakheel A, Gao A, Liu LW, Lang AE, Hazrati LN (2015) Colonic mucosal alpha-synuclein lacks specificity as a biomarker for Parkinson disease. Neurology 609–616.

Volpicelli-Daley LA, Gamble KL, Schultheiss CE, Riddle DM, West AB, Lee VM-Y (2014) Formation of α-synuclein Lewy neurite-like aggregates in axons impedes the transport of distinct endosomes. Mol Biol Cell 25:4010–4023.

Volpicelli-daley LA, Luk KC, Patel TP, Tanik SA, Dawn M, Stieber A, Meany DF, Trojanowski JQ, Lee VM (2012) Exogenous Alpha-Synuclein Fibrils Induce Lewy Body Pathology Leading to Synaptic Dysfunction and Neuron Death. Neuron 72:57–71.

Von Campenhausen S, Bornschein B, Wick R, Bötzel K, Sampaio C, Poewe W, Oertel W, Siebert U, Berger K, Dodel R (2005) Prevalence and incidence of Parkinson's disease in Europe. Eur Neuropsychopharmacol 15:473–490.

Wang L, Das U, Scott DA, Tang Y, McLean PJ, Roy S (2014) α-Synuclein Multimers Cluster Synaptic Vesicles and Attenuate Recycling. Curr Biol 24:2319–2326.

Wang L, Fleming SM, Chesselet M-F, Taché Y (2008) Abnormal colonic motility in mice overexpressing human wild-type alpha-synuclein. Neuroreport 19:873–876.

Wang W et al. (2011) A soluble alpha-synuclein construct forms a dynamic tetramer. Proc Natl Acad Sci 108:17797–17802.

Weinreb PH, Zhen W, Poon AW, Conway KA, Lansbury PT (1996) NACP, a protein implicated in Alzheimer's disease and learning, is natively unfolded. Biochemistry 35:13709–13715.

Winkler EA, Sengillo JD, Sagare AP, Zhao Z, Ma Q, Zuniga E, Wang Y, Zhong Z, Sullivan JS, Griffin JH, Cleveland DW, Zlokovic B V (2014) Blood-spinal cord barrier disruption contributes to early motor-neuron degeneration in ALS-model mice. Proc Natl Acad Sci U S A 111:1035–1042.

Winslow AR, Chen C, Corrochano S, Acevedo-arozena A, Gordon DE, Peden AA, Lichtenberg M, Menzies FM, Ravikumar B, Imarisio S, Brown S, Kane CJO, Rubinsztein DC (2010) Alpha-Synuclein impairs macroautophagy: implications for Parkinson's disease. J Cell Biol 190:1023–1037.

Withers GS, George JM, Banker GA, Clayton DF (1997) Delayed localization of synelfin (synuclein, NACP) to presynaptic terminals in cultured rat hippocampal neurons. Dev Brain Res 99:87–94.

Xiang W, Schlachetzki JCM, Helling S, Bussmann JC, Berlinghof M, Schäffer TE, Marcus K, Winkler J, Klucken J, Becker C-M (2013) Oxidative stress-induced posttranslational modifications of alpha-synuclein: Specific modification of alpha-synuclein by 4-hydroxy-2-nonenal increases dopaminergic toxicity. Mol Cell Neurosci 54:71–83.

Yahr MD, Duvoisin RC, Schear MJ (1969) Treatment of Parkinsonism With Levodopa. Arch Neurol 21:343–354.

Yang Q, She H, Gearing M, Colla E, Lee M, Shacka J, Mao Z (2009) Regulation of Neuronal Survival Factor MEF2D by Chaperone- Mediated Autophagy. Science 323:124–127.

Yu Z, Xu X, Xiang Z, Zhou J, Zhang Z, Hu C, He C (2010) Nitrated α-synuclein induces the loss of dopaminergic neurons in the substantia nigra of rats. PLoS One 5:9956.

Zarranz JJ, Alegre J, Gómez-Esteban JC, Lezcano E, Ros R, Ampuero I, Vidal L, Hoenicka J, Rodriguez O, Atarés B, Llorens V, Gomez Tortosa E, Del Ser T, Muñoz DG, De Yebenes JG (2004) The New Mutation, E46K, of Alpha-Synuclein Causes Parkinson and Lewy Body Dementia. Ann Neurol 55:164–173.

Zhou J, Broe M, Huang Y, Anderson JP, Gai WP, Milward EA, Porritt M, Howells D, Hughes AJ, Wang X, Halliday GM (2011) Changes in the solubility and phosphorylation of α-synuclein over the course of Parkinson's disease. Acta Neuropathol 121:695–704.

Zhu M, Qin ZJ, Hu D, Munishkina LA, Fink AL (2006) Alpha-Synuclein Can Function As an Antioxidant Preventing Oxidation of Unsaturated Lipid in Vesicles. Biochemistry 45:8135–8142.

Zimprich A et al. (2004) Mutations in LRRK2 cause autosomal-dominant parkinsonism with pleomorphic pathology. Neuron 44:601–607.